CONTROL OF COMBUSTION ZONE SOOT FORMATION IN A SEMI-CLOSED CYCLE GAS TURBINE

By

WILLIAM J. ELLIS, JR.

A THESIS PRESENTED TO THE GRADUATE SCHOOL
OF THE UNIVERSITY OF FLORIDA IN PARTIAL FULFILLMENT
OF THE REQUIREMENTS FOR THE DEGREE OF
MASTER OF SCIENCE

UNIVERSITY OF FLORIDA

2008

To my sister, Diana Brady, for her confidence and encouragement.

ACKNOWLEDGMENTS

This research was sponsored, in part, by the Department of Mechanical and Aerospace Engineering of the University of Florida, JEA Electric System of Jacksonville Florida, and the State University System of Florida Turbine Initiative. I am indebted to my supervisory committee members, (Dr. William E. Lear, Jr., Dr. David W. Hahn and Dr. David W. Mikolaitis) for their guidance and participation. I extend special thanks to John F. Crittenden, Jr., for his perspective and assistance regarding operation of the experimental set-up.

TABLE OF CONTENTS

Page

ACKNOWLEDGMENTS 4

LIST OF TABLES 8

LIST OF FIGURES 9

LIST OF TERMS 11

Roman 11
Greek 12
Subscripts 12

ABSTRACT 14

CHAPTER

1 INTRODUCTION 16

2 EXPERIMENTAL APPARATUS 20

Test Engine 20
Vapor Absorbsion Refrigeration System (Vars) 22
Recuperator And Warm Gas Cooler 23
Instrumentation 23
Optical Measurement 23
Gas Analysis 24
Load Measurement 25
Dynamometer 25
Condensed water 25
Engine Speed Measurement 25
Flow Measurement 25
Air and Recirculation 25
Fuel 25
Temperature Measurement 26
Pressure Measurement 26
Digital Acquisition System (Daq) 27
Signal conditioning 27
Operator interface terminal 27

3 THEORETICAL BASIS FOR DATA ANALYSIS 29

Two-Color Pyrometry 29
Soot Temperature Calculation 29
Soot Volume Fraction 30

Gas Composition 32
Inlet Air Composition. 32
Recirculation Gas Composition from Exhaust Analysis. 33
Oxidizer (Air + Recirculation Mixture). 35
Equivalence Ratio Φ 36
F/A Mass Ratio (Fuel/ Air-Recirculation Mix). 36
Stoichiometric F/A Mass Ratio (Fuel/ Air-Recirculation Mix). 38

4 EXPERIMENTAL METHOD 40

Pre-Test Setup 40
Start-Up, Operation and Shut-Down 41
Data Acquisition 42

5 DATA REDUCTION AND ANALYSIS 44

Data Post-Processing 44
Spectrometer 44
Data Acquisition System 45
Data Analysis 46
Soot Temperature And Volume Fraction 46
Sapphire window transmission 46
Sampling distance 47
Optical fiber acceptance angle 48
Gas Analysis 49
Equivalence Ratio 50
Adiabatic Flame Temperature 50

6 RESULTS AND DISCUSSION 53

Combustion Zone Parameters 54
Regression Analysis Of F_{vr} Based on Combustion Zone Parameters 56
Measurement Error Analysis 59

7 CONCLUSIONS 94

8 RECOMMENDATIONS 96

APPENDIX

A OPERATING PROCEDURES 99

The HPRTE Setup Procedure, ... 99
The VARS Operating Procedure 103
Lab Data Acquisition System Procedure 108
Spectrometer Operating Procedure 112
The COSA 1600 IR Gas Analyzer Operating Procedure 114
Digital Camera Set-up Procedure 116

B DATA SHEETS 118
C RELEVANT DATA 126
Measurement Error Analysis 129
LIST OF REFERENCES 131
BIOGRAPHICAL SKETCH 133

LIST OF TABLES

Table page

6-1 Regression equation coefficients for soot temperature and adiabatic flame temperature 61

6-2 Regression equation coefficients for soot volume fraction ratio 61

6-3 Data uncertainty for major parameters 61

C-1 Processed data 126

C-2 Sample Labview output 128

LIST OF FIGURES

Figure		page
3-1	Block diagram of HPRTE.	28
5-1	Geometry and dimensions used to correct emission intensity for sampling distance and optical fiber acceptance angle	52
6-1	Soot volume fraction ratio vs. combustor inlet O_2 %	62
6-2	Emissivity at 525.03 nm vs. % O_2	63
6-3	Emissivity at 675.01 nm vs. % O_2	64
6-4	Soot volume fraction ratio vs. combustor inlet equivalence ratio	65
6-5	Soot volume fraction ratio vs. combustion pressure	66
6-6	Soot volume fraction ratio vs. oxygen concentration at high fuel flow	67
6-7	Soot volume fraction ratio vs. soot temperature	68
6-8	Soot volume fraction ratio vs. adiabatic flame temperature	69
6-9	Soot temperature vs. combustor inlet percent oxygen	70
6-10	Soot temperature vs. absolute combustion pressure	71
6-11	Soot temperature vs. combustor inlet equivalence ratio	72
6-12	Adiabatic flame temperature vs. combustor inlet percent oxygen	73
6-13	Adiabatic flame temperature vs. combustion pressure	74
6-14	Adiabatic flame temperature vs. combustor inlet equivalence ratio	75
6-15	Soot temperature/adiabatic flame temperature vs. combustor inlet % O_2	76
6-16	Soot temperature/adiabatic flame temperature vs. combustion pressure	77
6-17	Soot temperature/adiabatic flame temperature vs. equivalence ratio	78
6-18	Regression and data soot temperature vs. combustor inlet percent oxygen	79
6-19	Regression and data adiabatic flame temperature vs. combustor inlet percent	80
6-20	Run data and regression F_{vr} vs. combustor inlet % O_2 using T_{soot} for the temperature parameter	81

6-21 Run data and regression F_{vr} vs. combustor inlet % O_2 using T_{ad} for the temperature parameter....82

6-22 Synthetic F_{vR} vs. P_{comb}, $\Phi = 0.4$ with 15 % and 20 % O_2 using T_{soot}....83

6-23 Synthetic F_{vR} vs. P_{comb}, $\Phi = 0.65$ with 15 % and 20 % combustor inlet O_2 using T_{soot}....84

6-24 Synthetic F_{vR} vs. P_{comb}, $\Phi = 0.4$ with 15 % and 20 % combustor inlet O_2 using T_{ad}....85

6-25 Synthetic F_{vR} vs. P_{comb}, $\Phi = 0.65$ with 15 % and 20 % combustor inlet O_2 using T_{ad}....86

6-26 Run data and extreme case synthetic F_{vR} vs. combustor inlet % O_2 using T_{soot}....87

6-27 Run data and extreme case synthetic F_{vR} vs. combustor inlet % O_2 using T_{ad}....88

6-28 Run data and extreme case synthetic F_{vR} vs. combustor inlet equivalence ratio using T_{soot}....89

6-29 Run data and extreme case synthetic F_{vR} vs. combustor inlet equivalence ratio using T_{ad}....90

6-30 Synthetic F_{vR} vs. combustor inlet % O_2 with variable combustor inlet Φ....91

6-31 Synthetic T_{soot} vs. combustor inlet % O_2 with constant P_{comb}....92

6-32 Synthetic T_{soot} vs. P_{comb} with constant combustor inlet % O_2....93

LIST OF TERMS

Roman

a	Regression coefficient
A	Cross sectional area or stoichiometric moles of air
C_1	Plank's first constant
C_2	Plank's second constant
C_{abs}	Particle absorption cross section
C_d	Discharge coefficient
C_{ext}	Particle extinction cross section
C_{scat}	Particle scattering cross section
d	Particle diameter
F/A	Fuel-to-air ratio
F_v	Soot volume fraction
F_{vmax}	Maximum soot volume fraction
F_{vR}	Soot volume fraction ratio
I	Emission intensity
ik	Imaginary part of the complex refractive index
K	Mole ratio
K_{ext}	Extinction coefficient
L	Optical path length
MW	Molecular weight
m	Complex refractive index
$\dot{m}$	Mass flow rate
N	Particle density

n	Moles or real part of the complex refractive index
$\dot{n}$	Mole flow rate
P	Pressure
R	Mass-specific gas constant or recirculation ratio
T	Temperature
V	Velocity or valve
$\dot{V}$	Volumetric flow rate

Greek

α	Particle size parameter
β	Venturi contraction ratio
Δ	Change in an associated term
ε	Emissivity
θ	Optical properties parameter
λ	Wavelength
ρ	Density
σ	Stefan-Boltzmann constant
Φ	Equivalence ratio
χ	Mole fraction

Subscripts

$_0$	Reference state, 300 Kelvin
$_1$	State one
$_2$	State two
$_{amb}$	Ambient
$_b$	Blackbody

Bnr	Combustor liner
comb	Combustor
db	Dry bulb
dry	Dry gas mixture
fuel	Property of fuel
H2O	Property of water
HPRE	High pressure recuperator exit
i	i^{th} constituent of a mixture
m	Mass basis
MAI	Main air inlet
max	Maximum observed value
n	Molar basis
N2	Property of nitrogen
O2	Property of oxygen
ox	Reactant gas mixture
ratio	Ratio of parameters
rec	Recirculation
sat	Property at saturation conditions
soot	Value for soot
stoic	Stoichiometric
throat	Property at bell mouth throat
wb	Wet bulb

Abstract of Thesis Presented to the Graduate School
of the University of Florida in Partial Fulfillment of the
Requirements for the Degree of Master of Science

COMBUSTION ZONE SOOT BEHAVIOR IN A SEMI-CLOSED CYCLE GAS TURBINE

By

William J. Ellis, Jr.

December 2008

Chair: William E. Lear, Jr.
Major: Mechanical Engineering

Spectroscopic measurements were made on the primary zone flame of a constant speed, semi-closed cycle, and recuperated gas turbine. This was undertaken at various loads while introducing cooled exhaust gas into the combustor reactant stream as a diluent. Operating conditions included equivalence ratios from 0.42 to 0.64 and reactant oxygen concentration from 15.4 to 20.7% at an average combustion pressure of 34.8 psia. The results demonstrated a power relationship between soot volume fraction and the oxygen concentration in the reactant gas mixture. An inverse power relationship between soot volume fraction and combustion pressure or equivalence ratio was observed. Soot formation was reduced by an order of magnitude when oxygen concentration was reduced to 17.5%. Soot temperature was found to be independent of equivalence ratio and more useful in predicting soot volume fraction than the adiabatic flame temperature. Two predictive models, based on data regression analysis, were developed for soot temperature as a function of pressure and oxygen concentration and for soot volume fraction as a function of equivalence ratio, oxygen concentration, soot temperature and combustion pressure. A third model was developed for adiabatic flame temperature as a function of equivalence ratio, oxygen concentration and combustion pressure.

The models demonstrate a close agreement with data and predict soot temperature will increase with combustion pressure and oxygen concentration, while soot volume fraction increases with oxygen concentration but decreases with combustion pressure. The adiabatic flame temperature model predicts increasing temperature with both combustion pressure and equivalence ratio.

CHAPTER 1
INTRODUCTION

Soot produced by various combustion processes has been studied with increasing interest in recent decades. This is the result of concerns regarding health, climate change and efficient utilization of resources. There is growing evidence from field observations that a soot aerosol layer exists at 10-11 km altitude [1, 2]. A correlation between the observed soot mass concentration and calculated fuel usage from air traffic suggests that aircraft fuel combustion may be the principal source of the soot aerosol layer in the stratosphere [7]. High altitude emission of soot particles acting as condensation nuclei may substantially affect the cirrus cloud formation [3]. Arguably, the effect of atmospheric soot levels could be to perturb the Earth's energy balance by altering these cloud formations. If the impact of this perturbation is significant, it might be expected to lead to changes in climate [4, 5], although the effect on global temperature is still controversial due to complex interactions with other aerosols. Soot, as a component of particulate matter (PM) air pollution, has been the subject of hundreds of investigations over the last ten years. It is now generally accepted that these pollutants are a significant contributor to illness and mortality rates. The influence is so strong that the EPA has issued periodically reviewed standards on PM emissions as required by the Clean Air Act. There is evidence of a nearly linear relation between increased risk of premature mortality and PM pollution [6].

The performance of gas turbines has continuously improved since their first practical application. With their performance, so has their popularity increased as appropriate application of the technology broadens. In aviation they are the primary choice of propulsion for all but the smallest aircraft, and as a stationary power source, they are now practical for tens of kilowatts to multi- megawatt generation facilities.

This popularity can be expected to increase owing to the low cost, high efficiency, simplicity, reliability, multi-fuel capability, fast start-up and short facility construction time. Gas turbine emissions are therefore of primary concern [7]. For civilian use, health, energy efficiency and environmental effects are the main priority. In military applications, the impact of efficiency on fuel logistics and mission capability as well as the exhaust signature are more important issues.

At the least, soot emissions represent available energy that is not utilized. Beyond that, the impact of thermal radiation from soot on engine components must be mitigated as part of the performance improvements needed to further exploit the attractive characteristics of gas turbines. In particular, the life of combustor liners is strongly influenced by radiative exchange with soot produced in the flame. Soot production is enhanced at the higher temperatures and pressures expected in new designs. At these conditions the size and concentration of soot particles allows them to radiate as black bodies in the infrared and this is the predominant heat load. The measure currently taken to control this effect involves additional film cooling over what otherwise might be required. This approach has a deleterious impact on engine performance by compromising temperature pattern factor, low power combustion efficiency and exhaust pollutants such as carbon monoxide and unburned hydrocarbons [8, 9].

Recent investigations of the soot formation mechanism generally resolve it into four phases. These are nucleation, coagulation, surface reactions and agglomeration. The source of carbon in the process involves both vapor-phase reactions and liquid-phase pyrolysis. All of the phases are affected by local temperature, pressure and oxygen concentration, as well as fuel type. Research suggests that in regard to local temperature, soot burnout ceases below approximately 1300 K and soot formation requires approximately 1600 K for nucleation [10].

The effect of molecular oxygen may, at high temperature, increase radical species and actually promote soot formation, rather than oxidation [11]. Further, soot volume fraction has been observed to be approximately proportional to a power of the absolute pressure with the exponent displaying variability depending on pressure regime [12-15].

Researchers have also been examining the impact of high temperature combustion air with and without reduced oxygen concentration as well as more typical air temperatures and reduced oxygen concentration on combustion and flame characteristics. These studies generally involve near-atmospheric pressures and preheat ranging from 540 R to 3600 R, with the goal of efficiency increases accompanied by reduced size and pollution for industrial boilers and furnaces.

Observations of the effect of reducing oxygen concentration, through dilution with recirculated exhaust or inert gases, include a reduction in soot production, with its accompanying flame luminosity, C_2 species, CO, unburned hydrocarbons and NO_x. When N_2 is used as the diluent however, NO_x reduction is dependent on conditions. As preheat temperatures increase in concert with dilution, temperature gradients are seen to diminish as the reaction zone becomes more distributed. When temperatures approach maximum and O_2 concentration is reduced below 15% to a minimum of about 2%, the flame color may transform to blue, blue-green or become colorless, with combustion being nearly homogeneous and fully distributed throughout the combustion chamber [16-21].

This behavior has been referred to as “Flameless” or “Mild” combustion in the literature. Although the peak flame temperature is reduced, the volumetric energy release tends to be higher since the reaction zone is distributed throughout the combustion chamber rather than having a peak near the point of fuel introduction.

Thus, a higher mean temperature can be maintained without exceeding material limits. This is somewhat analogous to the temperature pattern factor in gas turbines.

These furnace experiments did not address how the soot formation mechanism was modified by operating conditions, only methods by which it might be accomplished. Similarly, the present study was an evaluation of practical means by which one or more of the phases of soot formation could be interrupted and thus reduce or eliminate soot formation in the combustion zone of a gas turbine. This was accomplished by introducing cooled combustion products into the combustion air stream as a diluent and preheating the mixture by exhaust heat recuperation. Quantitative information on soot volume fraction and temperature behavior in the combustion zone was obtained using infrared absorbsion gas analysis and two color pyrometry via a spectrometer viewing the combustion flame through a sapphire window. The purpose of this investigation was to develop design tools making it possible to predict and control soot formation and extend the performance capability of gas turbine technology.

CHAPTER 2
EXPERIMENTAL APPARATUS

Test Engine

The experimental combustion rig used for this investigation is the High Pressure Recuperative Turbine Engine, (HPRTE) (Fig. 3-1), developed by the University of Florida Energy & Gasdynamic Systems Laboratory. The engine is augmented with a vapor absorbsion refrigeration system and can be operated with below ambient inlet temperature in what is referred to as the PoWER cycle. It is an independent twin spool, turbo shaft engine with recuperation and the capability to recirculate exhaust gas cooled by chilled water and vapor absorbsion refrigeration. This allows operation in a semi-closed cycle configuration.

An abbreviated description of capabilities and operation of the HPRTE is given here. Detailed construction and capabilities of the HPRTE has been documented by Howell [27]. The core or high pressure section of the HPTRE is a Rover, model 1S-60, 60 hp, turbo shaft engine with a design mass flow rate of 1.33 lbs/s and a pressure ratio of 2.8. This engine was produced in the mid-twentieth century as part of an educational package. It consisted of the Rover engine and a water-brake dynamometer, manufactured by Heenan & Froude, on a common frame with a stand alone fuel delivery system. Mechanical instrumentation provided data for operating performance evaluation. In order to investigate the performance of a pressurized, semi-closed cycle, this package was augmented or upgraded with electronic analog and digital instrumentation to provide more accurate and detailed information on the many components of the system. An additional fuel tank and fuel heat exchanger (FC) has also been added to allow testing of multiple fuels at controlled temperature.

The external flow path has been modified considerably to accommodate a Garret GT 4294-731376-1 turbocharger used in the low pressure section, as well as ducting between various heat exchangers and flow controls, to facilitate recirculation of exhaust gases. Internally, the High Pressure Compressor (HPC) discharge has been changed to redirect flow to a specially constructed recuperator (RECUP). Also, the combustor liner has been modified by welding 18 ga, perforated stainless steel restrictor plates, having straight pattern 0.125" holes on a 0.25" pitch, over the dilution flow passages. There were two reasons for this. The return duct from the RECUP discharged over one of the passages causing an asymmetric temperature distribution at the high pressure turbine (HPT) exit. A single restrictor plate improved this condition. Three more plates were attached over the remaining passages for this research. It was reasoned that higher primary zone flow, resulting from the addition of these plates, would extend the level of recirculation that could be tolerated, without extinguishing the flame due to reduced oxygen concentration.

In operation, the HPT discharges into the RECUP where thermal energy is transferred to the combustor (Bnr) inlet gas stream. Exhaust gas may discharged to the stack, or be diverted to the low pressure turbine (LPT) and/or the recirculation path. Recirculated gas is cooled by three custom heat exchangers in series. The first is the Hot Gas Cooler (HGC), which rejects heat to the Vapor Absorbsion Refrigeration System (VARS) and generates refrigerant vapor for that process. The second, designated as the Warm Gas Cooler (WGC), rejects heat to the local Process Chilled Water (PCW) supply. The third is the VARS evaporator or Cold Gas Cooler (CGC) where additional heat is rejected providing the capability to cool the recirculated gases below ambient temperature.

Recirculated exhaust gas is mixed with fresh air from the Main Air Inlet (MAI) and the Low Pressure Compressor inlet (LPCI) ahead of the HPC inlet. Discharge from the HPC is preheated in the RECUP before entering the Bnr.

The HPRTE may be operated in open cycle, with air supplied through the MAI and LPCI (in high pressure mode) with all exhaust sent to the stack. In semi-closed cycle mode, the recirculation control valve (V_R) is opened, allowing cooled exhaust gas to flow to the mixing junction just up stream of the HPC inlet. This provides a parallel flow path and reduces MAI flow simultaneously. Once V_R is fully opened, the amount of recirculation flow may be increased, within limits, by throttling the MAI valve (V_{MAI}). The mass Recirculation ratio R_m, defined as the mass of recirculated gas flow divided by the mass of ambient air flow was limited to a maximum of ~1.0 when throttling V_{MAI}, after fully opening V_R. The capability to pressurize the core engine was not exploited in this investigation. To do so, with or without recirculation, the boost control valve (V_B) would be throttled to divert exhaust flow to the LPT. As flow through the LPC increases, so does recirculation flow due to the higher supply pressure from the throttled exhaust. Both V_R and V_B must be operated in unison in order to control R_m. As the pressure ratio of the LPC approaches 1.0, VMAI must also be throttled and eventually closed to prevent reverse flow. In the current configuration, the LPC can achieve a maximum pressure ratio of ~ 1.4. The WGC chilled water flow is generally unrestricted when the HPRTE is in operation, however the VARS performance must be matched to heat load as recirculation gas flow changes in order to maintain stable behavior and desired HPC inlet temperature.

Vapor Absorbsion Refrigeration System (Vars)

The VARS is a single effect, continuous operation, ammonia absorbsion refrigeration system, designed, built and installed by Energy Concepts of Annapolis Maryland. The VARS has a design performance of 19 tons refrigeration with a COP of 0.85.

This system removes heat from the recirculated exhaust gases via the ammonia vapor generator and evaporator discussed above as the HGC and CGC respectively. VARS process heat is rejected to the PCW system.

Recuperator And Warm Gas Cooler

The RECUP and WGC heat exchangers were both custom built by Elanco Inc. of Newark Delaware. They are both shell and tube designs with an effectiveness of 0.51 and 0.85 respectively.

Instrumentation

During test runs of the HPRTE data is recorded in two ways, manually and digitally. The manual instruments, including thermometers, manometers and pressure gages, are generally redundant and are used to monitor parameters critical to the research and system health. This makes it possible to be aware of performance changes not being viewed at the moment on the digital system and also as a back-up in the event of data file corruption. The various instruments used for measurement are discussed here.

Optical Measurement

The engine combustion chamber has been modified by the addition of a 0.94 inch view diameter CeramTec sapphire window, P/N 17105-02-W. This allows observation of the flame in the primary combustion zone for video recording and the collection of data with the spectrometer.

All spectrometry hardware was supplied by Ocean Optics of Dunedin Florida, with the exception of one optical fiber assembly. The system is comprised of an optical fiber assembly and a S2000 spectrometer having a 500-770 nm bandwidth, equipped with a 1200 line grating blazed at 750 nm, a coated array, an L2 lens and a 10 μm slit. This unit relies on a 2000 pixel, Charged Coupled Device array (CCD) to measure emission intensity.

During the test program, two optical fiber assemblies were used. The first was damaged and replaced with a P600-5-VIS/NIR assembly. Specifications for the first fiber were not available, however calibration data was taken for both to account for performance differences. The spectral data samples were recorded using a laptop computer running Ocean Optics Spectrasuite software. The emissions from the flame were recorded in arbitrary units of total count, which is measured over a specific period defined as integration time. This time was chosen for each data point to prevent CCD saturation. Saturation occurs at slightly less than 4000 counts and the integration time selected during data acquisition, kept the total at 50-80% of that level to maximize signal to noise ratio. To convert the data to an absolute intensity needed for analysis, calibration curves were generated using an LS-1-CAL tungsten halogen standard.

Gas Analysis

The gas analyzer used in this investigation was a COSA model 1600-IR. The device utilizes infrared absorbsion to measure CO, CO_2 and unburned hydrocarbons as CH_4, and electrochemical cells for NO and O_2. Exhaust gas is sampled just prior to exiting the stack and passes through a ¼" x 18" stainless steel probe and 6' of neoprene hose to a condensate trap at the analyzer inlet. Data is recorded as actual percent or ppm concentration, which is to say neither on a "wet" or "dry" basis. Storage capacity is 50 data points which can be displayed on an LCD screen for transcription to a permanent record. The analyzer was calibrated using certified gas mixtures, of a typical concentration expected to be measured, based on previous testing with the HPRTE.

Load Measurement

Dynamometer

As stated in the engine description, shaft power is absorbed with a Heenan & Froude Dynamometer, equipped with a load cell on the moment arm. Documentation was no longer available for the load cell.

Condensed water

Condensed water was removed from the WGC and CGC using three peristaltic pumps. The pumps discharge into a reservoir supported by a load cell having a 72 pound capacity from Omega Engineering of Stamford CT.

Engine Speed Measurement

Shaft speed was measured at the dynamometer output flange using an ROS-W optical sensor and ACT-3 panel tachometer from Monarch Instruments of Amherst NH.

Flow Measurement

Air and Recirculation

Fresh air flow for the HPC (the LPC was not utilized) was measured using the MAI, original equipment bell mouth, provided with the system. The throat diameter is 4.41 inches. Recirculated exhaust gas flow was measured with a venturi (RCV), P/N V962900-CSI from Flow-Dyne of Fort Worth TX, having a throat diameter of 2.900 inches and a beta ratio of 0.4936. Factory calibration data was used for discharge coefficient calculations.

Fuel

A turbine flow meter, model number MF1/2X70B from Hoffer Flow Controls of Elizabeth City, NC was used to measure fuel flow in gallons per hour. This data was corrected for fuel density variations due to temperature in mass flow calculations.

Temperature Measurement

For the dry bulb temperature (Tdb) and wet bulb temperature (Twb) a psychrometer, catalog number 22010, from Industrial Instruments & Supplies of Southampton, PA was utilized. The percent RH was calculated during a run for each data point using the nomographic calculator supplied with the psychrometer. Combined with local barometric pressure, this information was used to determine the molecular weight, specific gas constant and density of the fresh air supply to the engine.

The remaining temperatures used in analysis were for the MAI, WGC exit/RCV inlet, HPR exit/Bnr inlet and the HPC inlet. All of these were ¼" type J thermocouples, of a length appropriate for each location, from Omega Engineering of Stamford CT.

Pressure Measurement

Pressure data was acquired with a selection of instruments and methods. Ambient barometric pressure was taken from data published by the University of Florida Department of Physics Weather Station on an hourly basis. Both current and archival data can be found at the web site http://www.phys.ufl.edu/weather/. The value used for analysis was an average of measurements taken during the time of day for each test run.

Three styles of manometer were utilized for data recording. The MAI bell mouth was an inclined manometer, with a fluid SG of 1.91. The RCV ΔP was measured with a U-Tube style, having a fluid SG 0.827 and the third was a column manometer with a fluid SG of 1.75 for the Bnr ΔP. For all manometers, fluid specific gravity was corrected for variation with temperature to obtain actual ΔP. The MAI inclined manometer was scaled for direct readout in inches of H_2O, which required the additional step of conversion to inches of fluid before the temperature correction.

Two other instruments were used for pressure data. The Bnr inlet was measured with a Bourdon Tube mechanical gauge and the RCV inlet was measured using a PX138 series pressure transducer from Omega Engineering.

Digital Acquisition System (Daq)

Signal conditioning

National Instruments Corp. of Austin, Texas products were used for signal conditioning and processing software. The hardware chassis was a four slot model SCXI-1000 which could be configured with a selection of modules depending on research needs. In this investigation, an SCXI-1100, two SCXI-1102's and an SCXI-1126 were needed. The SCXI-1100 module was utilized for pressure transducer, load cell and the engine tachometer signals and was equipped with an SCXI-1300, general purpose terminal block. All thermocouples for the engine proper were segregated on one of the SCXI-1102 modules. Thermocouples to monitor VARS performance were on the second SCXI-1102 module. Both were terminated using isothermal, cold junction compensated SCXI-1303 terminal blocks. The SCXI-1126 accepts frequency input from the fuel and PCW flow meters. It was complimented with an SCXI-1327 terminal block for extended voltage threshold level.

Operator interface terminal

Real time and post-processing of the data was accomplished with a Dell Optiplex 150 desk top computer operating at 1200 MHz with 256 Mb of RAM. Real time processing utilized LabVIEW 7.1 software from National Instruments. This version of LabVIEW saved the data in a two column .xls file. A sample of this output is shown in Appendix C. The first column was an index and the second was the data value. In the current configuration, the DAQ is continuously recording 63 parameters with an average scan rate of 1.3 seconds.

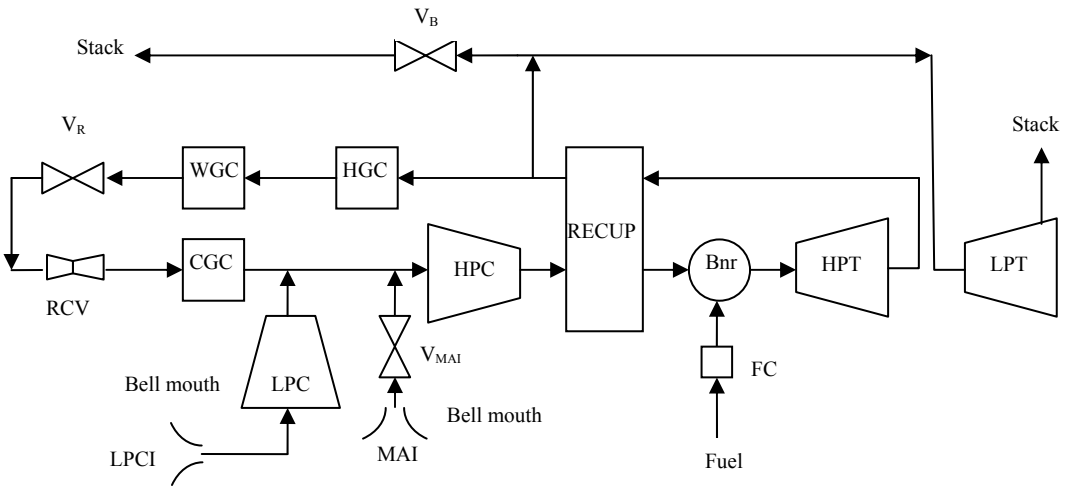

Figure 3-1. Block diagram of HPRTE.

CHAPTER 3
THEORETICAL BASIS FOR DATA ANALYSIS

Two-Color Pyrometry

The application of two-color pyrometry was introduced by Hottel and Broughton who utilized colored glass screens and an optical pyrometer [22]. Since that time there have been many advancements in instrumentation and data processing capability. However, the technique and results of their work are still in common use. The approach allows the calculation of soot temperature and volume fraction and has been utilized by many researchers. One example is the work of Zhao and Ladommatos [23] where the method is presented in detail. A brief description is shown here for convenience.

Soot Temperature Calculation

With a blackbody having an emission intensity $I_{b,\lambda}$ known at its surface, the temperature can be calculated at two wavelengths using Planck's equation for monochromatic emissive power and solving for $T_{\lambda 1}$ and $T_{\lambda 2}$.

$$I_{b,\lambda} = \frac{C_1}{\lambda^5 \left[e^{(C_2/\lambda T_\lambda)} - 1 \right]} \tag{3-1}$$

$C_1 = 3.7418 \times 10^{-16}$ W-m^2 and $C_2 = 1.4388 \times 10^{-2}$ m-K.

In two-color pyrometry it is convenient to define the Apparent Temperature T_a, where $I_{b,\lambda}(T_a) = I_\lambda(T)$. $I_{b,\lambda}(T_a)$ is the emission of a blackbody at T_a, equal to the intensity of a real emitter $I_\lambda(T)$, at the actual temperature T.

Then the monochromatic emissivity is given by Equation 3-2.

$$\varepsilon_\lambda = \frac{I_{b,\lambda}(T_a)}{I_{b,\lambda}(T)} \tag{3-2}$$

Combining 3-1 and 3-2 yields Equation 3-3.

$$\varepsilon_\lambda = \frac{e^{C_2/\lambda T} - 1}{e^{C_2/\lambda T_a} - 1} \tag{3-3}$$

Monochromatic emissivity for a flame is often estimated by the empirical relationship developed by Hottel and Broughton:

$$\varepsilon_\lambda = 1 - e^{\left(-K_{ext} L/\lambda^\theta\right)} \tag{3-4}$$

Equations 3-3 and 3-4 may be combined giving Equation 3-5.

$$K_{ext} L = -\lambda^\theta \ln\left(1 - \frac{e^{C_2/\lambda T} - 1}{e^{C_2/\lambda T_a} - 1}\right) \tag{3-5}$$

Writing 3-5 for two wavelengths and setting both cases equal gives Equation 3-6.

$$\left(1 - \frac{e^{C_2/\lambda_1 T} - 1}{e^{C_2/\lambda_1 T_{a1}} - 1}\right)^{\lambda_1^\theta} = \left(1 - \frac{e^{C_2/\lambda_2 T} - 1}{e^{C_2/\lambda_2 T_{a2}} - 1}\right)^{\lambda_2^\theta} \tag{3-6}$$

where θ is an optical properties parameter typically chosen as 1.39 for soot at visible wavelengths. K is an absorption coefficient proportional to the number density of soot particles and L is the geometric thickness of the flame along the optical path of detection. Equation 6 is solved for $T = T_{soot}$ with T_{a1} and T_{a2} from Equation 3-1. Then Equation 3-5 can be solved for KL.

Soot Volume Fraction

From Rayleigh theory, $K_{ext} = NC_{ext}$ and for an absorbing particle $C_{abs} >> C_{scat}$ so that $C_{ext} \sim C_{abs}$. Therefore K_{ext} can be expressed as in Equation 3-7.

$$NC_{abs} = \int_0^\infty N \frac{\lambda^2}{\pi} \alpha^3 IM\left[\frac{m^2 - 1}{m^2 + 2}\right] P(d)dd = NC_{ext} = K_{ext} \tag{3-7}$$

In Equation 3-7, N = Particle density, C_{ext} = particle extinction cross section, C_{abs} = particle absorption cross section, C_{scat} = particle scattering cross section, K_{ext} = extinction coefficient, $\alpha = \pi d/\lambda$, d = Particle diameter, λ = wavelength, m = n – ik, the complex refractive index and P(d) is a particle size distribution function. The soot volume fraction can be expressed as in Equation 3-8.

$$F_v = \int_0^\infty \frac{N\pi}{6} d^3 P(d) dd \tag{3-8}$$

Solving 7 and 8 for $\int_0^\infty d^3 P(d) dd$, setting both terms equal and solving for F_v gives Equation 3-9.

$$F_v = \frac{K_{ext}}{6\pi IM\left(\frac{m^2 - 1}{m^2 + 2}\right)} \tag{3-9}$$

Having T_{soot} and the optical path length L, the quantity K_{ext} is known from 3-5. From the work of Chang & Charlampopoulos [24], m can be found where;

$$n = 1.811 + 0.1263\ln\lambda + 0.027\ln^2\lambda + 0.0417\ln^3\lambda \tag{3-10}$$
$$k = 0.5821 + 0.1213\ln\lambda + 0.2309\ln^2\lambda - 0.01\ln^3\lambda. \tag{3-11}$$

Use of the Rayleigh approximation requires that the particle size parameter $\alpha = \pi d/\lambda << 1$. Soot particles are generally believed to range in diameter from 10-60 nm [25, 26]. Since measurements are being taken through a window in the mid region of the combustion zone, a diameter of ~ 35nm is assumed. This gives $\alpha \sim 0.21$ which is reasonable, particularly since data is presented as a volume fraction ratio. To implement solution of these relationships, the spectrometer must be calibrated for absolute irradiance with a standard source and the data must be corrected for sensing distance, view port transmission and optical fiber acceptance angle.

For the calculation of K_{ext}, the size of the flame must be assumed or measured to determine the optical path length L.

Gas Composition

Inlet Air Composition

Manual data is taken for the air ambient pressure, P_{amb}, dry bulb temperature, T_{db} and wet bulb temperature, T_{wb}. From this, the percent relative humidity (%RH) is known. A 'dry' total air pressure can then be calculated.

$$P_{dry} = P_{amb} - P_{H2O} \tag{3-12}$$

The partial pressure of H_2O, P_{H2O}, is found from %RH and the H_2O saturation pressure at T_{db}.

$$P_{H2O} = \frac{\%RH}{100} \times P_{sat} \tag{3-13}$$

Assuming dry air is 21% O_2 and 79% N_2, the dry partial pressure of each is calculated based on P_{dry}.

$$P_{O2} = \frac{P_{dry}}{4.76} \tag{3-14}$$

$$P_{N2} = 3.76 P_{O2} \tag{3-15}$$

Dividing the partial Pressures by P_{amb} gives the volume or mole fraction, χ_i, of the inlet air constituents.

$$\chi_{H2O} = \frac{P_{H2O}}{P_{amb}} \tag{3-16}$$

$$\chi_{O2} = \frac{P_{O2}}{P_{amb}} \tag{3-17}$$

$$\chi_{N2} = \frac{P_{N2}}{P_{amb}} \tag{3-18}$$

Given the mole fractions and molecular weights of the constituents, the inlet air molecular weight, MW_{MAI}, can be found.

$$MW_{MAI} = \sum (\chi \times MW)_i \tag{3-19}$$

With this and the universal gas constant, the specific gas constant for the inlet air is known for flow calculations.

$$R_{MAI} = \frac{1545}{MW_{air}} \frac{ft - lbf}{lbm - R} \tag{3-20}$$

Recirculation Gas Composition From Exhaust Analysis

The exhaust gas must be cooled prior to analyzer sampling. Only CH_4, CO, CO_2, NO and O_2 are measured directly. Therefore an unknown quantity of water may condense changing the species concentration. The recirculated gases are cooled further before mixing with the ambient air at the compressor inlet, resulting in additional water condensation. As a result, only the relative concentration of measured species can be known for the recirculation flow from exhaust gas analyzer data. The actual composition of the exhaust gases is calculated through stoichiometry. The reaction equation 3-21 is used.

$$C_x H_y + A(\chi_{O_2} O_2 + \chi_{N_2} N_2 + \chi_{H_2O} H_2O) \rightarrow n_{CH_4} CH_4 + n_{CO} CO + n_{CO_2} CO_2 + n_{NO} NO + n_{O_2} O_2 + n_{H_2O} H_2O + n_{N_2} N_2 \tag{3-21}$$

In Equation 3-21, A is the known molar ambient air inlet flow per mole of fuel, n_i is the exhaust species moles per mole of fuel and χ_i is the inlet air constituent mole fraction.

From exhaust gas analysis, species volume percent and thus the molar ratio, expressed as K_i, is known for the constituents in Equations 3-22 through 3-26.

$$K_1 = n_{CH4} / n_{CO2} \tag{3-22}$$

$$K_2 = n_{CO} / n_{CO2} \tag{3-23}$$

$$K_3 = n_{CO2} / n_{CO2} = 1 \tag{3-24}$$

$$K_4 = n_{NO} / n_{CO2} \tag{3-25}$$

$$K_5 = n_{O2} / n_{CO2} \tag{3-26}$$

The unknown mole ratios are K_6 and K_7.

$$K_6 = n_{H2O} / n_{CO2} \tag{3-27}$$

$$K_7 = n_{N2} / n_{CO2} \tag{3-28}$$

Atomic balances for carbon, hydrogen and nitrogen can be written in terms of n_{CO2}, χ_i and K_i as shown with Equations 3-29, 3-30 and 3-31 respectively. These can be solved for n_{CO2}, K_6 and K_7 given x and y for a known fuel.

$$x = n_{CO2}\left(K_1 + K_2 + K_3\right) \tag{3-29}$$

$$y + 2A\chi_{H2O} = n_{CO2}\left(4K_1 + 2K_6\right) \tag{3-30}$$

$$2A\chi_{N2} = n_{CO2}\left(K_4 + 2K_7\right) \tag{3-31}$$

From test point data, the amount of water condensed from the recirculated exhaust gas is known, as is the fuel flow. Therefore the moles of water condensed per mole of fuel can be calculated. The moles of water in the exhaust gas per mole of fuel are known from K_6.

$$n_{H2O} = n_{CO2} \times K_6 \tag{3-32}$$

The moles of water condensed are subtracted from the moles of water in the exhaust, which then allows calculation of species mole fraction in the recirculated gas.

$$\chi_i = \frac{n_i}{\sum n} \tag{3-33}$$

Given the constituent mole fractions and molecular weights, the recirculated gas molecular weight, MW_{rec} can be found using Equation 3-34.

$$MW_{rec} = \sum\left(\chi \times MW\right)_i \tag{3-34}$$

With this and the universal gas constant, the specific gas constant for recirculation gas, R_{rec} is known for flow calculations.

$$R_{rec} = \frac{1545}{MW_{rec}} \frac{ft - lbf}{lbm - R} \tag{3-35}$$

Oxidizer (Air + Recirculation Mixture)

From the test data, inlet pressure, temperature and Δp are known for the fresh air intake bell mouth and the recirculation gas path venturi. With the specific gas constants, the density can be calculated for both recirculation gas and ambient air intake using the ideal gas law where

$$\rho = P / RT \tag{3-36}.$$

For the fresh air intake bell mouth, Bernoulli's equation can be applied to find the flow velocity at the throat. Assuming constant density and elevation, the equation can be solved for velocity.

$$V = \sqrt{\frac{2g_c}{\rho}\left(P_{amb} - P_{throat}\right)} \tag{3-37}$$

The area of the bell mouth throat is known, therefore ambient air intake mass flow, $\dot{m}_{MAI}$ can be solved for.

$$\dot{m}_{MAI} = \left(\rho V A\right)_{MAI} \tag{3-38}$$

For the recirculation venturi, the flow velocity is slightly more complex due to losses and geometric constraints. These are accounted for with the discharge coefficient, C_d, which is published by the manufacturer along with the physical dimensions of the venturi. Velocity is then calculated.

$$V = C_d \sqrt{\frac{2g_c \Delta P}{\rho\left(1 - \beta^4\right)}} \tag{3-39}$$

Here β is the contraction ratio equal to the throat diameter divided by the entrance diameter. The area of the venturi throat is known, therefore recirculated gas mass flow, $\dot{m}_{rec}$, can be solved for.

$$\dot{m}_{rec} = (\rho V A)_{rec} \tag{3-40}$$

With this information the mass basis recirculation ratio, Rm, is known.

$$R_m = \frac{\dot{m}_{rec}}{\dot{m}_{MAI}} \tag{3-41}$$

Given the MW of the mixtures, a mole basis recirculation ratio, R_n can be calculated.

$$R_n = R_m \frac{MW_{air}}{MW_{rec}} \tag{3-42}$$

The MW for the air/recirculation mixture or oxidizer, can then be found for use in equivalence ratio calculations.

$$MWox = \frac{MW_{air} + R_n MW_{rec}}{1 + R_n} \tag{3-43}$$

Equivalence Ratio Φ

F/A Mass Ratio (Fuel/ Air-Recirculation Mix)

If total oxidizer and fuel mass flow is known, it is necessary to determine the portion of oxidizer flowing to the primary zone in order to calculate Φ. This was investigated in two ways. Test data was available for the gas turbine in an unmodified condition while operating at maximum design power. Assuming a Φ of 1, the primary air mass flow could be calculated by balancing the reaction equation.

$$C_x H_y + A(\ \chi_{O_2} O_2 + \chi_{N_2} N_2\ ) \rightarrow (B)CO_2 + (C)H_2O + (D)N_2 \tag{3-44}$$

The fuel molecular formula was assumed to be that of n-Dodecane, $C_{12}H_{26}$, with a molecular weight, MW, of 170.341. Fuel and air volumetric flow and density were known, allowing the calculation of flow on a mass and molar basis. Solving Equation 3-44 for 'A' the moles of air per mole of fuel and multiplying by the molar flow of fuel gave the flow of air on a mole basis. This was multiplied by the MW of dry air, 28.85, giving air mass flow into the primary zone. Dividing this value by the total inlet flow gave the primary flow fraction.

In the second method all air passages in the combustor liner were measured and the flow areas apportioned to primary or dilution flow according to their location. Both methods agreed within 0.1% indicating that, on average, the passages had similar flow coefficients. The primary flow fraction was 0.241-0.242 of the total.

For this research, orifice plates were welded over the dilution flow passages to change flow distribution. This reduced the total flow area and increased the portion allotted to the primary zone, resulting in a primary flow fraction of 0.428.

The fuel flow $\dot{V}$ was measured volumetrically during the test runs. Fuel mass flow rate, $\dot{m}_{fuel}$, is calculated using fuel density corrected according to temperature with the following relation developed by the American Petroleum Institute:

$$\rho_{fuel} = \left[0.002 \times \left(T_0 - T_{fuel}\right) + 1\right] \times \rho_0 \qquad (3\text{-}45),$$

where T_0 is the temperature at which the baseline density, ρ_0 was measured. Fuel mass flow rate was then found with Equation 3-46.

$$\dot{m}_{fuel} = \left(\rho \dot{V}\right)_{fuel} \qquad (3\text{-}46)$$

The mass flow of the inlet air/recirculation gas mixture, $\dot{m}_{ox}$, is equal to, the sum of $\dot{m}_{MAI}$ and $\dot{m}_{rec}$.

$$\dot{m}_{ox} = \dot{m}_{MAI} + \dot{m}_{rec} \tag{3-47}$$

The fuel- air ratio can then be determined.

$$F/A = \frac{\dot{m}_{fuel}}{0.428 \times \dot{m}_{ox}} \tag{3-48}$$

Stoichiometric F/A Mass Ratio (Fuel/ Air-Recirculation Mix)

Given the molecular weight, species mole fractions and mole recirculation ratio, R_n, of the air mixture with the formula and molecular weight of the fuel, the stoichiometric fuel-oxidizer ratio, F/A_{stoic}, can be found. Beginning with the combustion equation,

$$\begin{aligned} &C_x H_Y + (A)\left[\begin{array}{l}(\chi_{O2}O_2 + \chi_{N2}N_2 + \chi_{H2O}H_2O)_{MAI} + \\ R_n * (\chi_{CH4}CH_4 + \chi_{CO}CO + \chi_{CO2}CO_2 + \chi_{NO}NO + \chi_{O2}O_2 + \chi_{H2O}H_2O)\end{array}\right] \\ &\rightarrow (B)CO_2 + (C)H_2O + (D)N_2 \end{aligned} \tag{3-49}$$

Atomic balances can then be written for carbon, hydrogen and oxygen in Equations 3-50, 3-51 and 3-52 respectively.

$$x + AR_n(\chi_{CH4}CH_4 + \chi_{CO}CO + \chi_{CO2}CO_2)_{rec} = B \tag{3-50}$$

$$y + A(\chi_{H2O}H_2O)_{MAI} + AR_n(4\chi_{CH4}CH_4 + 2\chi_{H2O}H_2O)_{rec} = 2C \tag{3-51}$$

$$A(2\chi_{O2}O_2 + \chi_{H2O}H_2O)_{MAI} + AR_n(\chi_{CO}CO + 2\chi_{CO2}CO_2 + \chi_{NO}NO + 2\chi_{O2}O_2 + \chi_{H2O}H_2O)_{rec} = 2B + C \tag{3-52}$$

Combining these equations allows solving for A, the stoichiometric moles of ambient air per mole of fuel.

$$A = \frac{2x + 1/2y}{(2\chi_{O2}O_2 - \chi_{H2O}H_2O)_{MAI} + R_n(-4\chi_{CH4}CH_4 - \chi_{CO}CO + \chi_{NO}NO + 2\chi_{O2}O_2)_{rec}} \tag{3-53}$$

The stoichiometric moles of oxidizer per mole of fuel is found with Equation 3-54.

$$n_{ox} = A(1 + R_n) \tag{3-54}$$

The stoichiometric fuel-oxidizer ratio is found with Equation 3-55.

$$F/A_{stoic} = \frac{(1) \times MW_{fuel}}{n_{ox} \times MW_{ox}} \tag{3-55}$$

Lastly the equivalence ratio, Φ, can be calculated.

$$\Phi = \frac{F/A_{ACT}}{F/A_{STOIC}} \tag{3-56}$$

CHAPTER 4
EXPERIMENTAL METHOD

The HPRTE is a complex system and optimally requires eight individuals for the tasks of gas analysis, DAQ operation, pressure data recording, temperature recording, VARS operation and data recording, engine room watch data, operator panel data and test run oversight. In order to accomplish the goals of this research, consistent setup, operation and data acquisition was essential. With the exception of test run oversight, specific procedures and/ or data recording sheets were written for each task. In addition, a test plan and required data matrix was necessary for the overall program of testing as well as the individual test runs.

In the case of test run oversight, a senior individual had the responsibility to monitor the health of the test rig and progress of the test. This was accomplished by examining critical data as it was taken by others and evaluating whether the test run needed to be modified in real time. Each individual taking data had the responsibility of making the overseer aware of potential problems developing. Examples of possible action by the overseer would be emergency shutdown due to high turbine inlet temperature transients or reducing data points for the test due to limited available fuel.

Pre-Test Setup

Before the start of the test program, thermocouples, pressure transducers and manometers were checked for calibration. Thermocouples were checked using a boiling water bath and an insulated ice water bath. Pressure transducers and manometers were calibrated using an Ametek portable pressure tester, model CPS-200. Once the test program had begun, the system was set up the evening before each test to minimize delays from minor issues. Engine preparations included filling the fuel tank, checking lubricating oil level, setting flow control valves and verifying battery charge for the starter and ignition systems.

Instrumentation and audio/video systems were checked for proper operation and left on overnight. This was particularly important to stabilize cabinet temperature for the DAQ cold junction temperature compensation. Any systems that could not remain on overnight were activated the morning of the test. This included the gas analyzer, which was battery powered and had internal heaters to maintain a consistent operating temperature for the IR bench. PCW flow to heat exchangers and the VARS were also started in the morning to avoid excessive condensation of ambient water vapor in the laboratory. While the spectrometer was set up the night before the test runs, baseline data was taken the morning of a test, with no light input, to record signal noise. Also, data was recorded with the optical fiber in the test position, to quantify any ambient light circumventing the light shields of the mounting system. Typical set-up procedures are illustrated in Appendix A.

Start-Up, Operation And Shut-Down

After checking communications and instrumentation for proper operation, recording offsets and ambient conditions, the start-up sequence was initiated. This involved verifying the status of a number of electrical panel switches and the fuel system as well as starting condensate pumps. When the electric starter was engaged, no fuel was allowed to flow until a 300 rpm minimum speed was achieved. This greatly reduced fuel build up in the combustion chamber prior to ignition. For the same reason, fuel rate was throttled to approximately 50% of governor demand until the engine was self sustaining at about 2600 rpm. At that point, fuel rate was increased until unrestricted and the engine fuel rate was controlled by the governor at minimum load condition. During warm-up, dynamometer water flow was set at its operating level of 5 gpm, for the remainder of the run.

Once the engine was considered to be running at a stable equilibrium, indicated by a steady recuperator exit temperature, data acquisition could begin or adjustments made to reach the required test point. System shut-down was essentially the reverse of start-up and a typical example of the procedure is shown in Appendix A.

Data Acquisition

Low load data points, defined by the run test plan, were approached by gradually increasing the load on the engine, either with the dynamometer or by throttling V_{MAI}, in the case of high recirculation points. This was necessary because at low loads, insufficient heat is available to the VARS vapor generator and it would remain in standby mode. Under these circumstances, the HPCI temperature could approach design limits. As the load was increased and sufficient heat became available, the VARS would switch into operating mode and cool the recirculated gases flowing to the compressor. Once this occurred, transitions between data points could be accomplished more quickly.

In general, data points were approached by setting a shaft load with the dynamometer and then opening V_R to increase RCV dp. Each data point in the test matrix represented a 0.5" change in dp, at the same load, or a 25% increase in shaft load at the same dp. Recirculation could be increased by opening V_R up to about 4.0" dp across RCV, with both V_R and V_{MAI} fully open. To reach higher recirculation ratios, V_{MAI} would be throttled to increase RCV dp, again in 0.5" increments. Once run point adjustments were made, time was allowed for the recuperator exit temperature to stabilize before taking data. This was augmented with a stable HPCI temperature when the VARS was in operating mode. As stated previously, data was recorded continuously by the DAQ, within scan rate limits, and also manually by personnel on station. At the end of each run, measurements from the gas analyzer were transcribed to a data sheet which was collected along with all manual instrument data sheets.

Data from the spectrometer and DAQ were copied and stored electronically for post-processing. Examples of test plans, test data matrix and the manual data recording sheets are in Appendix B.

CHAPTER 5
DATA REDUCTION AND ANALYSIS

For data reduction, an Excel spreadsheet was created to calculate the results needed for analysis in this investigation. Pertinent data from the manual data sheets, including gas analysis, was transferred directly into the spread sheet while spectral and DAQ data required post-processing. Equations from Chapter 3 and noted here were incorporated into the analysis spreadsheet.

Data Post-Processing

Spectrometer

Spectrometer data was used to calculate soot temperature and volume fraction. To do so, absolute monochromatic emission intensity at each data point had to be known. The recorded data was in arbitrary units of counts requiring conversion to intensity. This was accomplished by taking data from a standard source of known emission intensity over the same integration time used for each test data point. The arbitrary units were equated to the known intensity of the standard provided by the manufacturer and a conversion factor was calculated.

In practice, emission intensity of the source was supplied by the manufacturer for discrete wavelengths at 10, 20, 25 and 50 nm intervals in tabulated form and having units of $\mu W/cm^2/nm$. These values were converted to $W/m^2/m$ for convenience in subsequent calculations. The values were then plotted and a 4^{th} order least squares polynomial curve fit was found giving the absolute intensity of the standard as a function of wavelength. Data was then recorded with the spectrometer, measuring the output of the source. Dividing the known absolute intensity of the source in $W/m^2/m$ by the counts recorded by the spectrometer gave a correction factor for each wavelength in $W/m^2/m/count$.

Multiplying these factors by the test data at each run point gave the measured monochromatic emission intensity at the optical fiber sampling location in $W/m^2/m$. This information was then entered into the data analysis spread sheet.

Data Acquisition System

The LabView software stores recorded data in two columns of an .xls file. The first is an index and the second is the data value. Post-processing was required to transfer the data to a file where all data was segregated into individual columns for each parameter. This was accomplished using a MatLab algorithm "edecimate" developed by Howell [27]. The data was then copied to an Excel spreadsheet, developed by the ECGDL providing data headers, incorporation of offsets, performance calculations and plots of interest.

Along with test parameters, the DAQ recorded the elapsed time (ET), in seconds, since recording was initiated. The ECGDL spread sheet included plots of forty nine different system parameters versus ET. An instability existed, which may be unique to this hardware/software combination, which advanced the recorded time by a number of seconds, typically in the range of 50 to 100 seconds, between two data scans. This ET anomaly did not always occur, but when it did, it was observable in the parameter vs. time plots and could happen more than once in a test run. Plots of the data were examined during post-processing and the ET corrected by subtracting the time advance from all subsequent data recordings and adding the average scan time between the two points where the anomaly occurred. As an example, consider two adjacent data points with a recorded ET of 945.9 sec. and 1019.7 sec. If the average scan time was 1.3 seconds, the ET for the second data point should have been 947.2 seconds. To implement the correction, the ET for the second and all subsequent data points would be reduced by (1019.7-947.2) or 72.5 seconds.

A second issue was signal noise. This was a random occurrence which caused stray data points with vastly different values than adjacent points taken one scan before or after. Again by examining the plots, these points were identified and the values corrected by averaging the adjacent point values.

Data Analysis

The total number of data points taken during this investigation was sixty five, with nine eliminated from consideration due to high or low spectrometer signals and one due to questionable gas analysis. For each of the remaining data points, extensive calculations were needed to ascertain the values pertinent to this research. To accomplish this task an Excel spread sheet was utilized to find the soot volume fraction, soot temperature, gas composition, constants and flow rate, mass and molar recirculation ratio, mass fuel flow, equivalence ratio and adiabatic flame temperature. It was also necessary to develop correlations for water vapor pressure and density as well as bell mouth and venturi performance. In the case of soot data, corrections were necessary due to physical constraints of the sampling method. All data was transcribed directly into the analysis spread sheet from post-processing files or the manual data sheets.

Soot Temperature And Volume Fraction

Soot emission values from the post-processing file had to be corrected to account for three sampling method constraints. These were, signal attenuation by the sapphire window, intensity reduction proportional to the square of the distance from the flame, and a sample area correction due to the acceptance angle of the optical fiber. With these corrections, the soot volume fraction and temperature were calculated according to the methods discussed in chapter 2.

Sapphire window transmission

Baseline spectral data was taken, with an arbitrary light source to determine the degree to which transparency might change during a run.

A transmission fraction was calculated for the window when clean and just after a run at both wavelengths of interest. It was assumed that contaminant buildup on the window during a run would change this fraction.

The transmission fraction was found to be 0.739 at both 525.03 nm and 675.01 nm with a clean window and 0.577 at the end of a typical run. The window was cleaned periodically during the test program in an attempt to maintain a somewhat consistent transmission performance run to run. Visual observations through the window during engine start-up suggested that the majority of contamination build-up occurred at that time. However it is likely that some additional deposition continued throughout the run. There was no method to quantify the build-up rate in real time and so an average value for transmission factor of 0.66 was used for all data. Over the full range of transmission, soot temperature and soot volume fraction ratio varied by +/- 0.25% compared to the average value. The emission intensity was corrected by dividing the post-processed value by the average transmission factor.

Sampling distance

The sampling plane of the optical fiber assembly was located 7.59 inches from the combustor centerline. The sampling distance correction was an inverse square relationship and required an estimate of the distance from the combustor centerline to the flame perimeter. The combustor liner inside diameter was known to be 4.6 inches. The fuel injector had a 90 degree cone angle and the distance from the injector face to the center of the sapphire window was known to be 1.36 inches, resulting in a nominal spray cone diameter of 2.72 inches at that location. The liner shape in the combustion zone approximated a sphere and the flame was considered to be essentially the same shape. No expedient method was available to verify the diameter of the flame so it was taken as the average of the fuel spray cone diameter and the liner inside diameter or 3.66 inches which is also taken to be the optical path length L.

The distance from centerline was one half this dimension or 1.83 inches. The distance correction factor was therefore equal to the square of the ratio 7.59/1.83 or 17.2. The emission intensity was corrected by multiplying the post-processed value by the correction factor.

Optical fiber acceptance angle

The acceptance angle represents the field of view of an optical fiber. A light ray approaching the fiber at an angle greater than the acceptance angle will not be propagated. When calibrating for absolute emission intensity, the full field of view of the fiber is exposed to the standard light source. When sampling an emission source through an aperture that is smaller than the field of view, a correction must be made for this reduction in area. The sampling geometry for the spectral data was such that the sapphire window functioned as an aperture. The fiber assembly used in this investigation had an acceptance angle of 24.8 degrees, giving a conical field of view with a base diameter of 1.62 inches at the plane of the window. The view diameter of the window however is 0.94 inches. These diameters were projected onto spheres intersecting the plane of the window and the surface areas calculated as $2\pi rh$. The ratio of these areas was 2.088/0.704 or 2.966. The emission intensity was corrected by multiplying the post-processed value by this ratio. The geometry of interest for distance and acceptance angle correction is illustrated in Figure 5-1.

With the corrected emission intensity at the perimeter of the flame, Equation 3-1 was solved for T_{a1} and T_{a2}. Using Equation 3-6, T_{soot} was found iteratively with the solver utility in Excel by setting the difference between the left and right side of Equation 3-6 equal to zero. $K_{ext}L$ was then calculated with Equation 3-5 and the soot volume fraction, F_v, from Equation 3-9. For all runs, the maximum F_v, defined as F_{vmax}, occurred at minimum load with no recirculation of exhaust gases.

The soot volume fraction, at any data point, was divided by F_{vmax} to establish a non-dimensional soot volume fraction ratio, F_{vR}, for investigating correlations between soot production and other parameters.

Gas Analysis

Exhaust gas analysis produced the information needed to calculate the constituent mole fractions, specific gas constant, molecular weight, density and mass flow rate of the recirculated gases. Combined with similar calculations for the ambient air intake, the composition of the mixture at the HPCI was known as well as the recirculation ratio on both a mass and mole basis. With this information, it was possible to determine the equivalence ratio and the adiabatic flame temperature.

Ambient air, T_{db}, %RH and P_{amb} were taken from the manual data and entered into the analysis spread sheet. Equations 3-12 through 3-20 and 3-36, 3-37 and 3-38 were applied giving the properties of interest and the ambient air intake flow. For expedience, a correlation for P_{sat} of H_2O versus T_{db}, having an accuracy of 0.19%, was developed from tabulated data [28] where

$$P_{sat} = 2.023E-11(T_{db})^5 + 1.089E-9(T_{db})^4 + 2.262E-7(T_{db})^3 + 3.546E-5(T_{db})^2 + 1.917E-4(T_{db}) + 3.820E-2 \quad (5\text{-}1)$$

Exhaust gas sample data for the percent by volume for CH_4, CO, CO_2, NO (ppm) and O_2 was entered into the spread sheet as input for Equations 3-22 through 3-35. This provided the properties of interest to calculate the recirculation gas flow using Equations 3-36, 3-39 and 3-40. Also for expedience, a correlation was developed for C_d versus $\Delta P/P$, having an accuracy of 0.032%, from the recirculation venturi manufacturers calibration data where

$$C_d = -2.187E+9\left(\frac{\Delta P}{P}\right)^6 + 1.774E+8\left(\frac{\Delta P}{P}\right)^5 - 5.772E+6\left(\frac{\Delta P}{P}\right)^4 + 9.689E+4\left(\frac{\Delta P}{P}\right)^{3^2} - 9.007E+2\left(\frac{\Delta P}{P}\right) + 4.754\left(\frac{\Delta P}{P}\right) + 9.744E-1 \quad (5\text{-}2)$$

Lastly, R_m, R_n and MW_{ox} were found utilizing Equations 3-41, 3-42 and 3-43.

Equivalence Ratio

The fuel was assumed to be comparable to n-Dodecane having a molecular formula of $C_{12}H_{26}$ and a molecular weight of 170.341. The baseline density ρ_0, was measured as 52.702 lb/ft^3 at a baseline temperature T_0, of 74^o F.

Volumetric fuel flow data, from the DAQ, was utilized along with Equations 3-45 and 3-46 to calculate $\dot{m}_{fuel}$. Combined with the results from gas analysis and Equations 3-47 and 3-48, the nominal F/A ratio was found.

Given x and y from the fuel formula, air and recirculation gas mole fractions and R_n from gas analysis, F/A_{stoic} was found from Equations 3-53, 3-54 and 3-55. Equivalence ratio Φ could then be calculated with Equation 3-56.

Adiabatic Flame Temperature

From gas analysis, the mass flow rate, constituent mole fractions and molecular weight of the air and recirculation gas were known. Similarly, the mass flow and molecular weight of the fuel were known. Given the molecular weight of the air and recirculation constituents and the primary flow fraction, the gas constituent flow on a molar basis, into the primary zone, $\dot{n}_i$, was calculated.

$$\dot{n}_i = .428\chi_i \frac{\dot{m}_i}{MW} \tag{5-3}$$

The mole basis fuel flow was calculated in the same way.

$$\dot{n}_{fuel} = \frac{\dot{m}_{fuel}}{MW_{fuel}} \tag{5-4}$$

The initial temperature and pressure of the reactants were needed to calculate the adiabatic flame temperature. The inlet temperature was taken at the HPRE duct just upstream of the combustor. The combustion pressure was not measured directly.The gage pressure P_{HPRE} was known at the same location as the HPRE temperature. Also known was the pressure drop across the combustor liner, ΔP_{BNR}, and P_{amb}. The absolute combustion pressure, P_{comb}, was therefore equal to

$$P_{comb} = P_{HPRE} - \Delta P_{BNR} + P_{amb} \tag{5-61}$$

With the quantity of all reactants entering the combustion zone known along with initial conditions, the adiabatic flame temperature was found using NASA CEA2 software. This program was available from the NASA web site http://www.grc.nasa.gov/WWW/CEAWeb/. The software has a Windows compatible graphical user interface for convenient data entry. It should be noted that the units of input and output data for the software are a mixture of SI and English.

The inputs required for CEA2 in this analysis were pressure, temperature, moles and chemical formula of the reactants. The fuel enthalpy of formation was also needed and was taken to be -292.162 kJ/gmole. The results were transcribed to the analysis spreadsheet for subsequent examination and plotting.

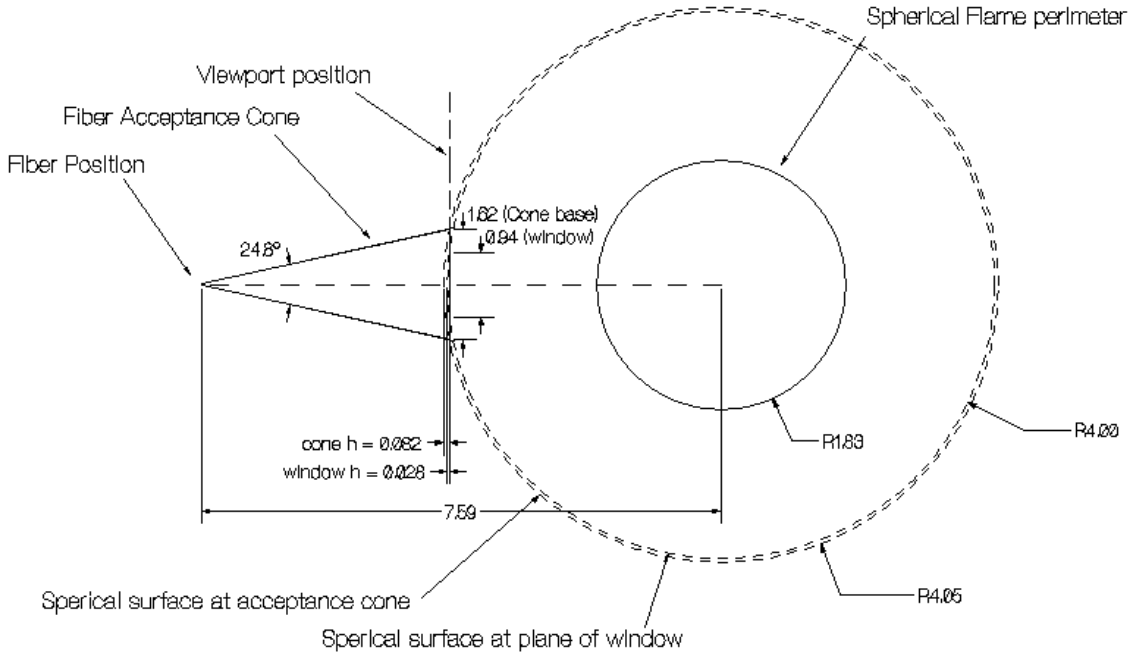

Figure 5-1. Geometry and dimensions used to correct emission intensity for sampling distance and optical fiber acceptance angle

CHAPTER 6
RESULTS AND DISCUSSION

The test program acquired data at fifty-five steady-state operating points, taken over nine test runs. Mass basis recirculation ratio ranged from 0 to 1.04, equivalence ratio ranged from 0.42 to 0.64, reactant oxygen concentration ranged from 15.4 to 20.7% and combustion pressure ranged from 33.1 to 36.1 psia. Soot Temperature and soot volume fraction ratio, calculated from spectral measurements, ranged from 3100 to 3720 Rankine and 0.01 to 1.00 respectively. The mean molecular weight of the inlet air, recirculated gas and exhaust gas was found to be 28.60 +/- 0.11, 28.58 +/- 0.24 and 28.59 +/- 0.12 respectively. The goal of this investigation was to determine what relationship existed between soot volume fraction and oxygen concentration, equivalence ratio, Φ, combustion pressure and local temperature, these being the primary variables in the combustion zone. All data analysis is based on a control volume about the combustor. With the combustor as the control volume in a semi-closed cycle gas turbine, defining an operating point must include combustor inlet Φ and O_2 percent for a constant speed machine. This is because each is a function of recirculation ratio and load. As recirculation ratio is increased and load is held constant, Φ will increase and O_2 percent will be reduced owing to the greater portion of exhaust gas in the reactants. The same is true when load is increased and recirculation ratio is held constant since at higher load the concentration of oxygen in the recirculated exhaust is reduced. At a specific load and recirculation ratio, there will be a particular pair of values for these parameters.

It was assumed that soot formation would be affected by oxygen concentration combustion pressure and local temperature according to results by other investigators. Further, it seemed reasonable that the amount of fuel in the combustion zone should also have a direct impact on F_v and that would be reflected by a Φ, O_2 percent pair.

Because of this, the impact of soot temperature, T_{soot}, and adiabatic flame temperature, T_{ad}, were both examined as a surrogate for local temperature. As previously stated, the maximum soot volume fraction, F_v was observed at minimum load and no recirculation of exhaust gas diluent. With a small increase in load, F_v quickly reduced to a minimum and then increased with load. This behavior was attributed to reduced fuel demand caused by the addition of a recuperator. The engine fuel injector was not modified from the original design and the lower fuel demand resulted in less than optimal fuel atomization. All soot volume fraction data presented was normalized with this maximum to give the soot volume fraction ratio, F_{vR}, used for plotting and correlation. In all cases F_v and F_{vR} followed the same relationships.

Combustion Zone Parameters

In Figure 6-1 F_{vR} was plotted against combustor inlet O_2%, accompanied with a least squares fit power curve trend line, and a relationship was clear. However, the high level of scatter suggested the impact of other parameters was significant.

Figure 6-2 and 6-3 reflect the behavior of emissivity as oxygen concentration changes. The emissivity is calculated using Equation 3-4 and all quantities are constant at each wavelength except K_{ext}. As K_{ext} becomes small so does emissivity. Note the similarity to Figure 1. This is to be expected since as soot volume fraction diminishes so does the number of particles or their absorbsion cross section or both. Thus K_{ext}, equal to NC_{abs}, would be reduced.

Figure 6-4 illustrates a similar, although mirrored relationship between F_{vR} and combustor inlet Φ. Again, a least squares fit power curve trend line is shown for comparison.

A plot of F_{vR} vs. Primary zone absolute pressure, P_{comb}, is presented in Figure 6-5. No trend was apparent but the pressure changes were very small, between 33.1 and 36.1 psia, due to the near constant speed, and therefore pressure ratio, of the machine. The main contribution to pressure change was from MAI throttling to increase exhaust recirculation flow.

It was of interest whether fuel atomization might have an obvious impact on the soot volume fraction ratio versus oxygen concentration relationship. Figure 6-6 shows data for which the fuel mass flow rate was between 91 and 98% of maximum. As can be seen, data points with nearly the same oxygen concentration can differ by a factor of almost 5 in their soot volume fraction ratios and there is no obvious trend. This suggests that, at least at high fuel flow rate conditions, fuel atomization was not a significant driver of soot formation. Having said this, it should be borne in mind that in this test engine, fuel flow, air flow and therefore equivalence ratio cannot be independently controlled. As oxygen percent decreases, Φ is increasing. The ability to hold Φ constant might present different results.

Figures 6-7 and 6-8, plot FvR vs. T_{soot} calculated from spectral measurements, or T_{ad} calculated with NASA CEA2. As in Figure 6-6, no direct relationship is apparent. For a specific machine and fuel, T_{soot} was expected to correlate with O_2 percent, P_{comb} and Φ. In Figures 6-9, 6-10 and 6-11, T_{soot} was plotted vs. these parameters. Again no obvious relationship was discernable.

Adiabatic flame temperature was examined in the same way in Figures 6-12 through 6-14. Results demonstrated the same lack of a distinct correlation. It was of interest whether a relationship existed between T_{soot} and T_{ad}. A temperature ratio was calculated as $T_{ratio} = T_{soot}/T_{ad}$. Tratio was plotted vs. O_2 percent, P_{comb} and Φ. In Figures 6-15 through 6-17, T_{ratio} was generally increasing with O_2 percent and P_{comb} while decreasing with Φ. A linear least squares trend line was shown to illustrate this behavior. Over all, the data T_{soot} was 3410 +/- 310 degrees R with and average of 3450 degrees R. T_{ad} was 2900 +/- 170 degrees R with an average of 2930 degrees R and T_{ratio} was 1.17 +/- 0.13 with an average of 1.18.

A multi-variant least squares exponential regression was performed for T_{soot} and T_{ad} on percent O2 and P_{comb} with and without Φ to determine the impact of each parameter and develop a correlation. The regression equation was the form of Equation 6-1.

$$Y = b * M_1^{X_1} * M_2^{X_2} * \cdots \quad (6\text{-}1)$$

Table 6-1 shows the resulting equation coefficients for each case.

In Figure 6-18 both the regression and data values of T_{soot} vs. O_2 percent were plotted with linear trend lines for comparison. The trends were nearly identical although the data values displayed much greater scatter. Both regression equations had essentially the same average error. With Φ included in the regression, the average error was 0.046%, without Φ the average error was 0.047% demonstrating a good correlation and also that Φ was not important to T_{soot} within the range of testing.

The same comparison was examined in Figure 6-19 for T_{ad}. Here the impact of Φ was clearly evident. When Φ was included in the regression the values followed data much more closely having an average error of 0.002%. When Φ was not included the results were comparable to the T_{soot} correlations with an average error of 0.045%

Regression Analysis Of F_{vr} Based On Combustion Zone Parameters

An exponential regression was carried out on F_{vR} using Φ, O_2%, P_{comb} and Tsoot or Tad as variables. The results of the T_{soot} regression suggested the model could be simplified, for the HPRTE at least, and T_{soot} was considered by proxy through O_2% and P_{comb}. However, a better fit to the data was achieved when T_{soot} was included in the regression directly and 6-1 implemented with four parameters for F_{vR}. Values for the coefficients are presented in Table 6-2.

The results of the analysis are shown in Figures 6-20 and 6-21 where actual F_{vR} and the regression F_{vR} was plotted vs. % O_2 in the reactant gas.

Input for the regression equation was the values for Φ, O_2%, P_{comb} and T_{soot} or T_{ad} measured or calculated from test data. Trend lines for both data and regression values of F_{vR} are a least squares fit for a power curve. While the T_{ad} correlation displayed a better curve fit, the average error was found to be 48% compared to 20% when T_{soot} was used for the temperature parameter.

In Figures 6-22 through 6-25 the pressure effects predicted by the regression were examined with Φ values of 0.4 and 0.65 and P_{comb} varied from 30 to 40 psia. Temperatures were calculated as, $T_{soot} = f(O_2\%, P_{comb})$ and Tad = f (O_2%, P_{comb}, Φ) for the calculation of F_{vR}. Here the regression reflected an inverse power relationship between F_{vR} and P_{comb} at any Φ or O_2% with the pressure exponent ranging from -1.93 to -4.70. Other investigations, [12-15], involving methane or ethylene, have shown a direct scaling with pressure and exponents of 1.2 at high pressure (290-580 psia) to 2 at low pressure (72-290 psia). Note that when T_{soot} is used as the temperature parameter, the pressure exponent is not a function of Φ.

Noting the trends illustrated in Figures 6-1, 6-4 and 6-22 through 25, two extreme synthetic data sets were calculated for F_{vR} using T_{soot} and T_{ad} to determine if the run points from the test data would fall between the minimum and maximum curves predicted by the regression. Using values from test data for minimum P_{comb} = 33.1 psia and Φ = 0.42, a maximum F_{vR} set was generated. In the same way using maximum P_{comb} = 36.1 psia and Φ = 0.64, a minimum F_{vR} set was generated. In Figure 6-26 and 6-27 these data sets are plotted along with the actual test data. The synthetic curves using Tsoot for the temperature parameter follow the run data quite well with 70% of the test points inside the bounded area and the remaining points following the curves closely. For the regression using Tad, only 50% of the data points plotted inside the boundary.

A similar Min/Max case was developed for FvR as a function of Φ. For the minimum case, O_2% was 15.4%, and P_{comb} was 36.1 psia. For the maximum case, O_2% was 20.7%, and P_{comb} was 33.1 psia. The results were plotted in Figure 6-28 and 6-29 along with the test data. While a few test points lie outside the bracketed region, they remain very near to the predicted limits when T_{soot} was used as the temperature parameter in Figure 6-28. In Figure 6-29 the regression is less convincing with more data points lying farther outside the curves.

The regression equation requires values for Φ, O_2%, P_{comb} and T to calculate F_{vR}. From the trends illustrated in Figures 6-20, 6-21 and 6-26 through 6-29, the Tsoot was selected as the more relevant temperature parameter compared to T_{ad}. It was desired to calculate synthetic values for F_{vR} and examine the predicted soot formation behavior as a function of Φ and O_2% only. To accomplish this, appropriate values for P_{comb} and temperature were needed that were comparable to actual run conditions. Examining all the test points, the average P_{comb} was found to be 34.8 psia. A constant value of 35 psia was therefore selected for P_{comb}. To obtain values for temperature, Equation 6-1 was used with the coefficients in Table 6-1, along with the chosen values for O_2% and P_{comb} as input variables for T_{soot}. Synthetic F_{vR} data was then generated with Φ ranging from 0.40 to 0.65, O_2% ranging from 15 to 21%, P_{comb} = 35 psia and T_{soot} = f (O_2%, P_{comb}). The results were plotted in Figure 6-30. The regression equation predicted that reducing O_2% would diminish F_{vR} at any equivalence ratio. However, this effect was much less pronounced at high Φ where F_{vR} approaches a linear relationship with O_2%.

While the prediction of lower F_{vR} with increasing Φ seemed counterintuitive, only four of the data points were at zero recirculation. Therefore, the test points were heavily weighted with reduced O_2% operating conditions.

As stated previously, combustor inlet Φ is a function of both load and O_2%. A reduction in O_2% increases Φ without an increase in load and diminishes F_{vR}. This behavior, illustrated in Figure 6-2 was reflected by the regression.

That F_{vR} would continue to increase with O_2% was also predicted. Obviously this investigation was limited to the ambient O_2% and soot formation behavior as lean blowout conditions are approached may not follow this model with certainty.

Similarly the regression suggests a minimum for F_{vR} at low O_2%. However, at any load, decreasing O_2% would drive Φ toward 1.0 and beyond. Soot formation behavior would be expected to change under those conditions. With a maximum Φ of 0.64 for this investigation, extrapolation of the model would not be useful.

In Figures 6-31 and 6-32 the behavior of the T_{soot} regression was examined by holding P_{comb} = 35 psia in 6-31 and O_2% = 18% in 6-32. The independent effects can be seen as a linear relationship for T_{soot} vs. O_2% and T_{soot} vs. P_{comb} respectively.

Measurement Error Analysis

The method of two-color pyrometry has been employed to study soot since the early 1900s. The usefulness of the method depends on knowing the optical properties of soot particles such as θ, the optical properties parameter, and the complex refractive index. Values found by different researchers vary widely and can affect results for soot temperature by +/- 25 K and results for soot volume fraction, F_v, by 20%-75% as demonstrated by di Stasio and Massoli [29]. The primary source of variability in the spectral data recorded in this research was related to the measured intensity correction due to the assumed optical fiber position, flame diameter and sapphire window transmission. In the case of T_{soot} this would affect results by an additional +/- 3 K. Regarding soot volume fraction ratio, F_{vR}, the uncertainty was increased by +/- 0.02.

It is important to note that all soot volume fraction calculations utilized the same assumptions for the optical properties and the physical configuration for data acquisition. Therefore the error quoted above for soot volume fraction, F_v, would largely cancel out when expressing the results as the soot volume fraction ratio F_{vR}.

The quantities percent oxygen, equivalence ratio and combustion pressure were calculated using data from the non-optical test facility instrumentation. The value of the combustion pressure, P_{comb}, is dependent on measurements from a Bourdon gage and two manometers. Since the gage performance is the overwhelming contributor to the inaccuracy of the calculated value, the uncertainty of the P_{comb} calculation is considered to be on the order of +/- 0.8 psi, using a 100 psi gage rated with an accuracy of +/- 0.75% of full scale. In the same way, the overwhelming contributor to the inaccuracy of percent oxygen and equivalence ratio calculations was the gas analyzer. All species measurements had an accuracy of either +/- 5% or much less than 1%. A simple root of the sum of the squares operation was performed using the accuracy for each gas constituent used in the calculations. The result was an uncertainty value of +/- 7% for both Φ and O_2%. These results are summarized in Table 6-3. The method of calculation can be found in Appendix C.

Table 6-1. Regression equation coefficients for soot temperature and adiabatic flame temperature

Parameter	-	X1 = % O_2	X2 = P_{comb}	X3 = Φ
Y	b	M_1	M_2	M_3
T_{soot}	2585.549	1.003	1.007	-
T_{soot}	3010.405	1.000	1.006	0.893
T_{ad}	3992.361	1.006	0.988	-
T_{ad}	1004.149	1.034	0.998	2.795

Table 6-2. Regression equation coefficients for soot volume fraction ratio

Parameter	-	X1 = % O_2	X2 = P_{comb}	X3 = Φ	X4 = T
Y	b	M_1	M_2	M_3	M4
$F_{vR} = f(T_{soot})$	1.464E+07	1.825	1.102	1.112E-04	9.919E-01
$F_{vR} = f(T_{ad})$	1.302E-06	7.111E+01	7.513E-01	4.948E+45	9.635E-01

Table 6-3. Data uncertainty for major parameters

Parameter	Uncertainty
F_{vR}	+/- 0.02
T_{soot}	+/- 28 K
P_{comb}	+/- 0.8 psi
Φ	+/- 7% of value
O_2%	+/- 7% of value

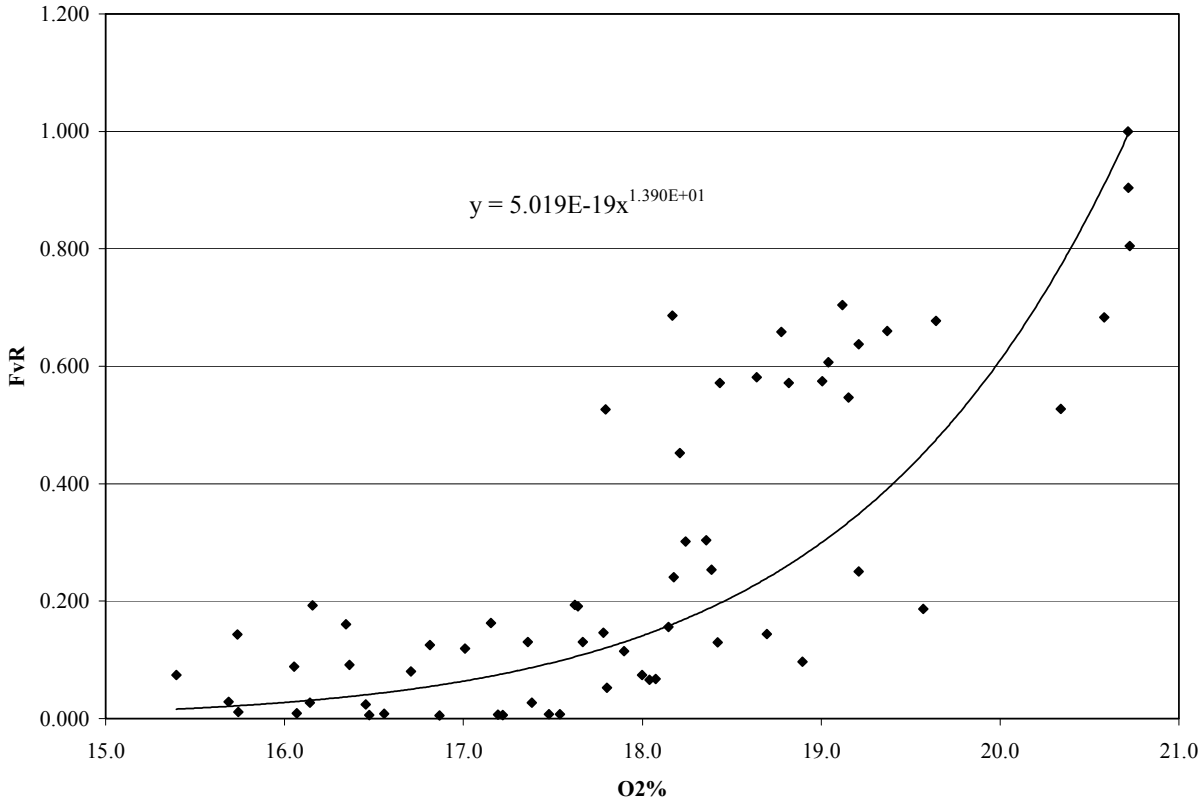

Figure 6-1. Soot volume fraction ratio vs. combustor inlet O_2%

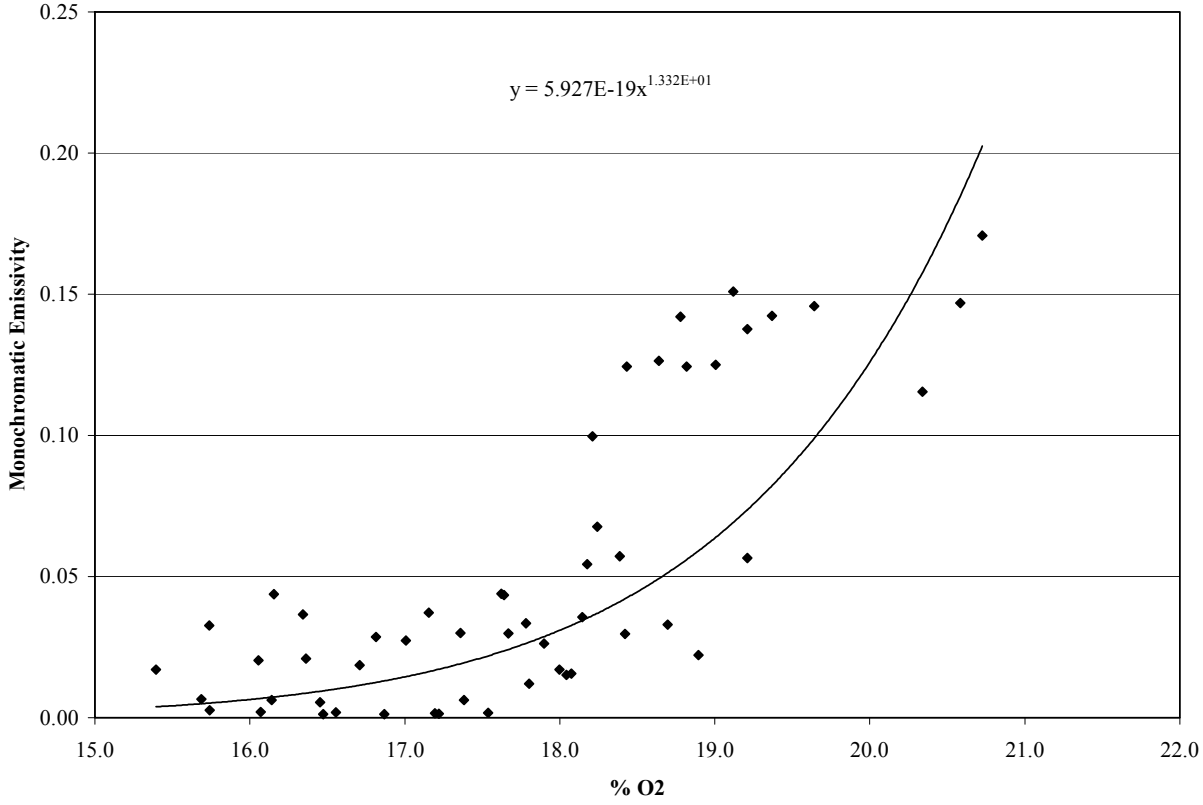

Figure 6-2. Emissivity at 525.03 nm vs. % O_2

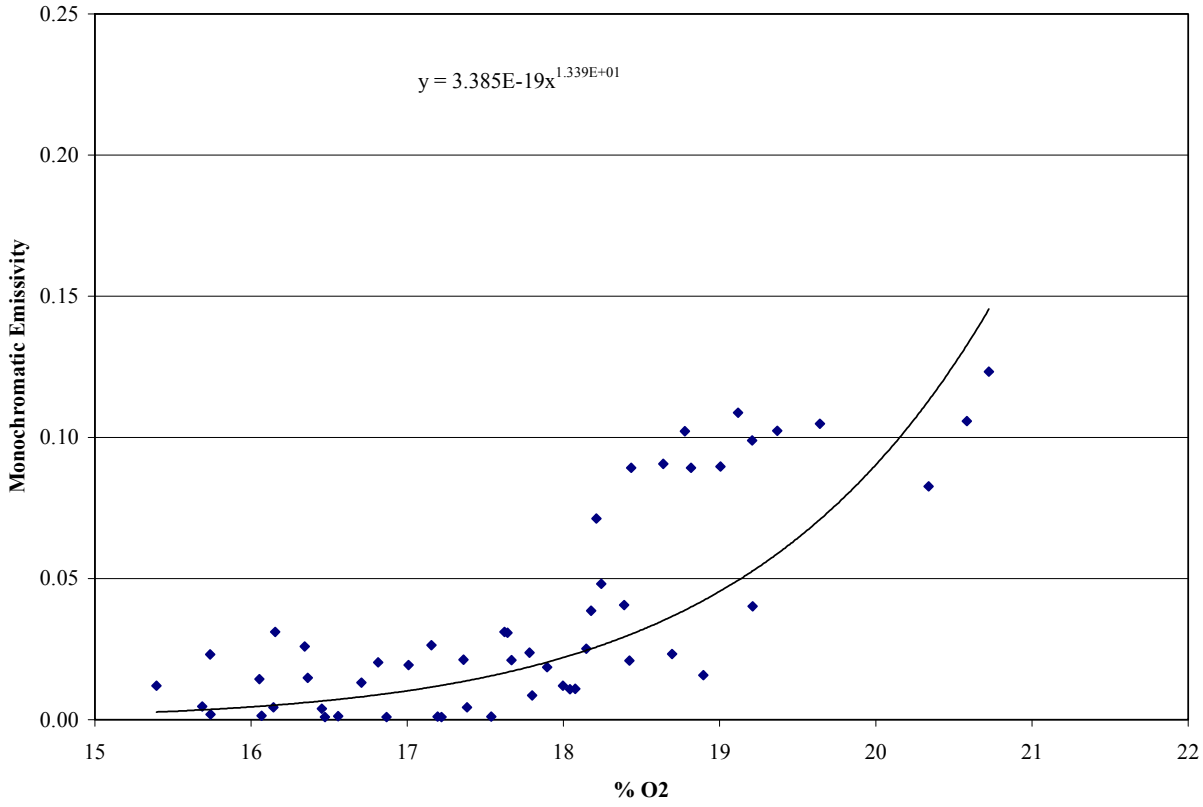

Figure 6-3. Emissivity at 675.01 nm vs. % O_2

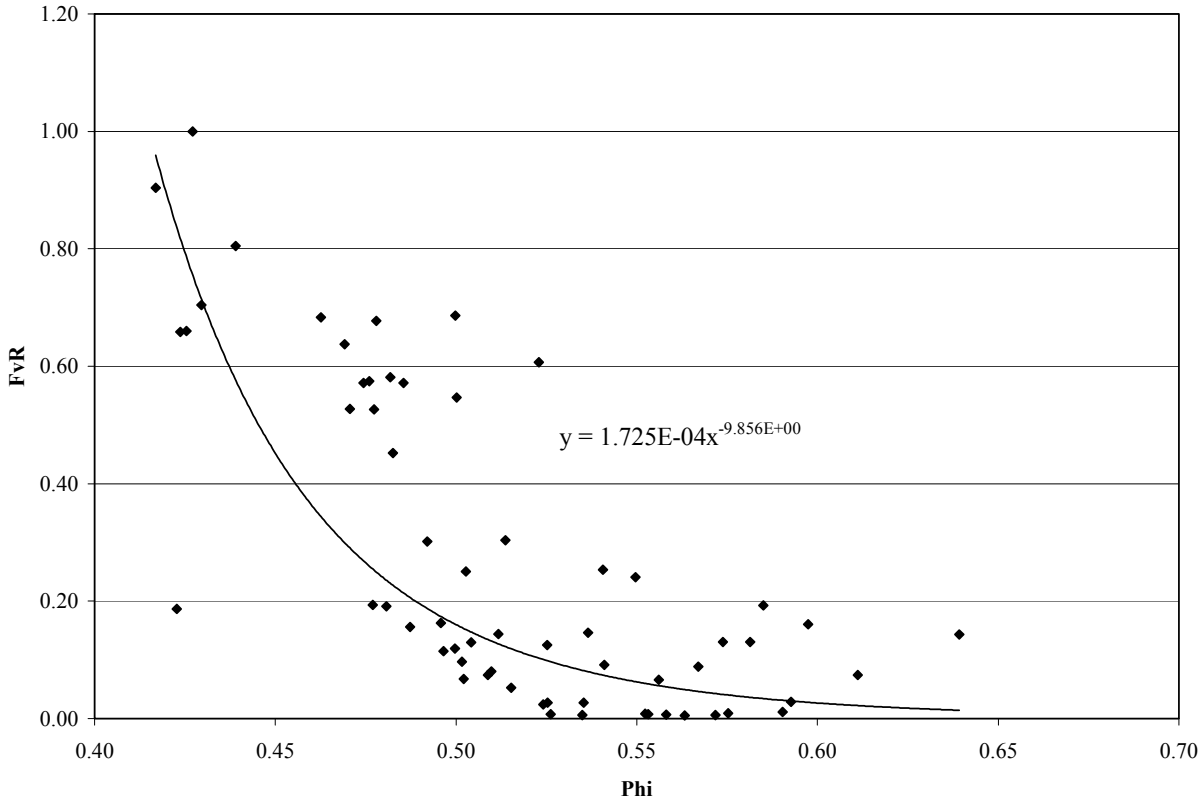

Figure 6-4. Soot volume fraction ratio vs. combustor inlet equivalence ratio

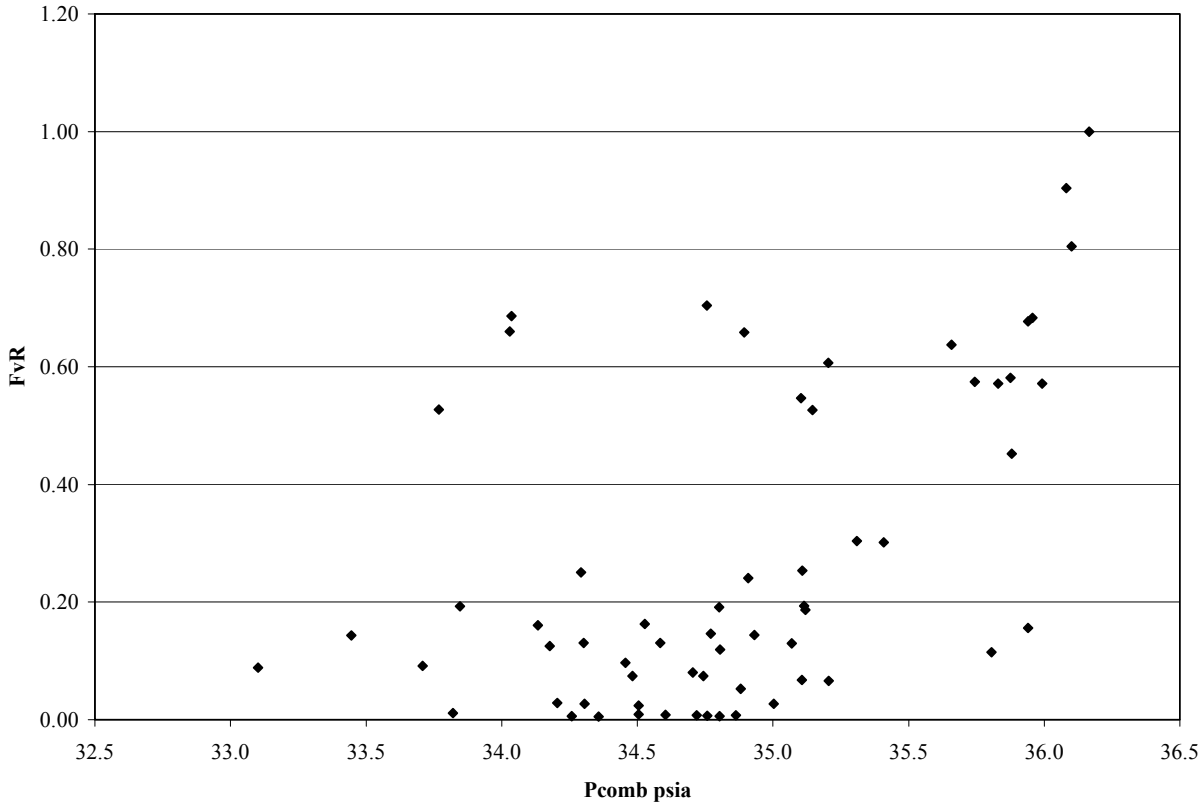

Figure 6-5. Soot volume fraction ratio vs. combustion pressure

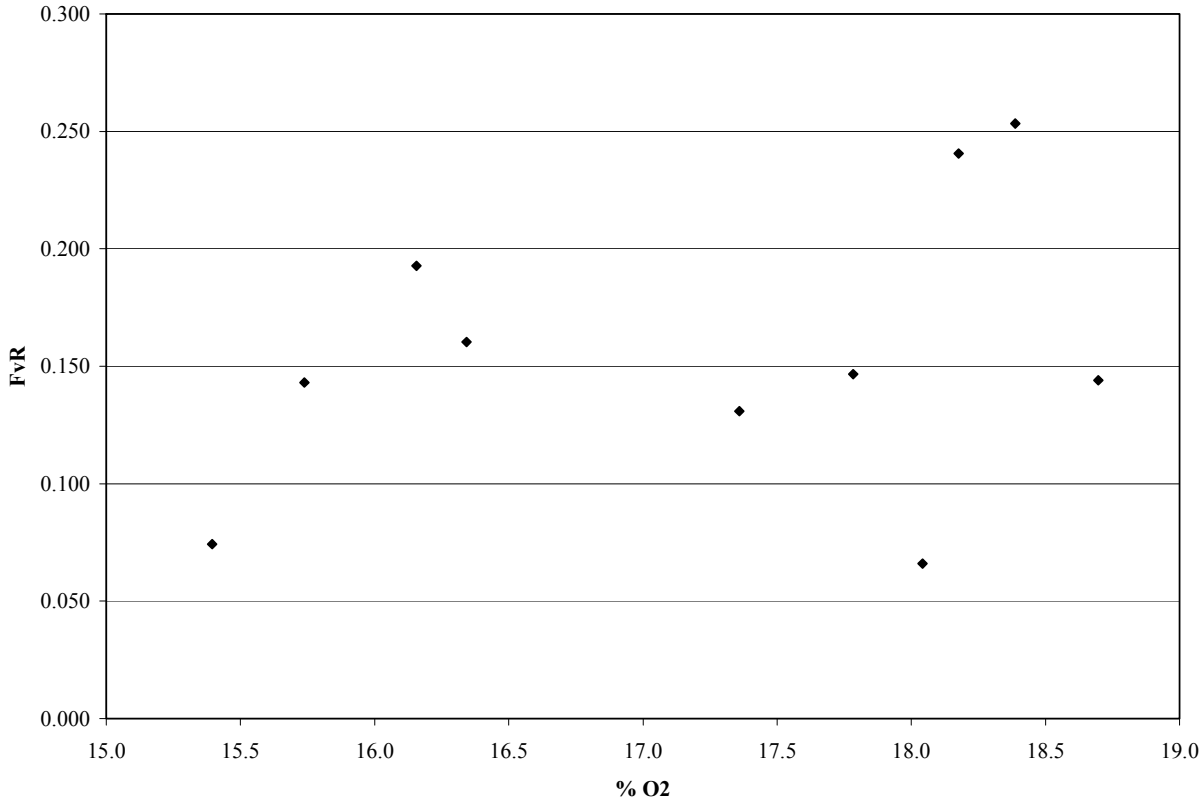

Figure 6-6. Soot volume fraction ratio vs. oxygen concentration at high fuel flow

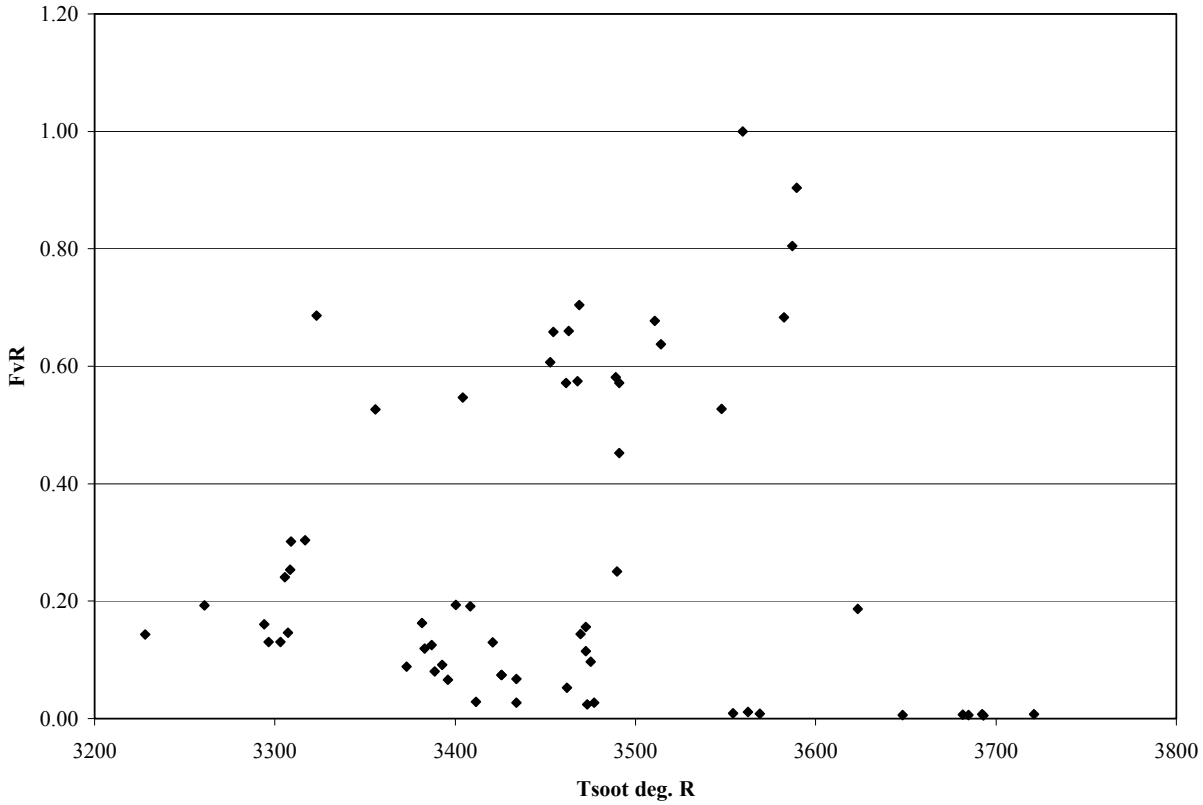

Figure 6-7. Soot volume fraction ratio vs. soot temperature

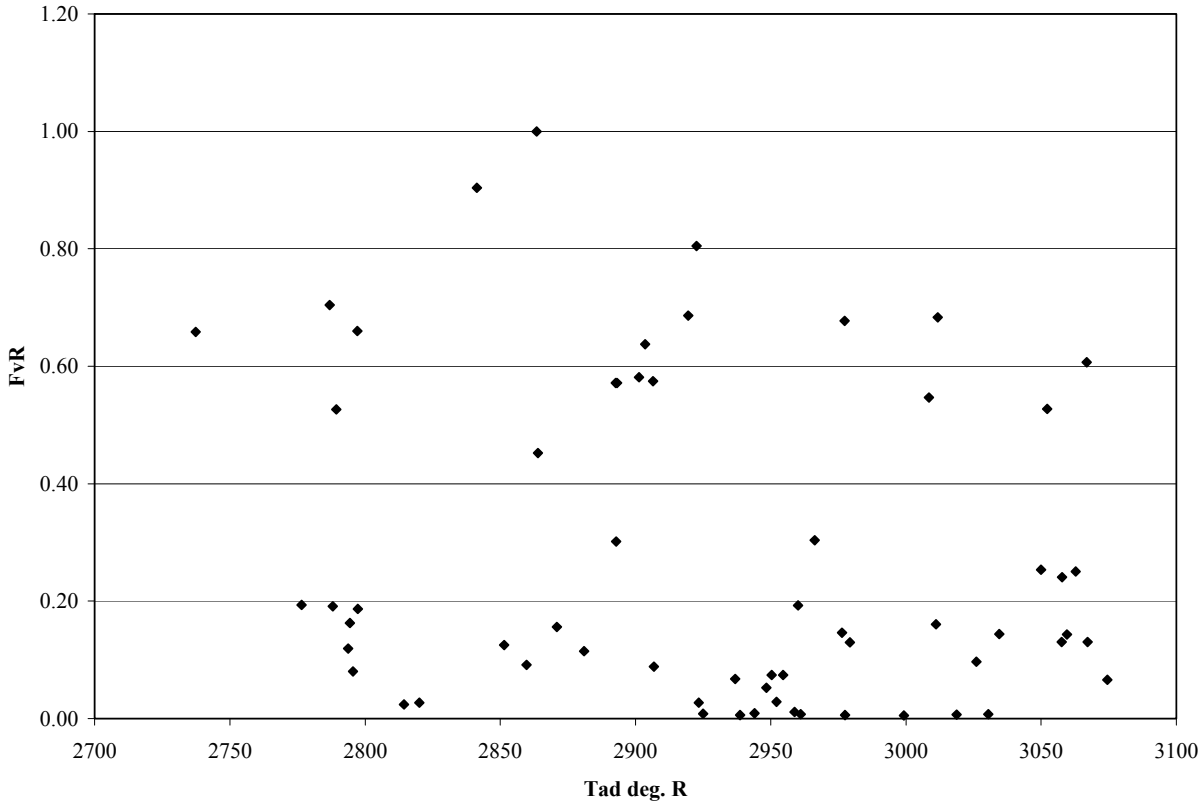

Figure 6-8. Soot volume fraction ratio vs. adiabatic flame temperature

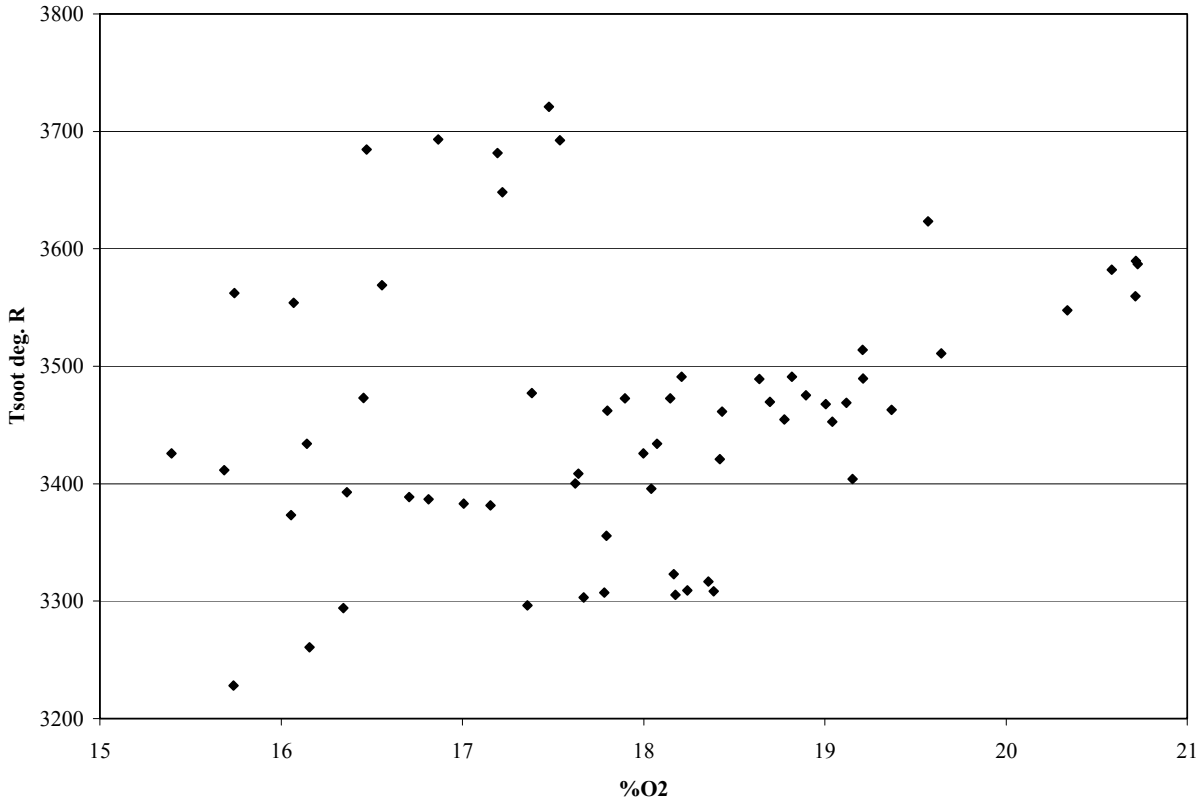

Figure 6-9. Soot temperature vs. combustor inlet percent oxygen

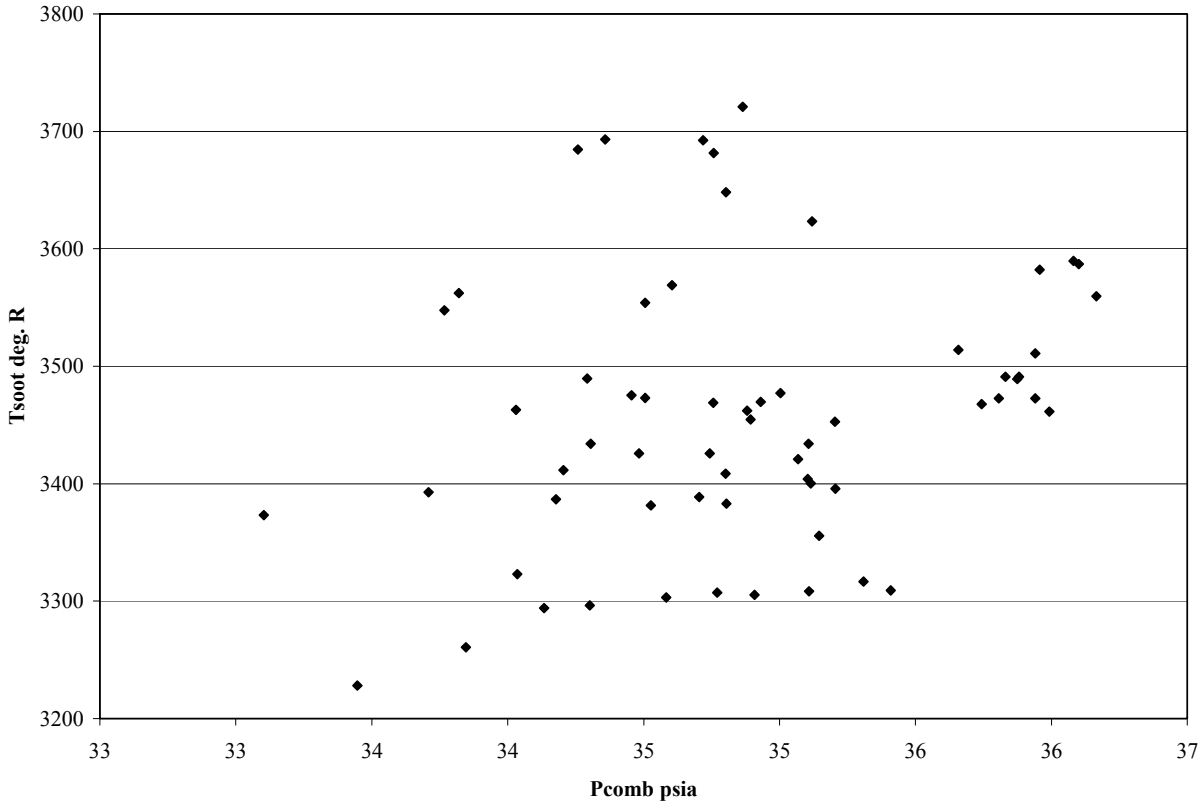

Figure 6-10. Soot temperature vs. absolute combustion pressure

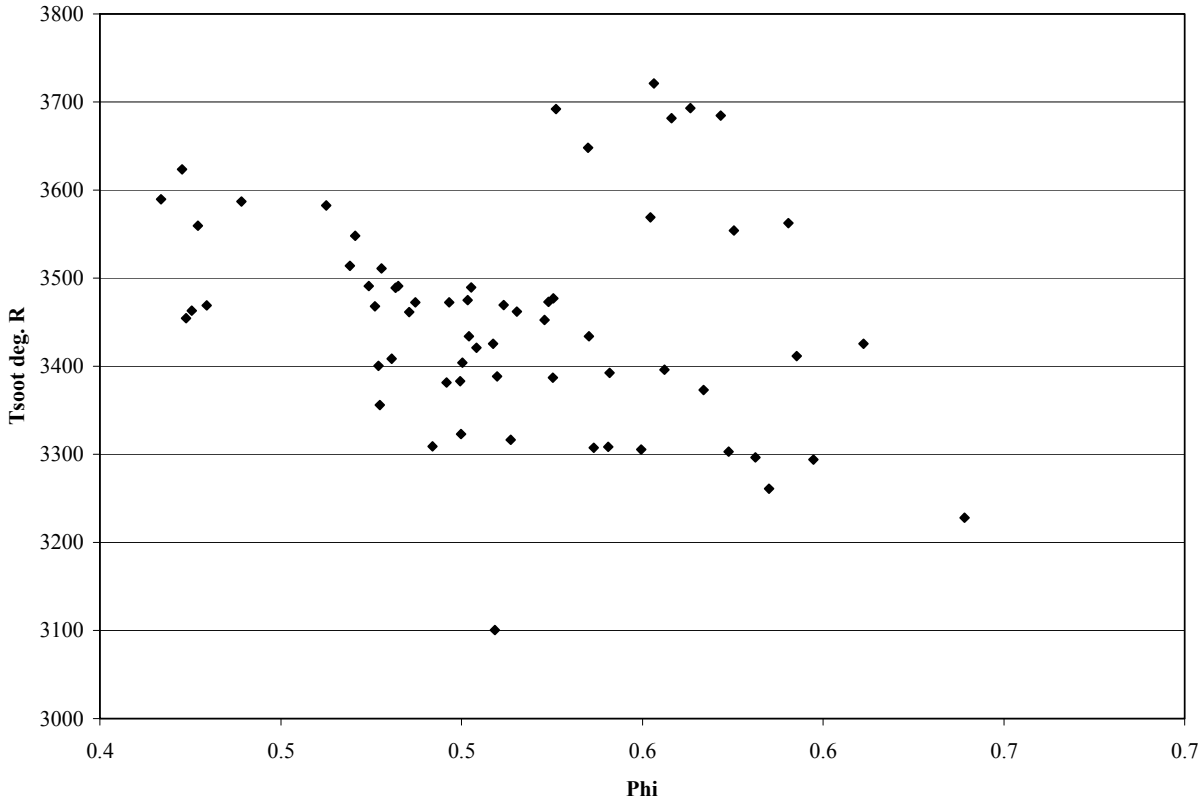

Figure 6-11. Soot temperature vs. combustor inlet equivalence ratio

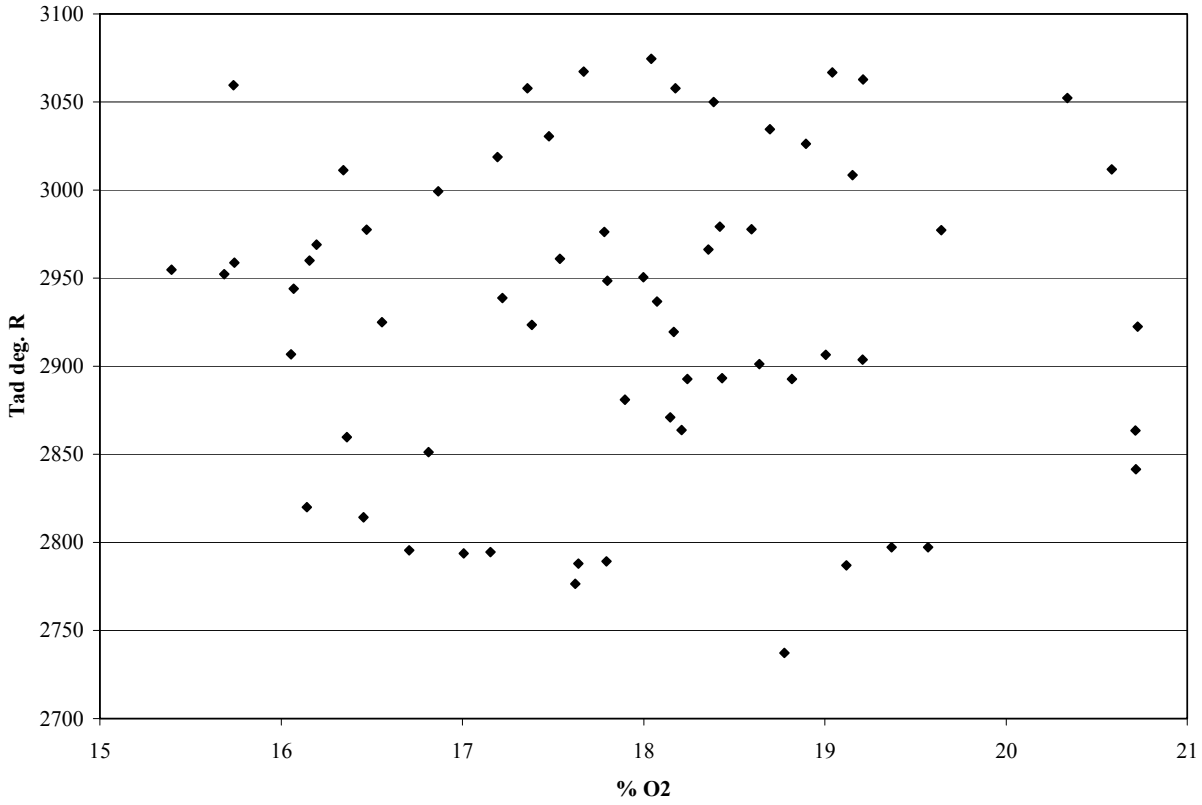

Figure 6-12. Adiabatic flame temperature vs. combustor inlet percent oxygen

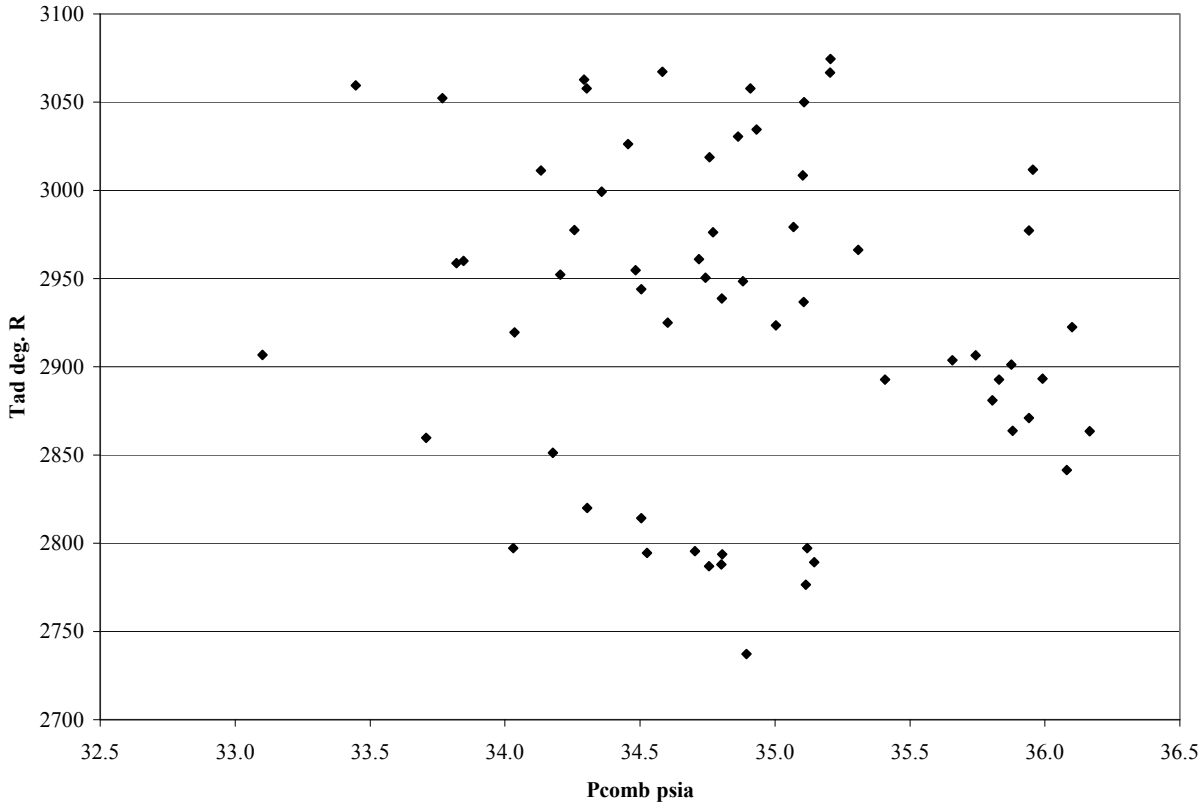

Figure 6-13. Adiabatic flame temperature vs. combustion pressure

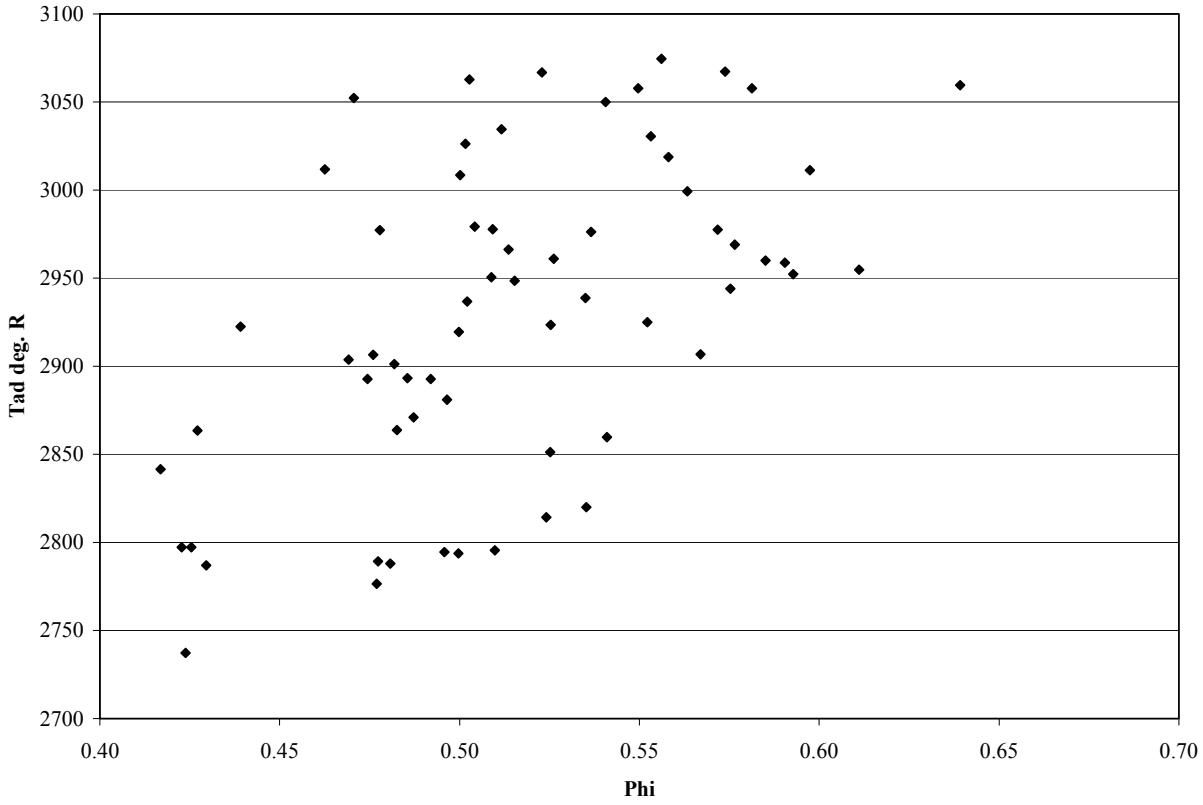

Figure 6-14. Adiabatic flame temperature vs. combustor inlet equivalence ratio

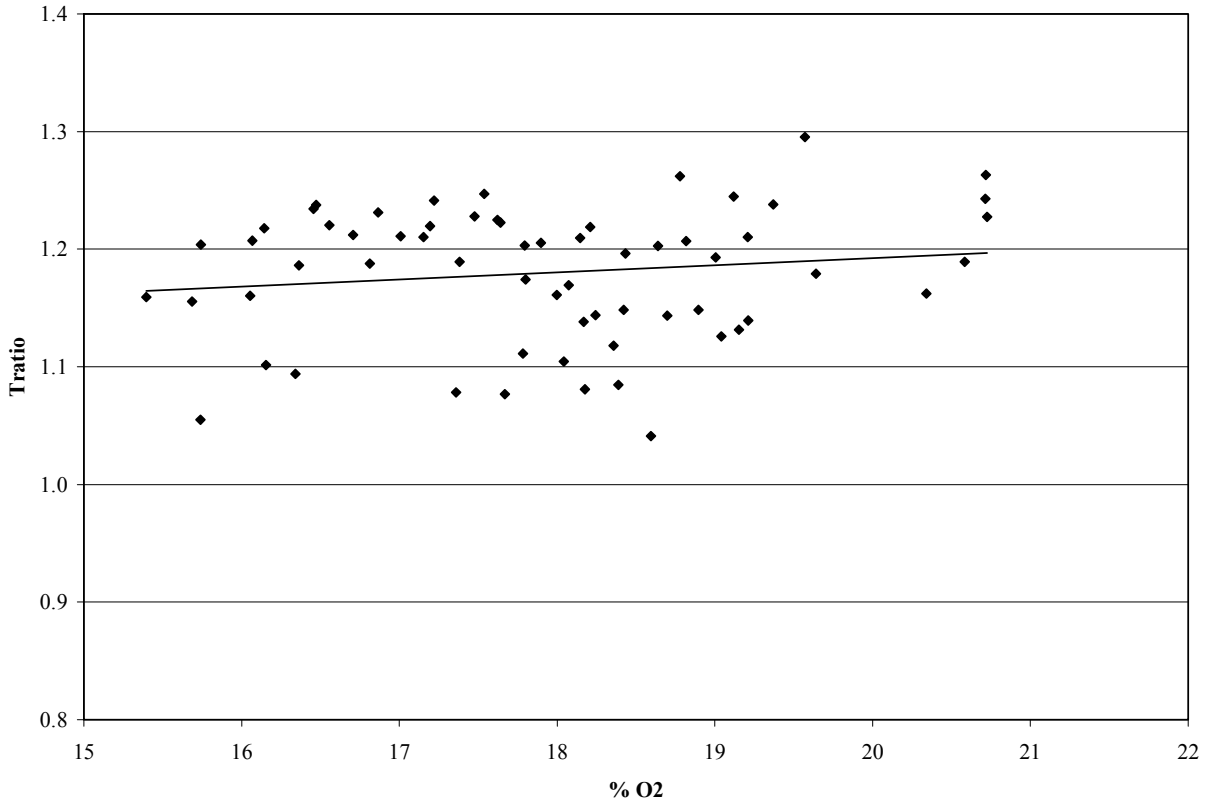

Figure 6-15. Soot temperature/adiabatic flame temperature vs. combustor inlet % O_2

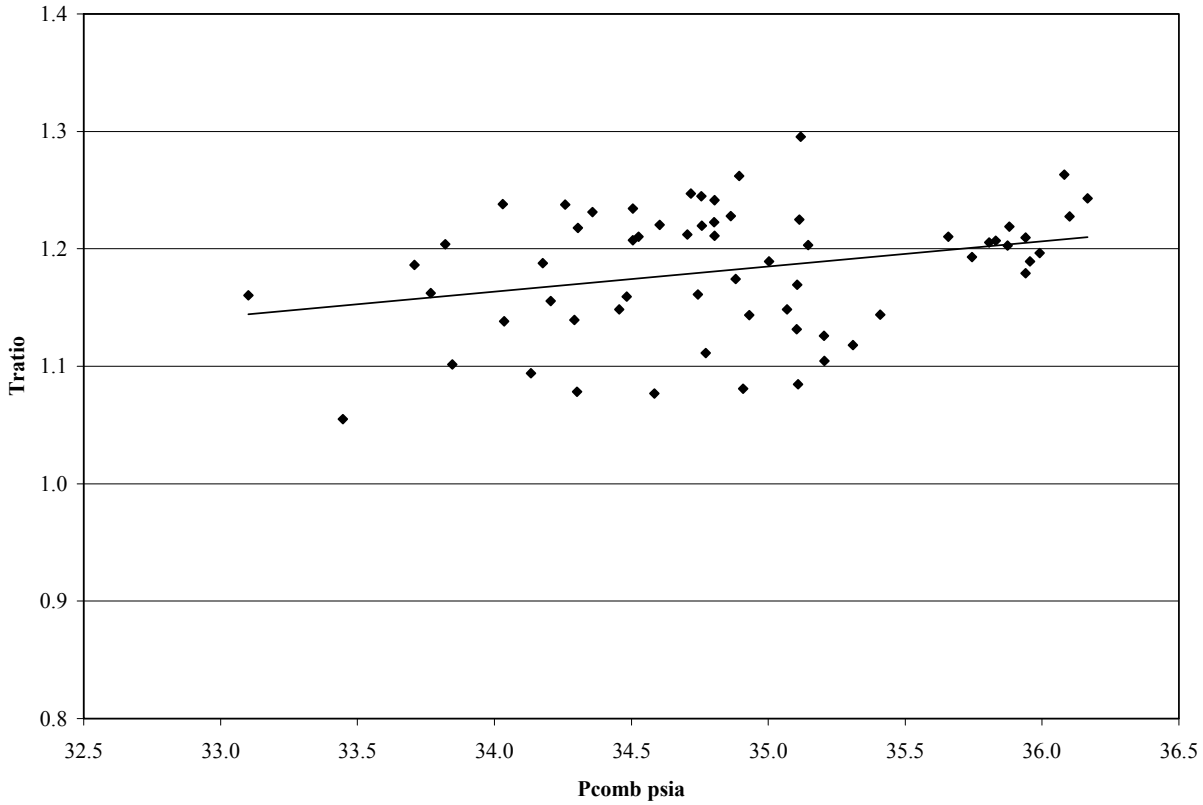

Figure 6-16. Soot temperature/adiabatic flame temperature vs. combustion pressure

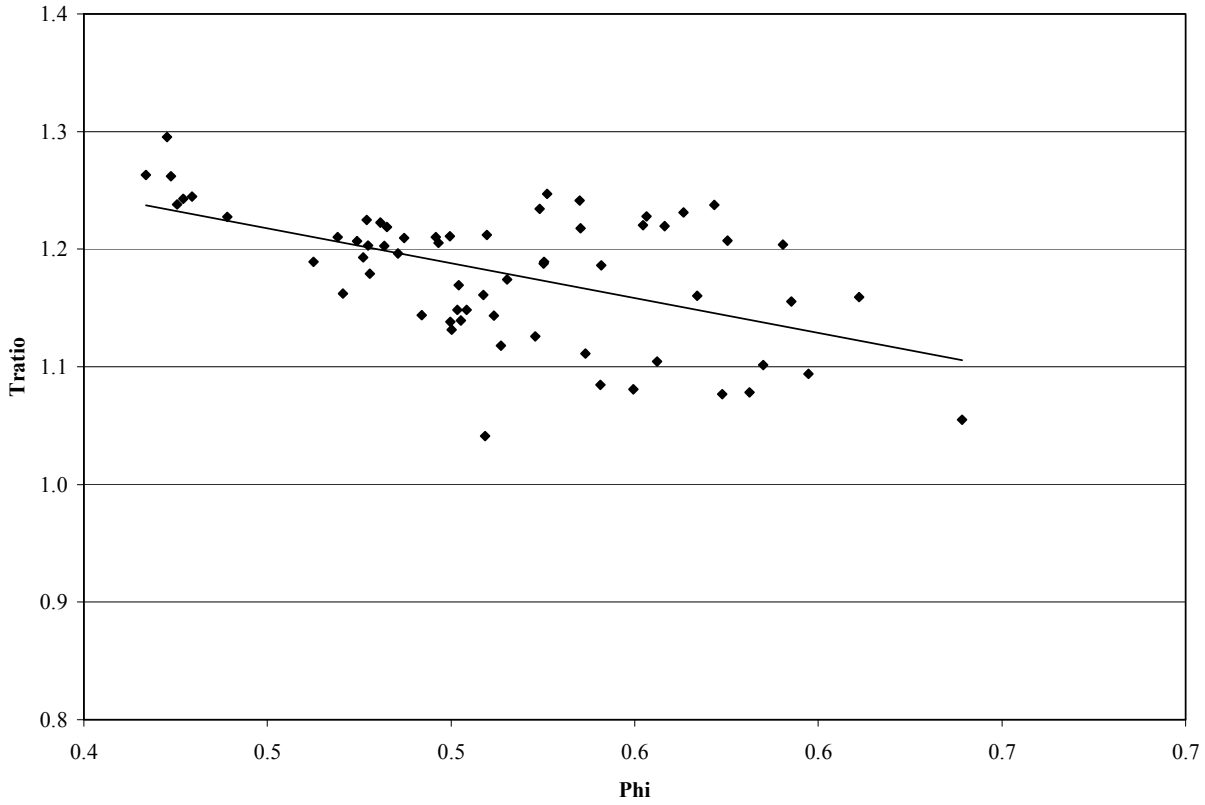

Figure 6-17. Soot temperature/adiabatic flame temperature vs. equivalence ratio

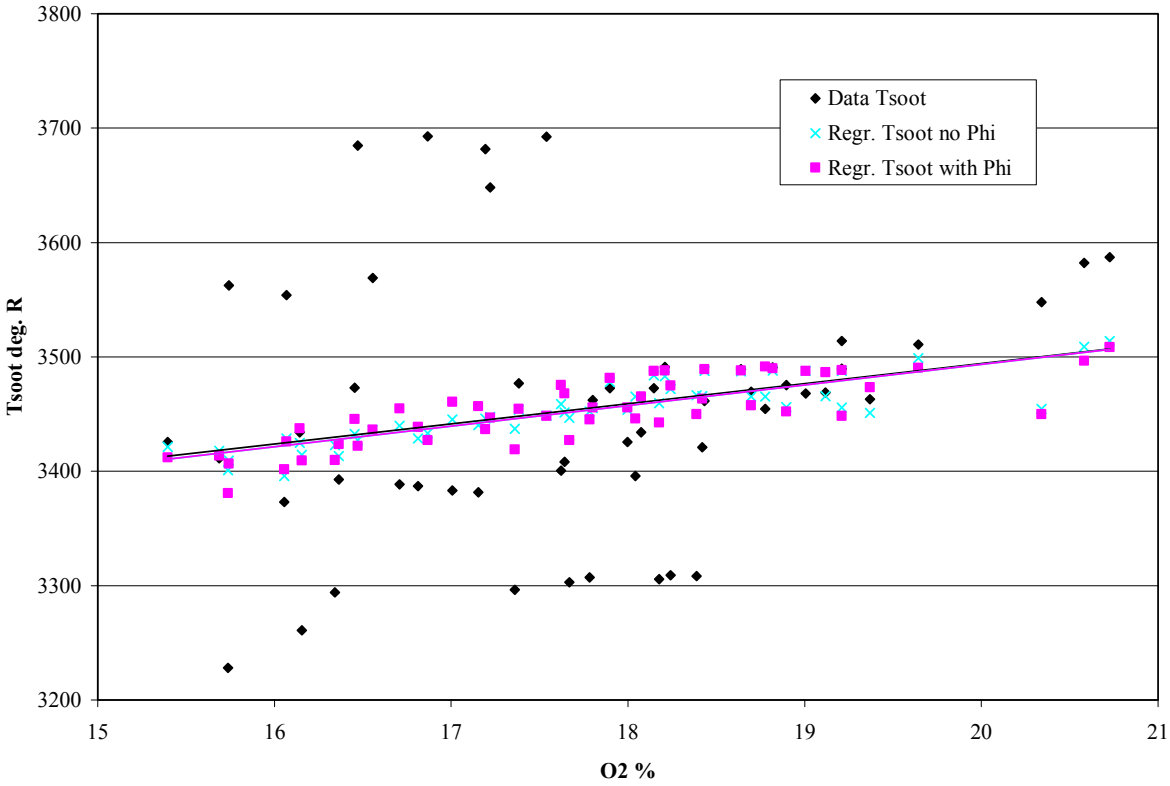

Figure 6-18. Regression and data soot temperature vs. combustor inlet percent oxygen

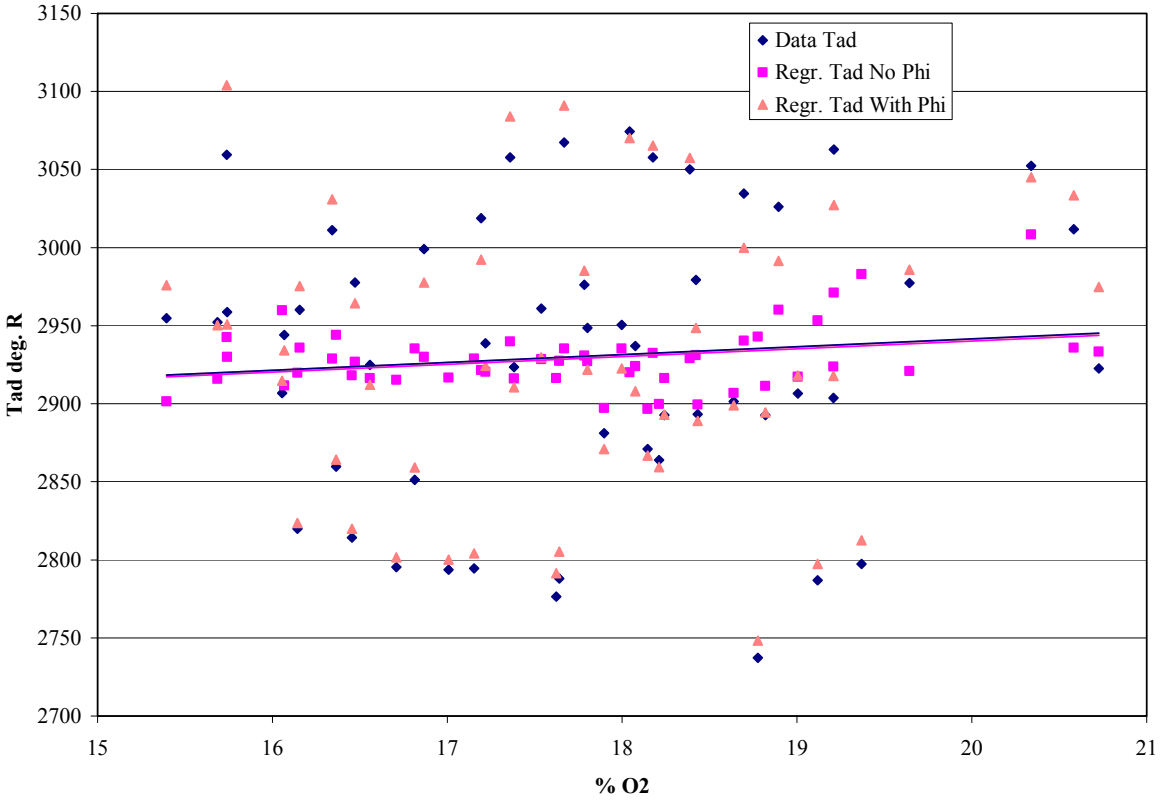

Figure 6-19. Regression and data adiabatic flame temperature vs. combustor inlet percent

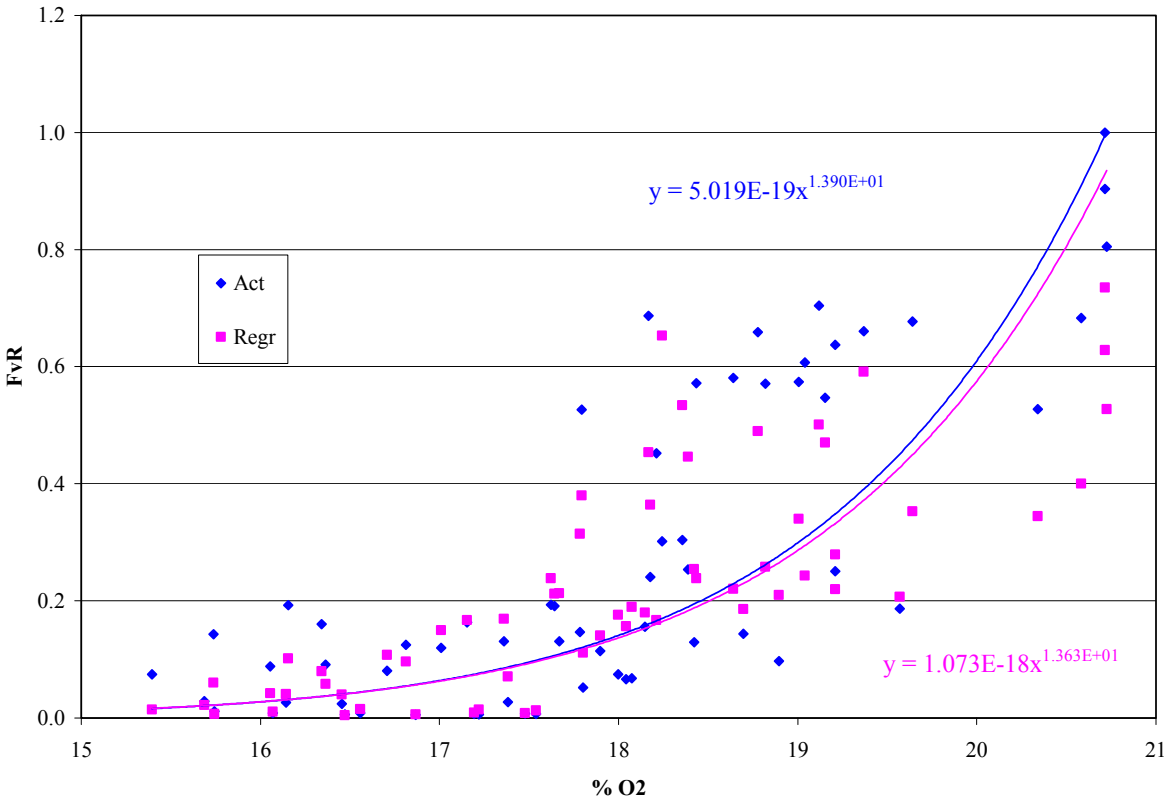

Figure 6-20. Run data and regression F_{vr} vs. combustor inlet % O_2 using T_{soot} for the temperature parameter

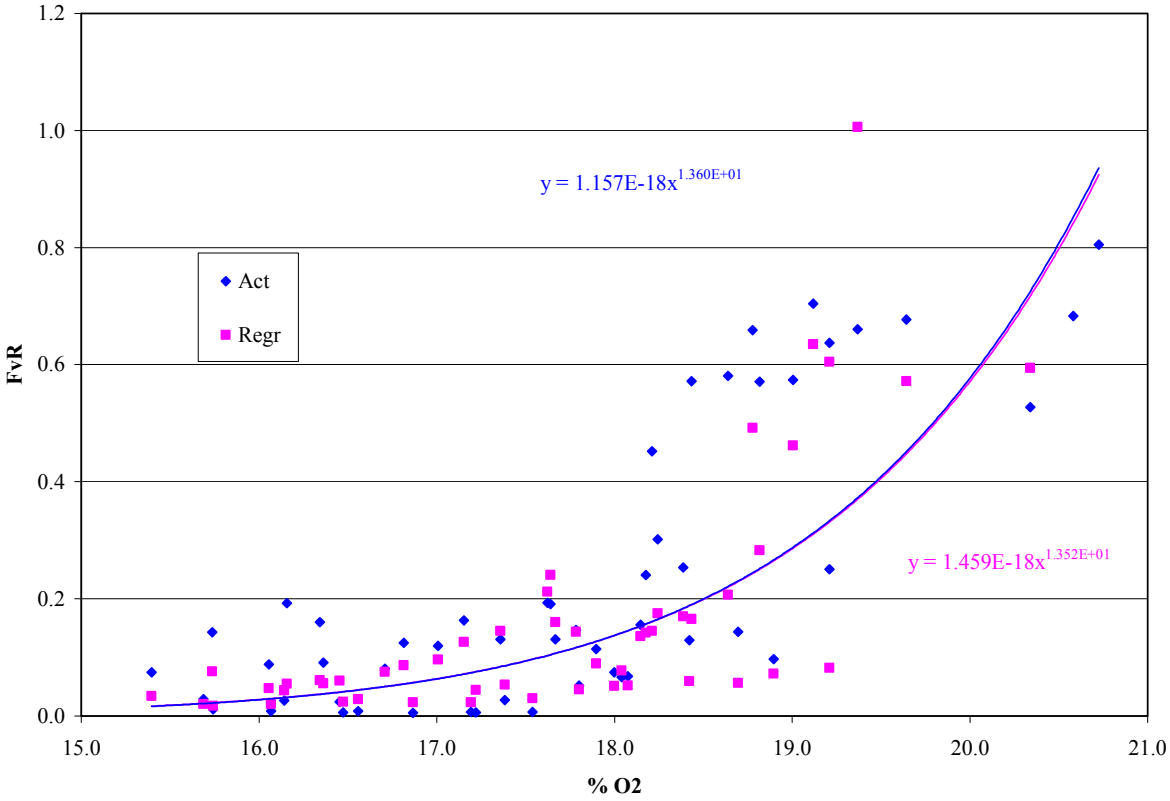

Figure 6-21. Run data and regression F_{vr} vs. combustor inlet % O_2 using T_{ad} for the temperature parameter

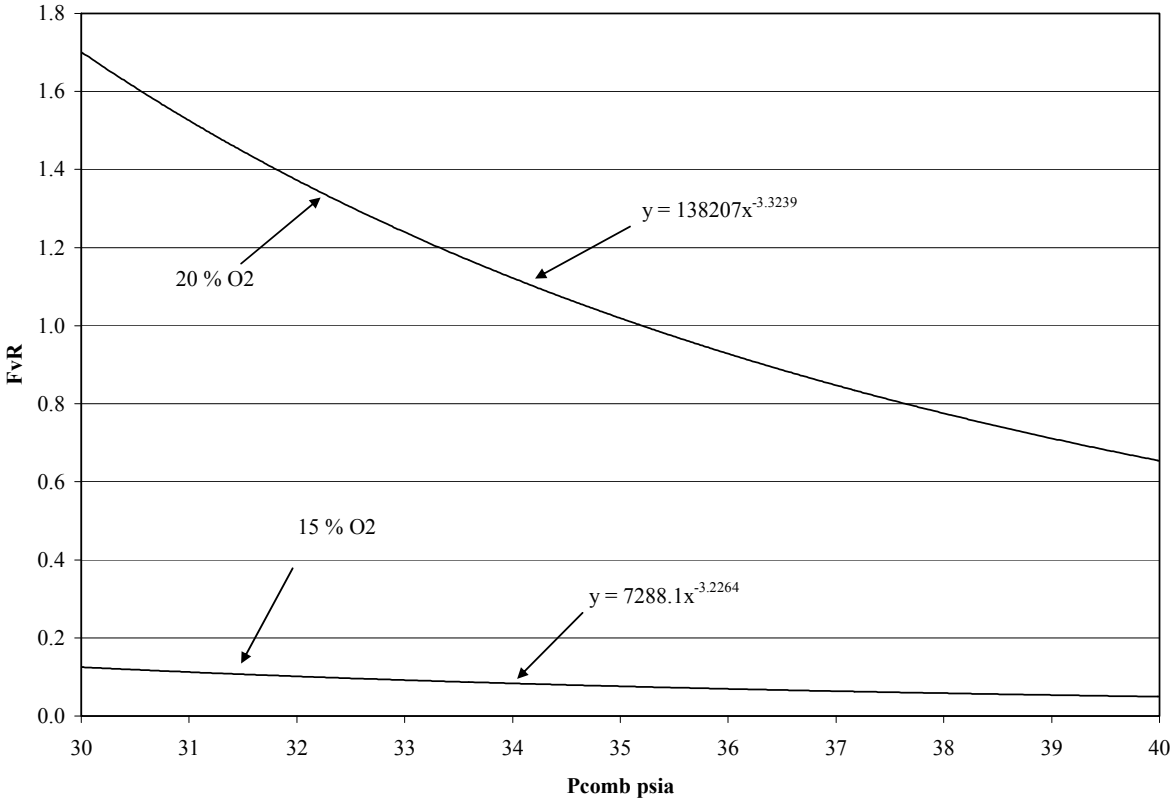

Figure 6-22. Synthetic F_{vR} vs. P_{comb}, $\Phi = 0.4$ with 15% and 20% O_2 using T_{soot}

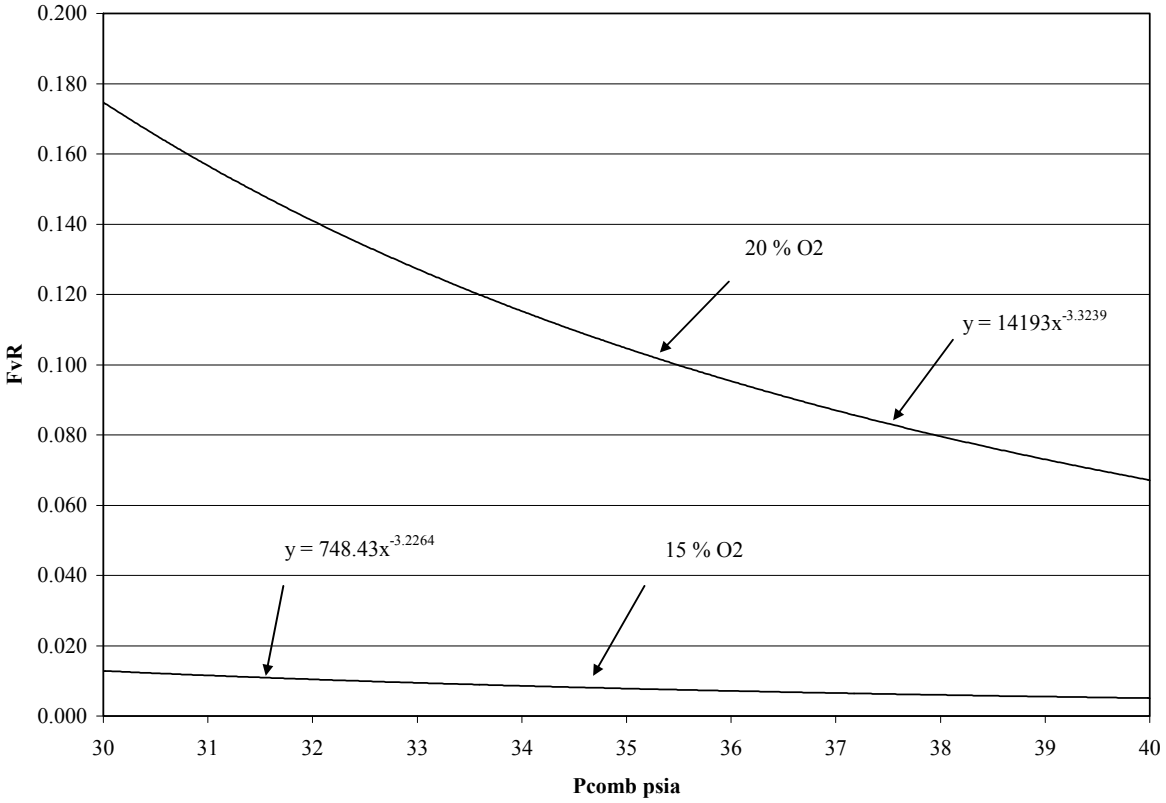

Figure 6-23. Synthetic F_{vR} vs. P_{comb}, $\Phi = 0.65$ with 15% and 20% combustor inlet O_2 using T_{soot}

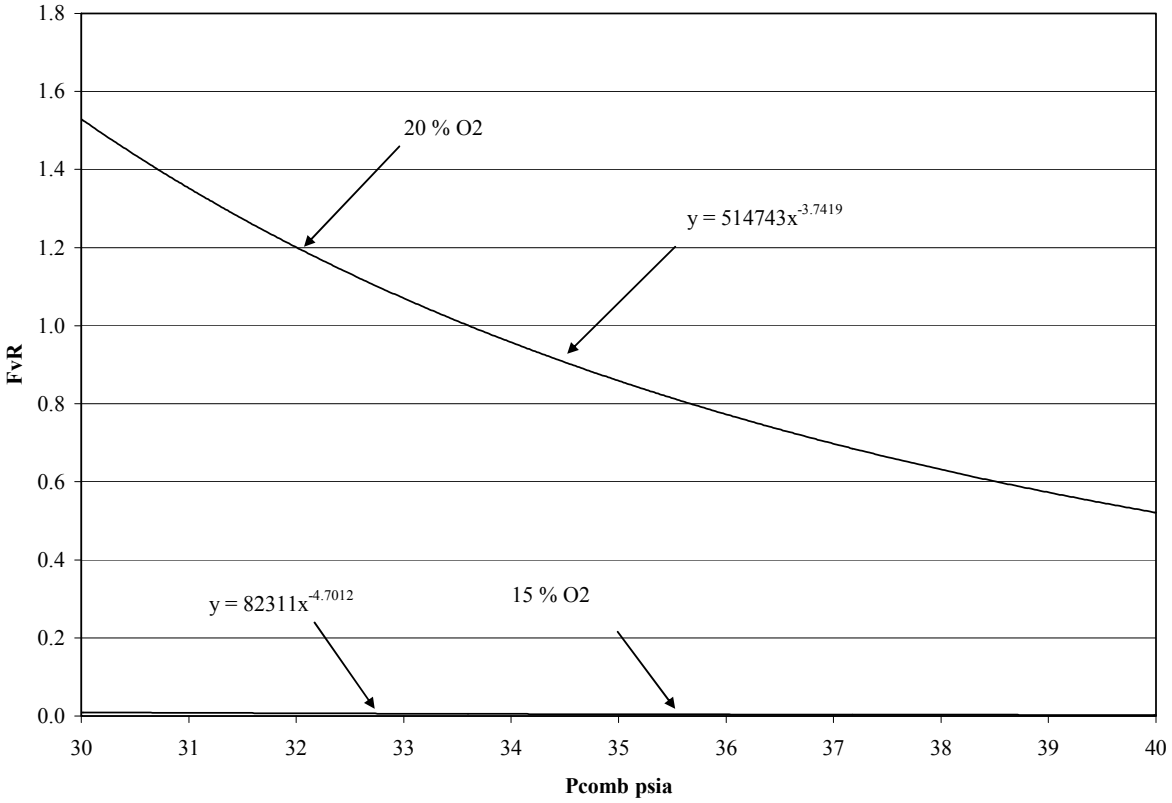

Figure 6-24. Synthetic F_{vR} vs. P_{comb}, $\Phi = 0.4$ with 15% and 20% combustor inlet O_2 using T_{ad}

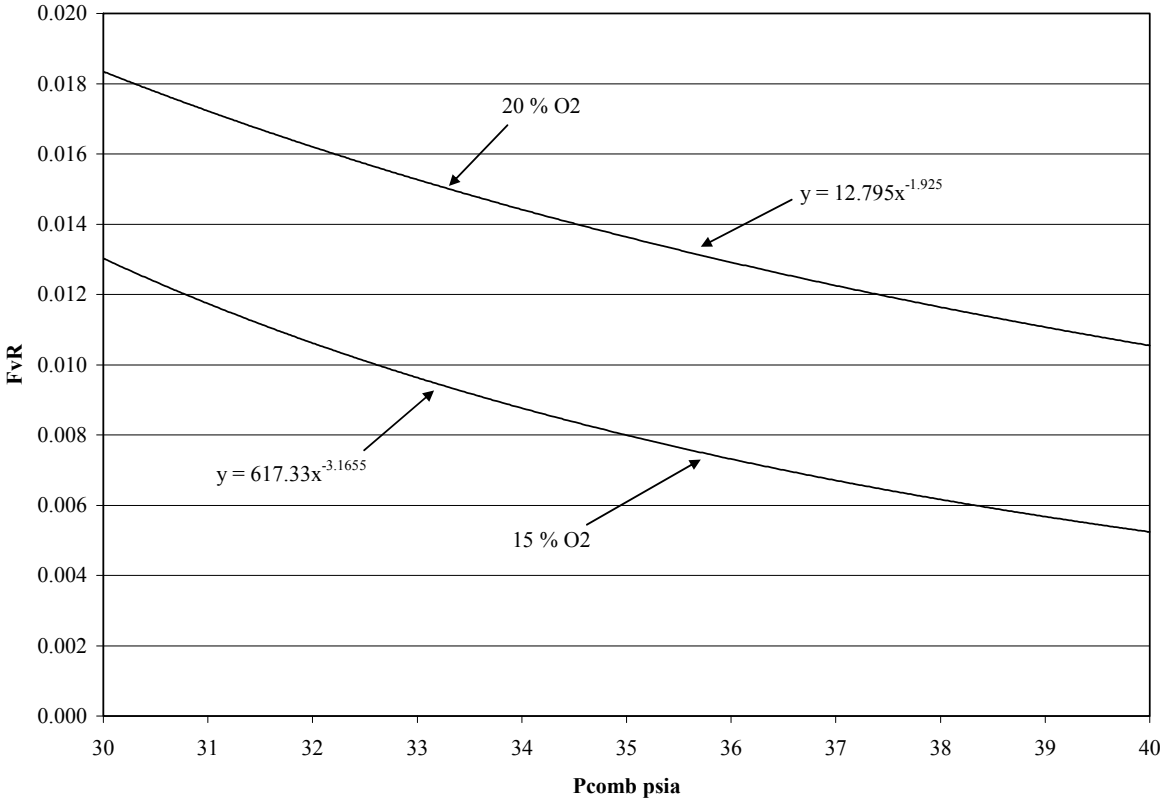

Figure 6-25. Synthetic F_{vR} vs. P_{comb}, $\Phi = 0.65$ with 15% and 20% combustor inlet O_2 using T_{ad}

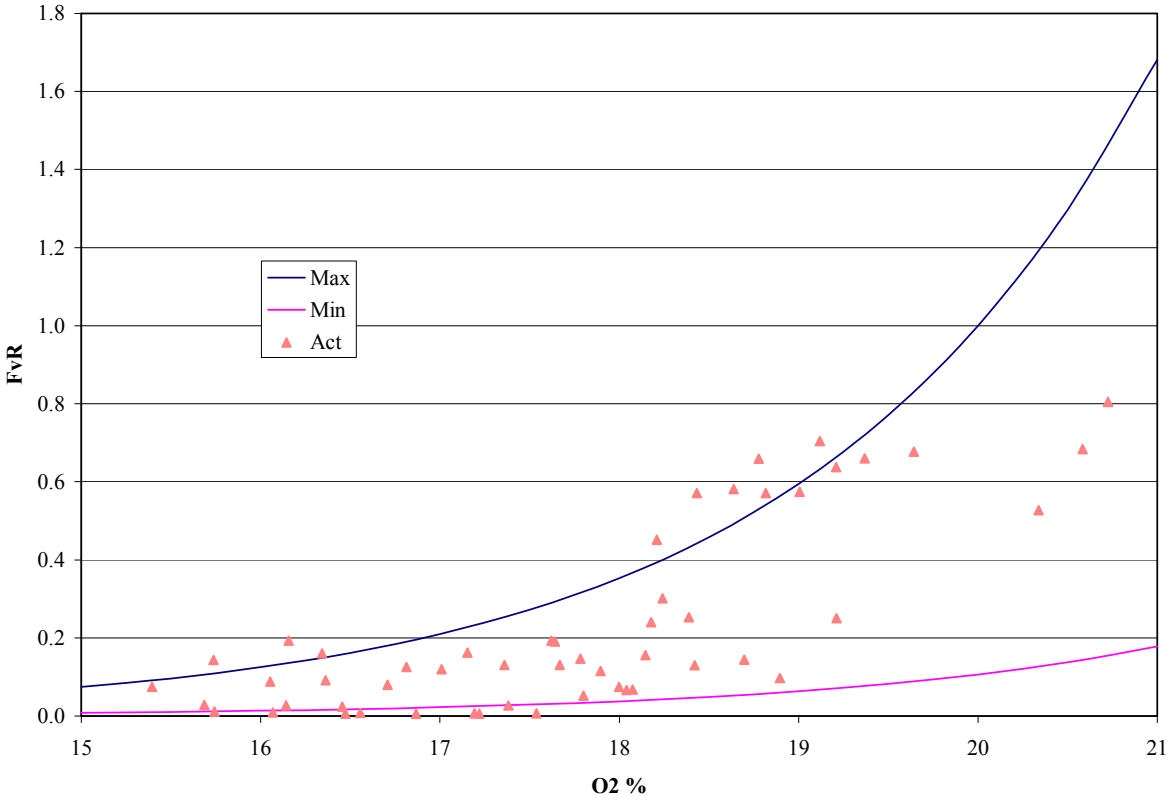

Figure 6-26. Run data and extreme case synthetic F_{vR} vs. combustor inlet % O_2 using T_{soot}

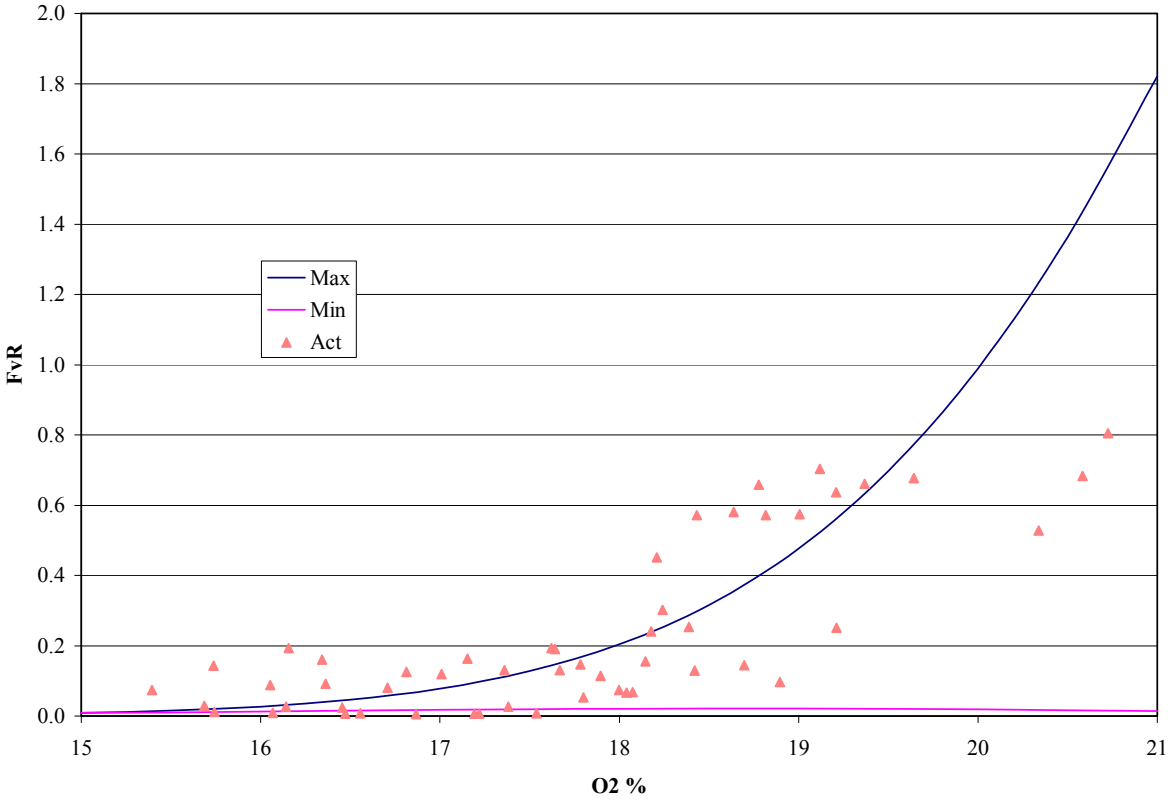

Figure 6-27. Run data and extreme case synthetic F_{vR} vs. combustor inlet % O_2 using T_{ad}

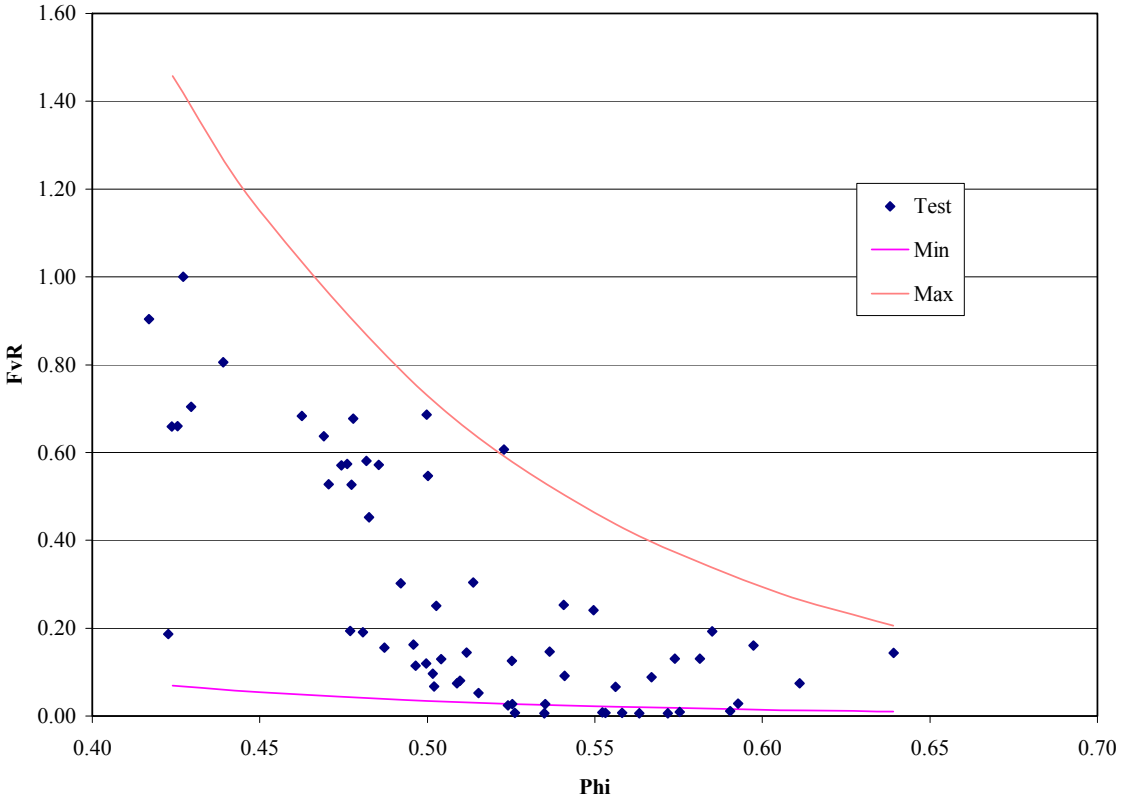

Figure 6-28. Run data and extreme case synthetic F_{vR} vs. combustor inlet equivalence ratio using T_{soot}

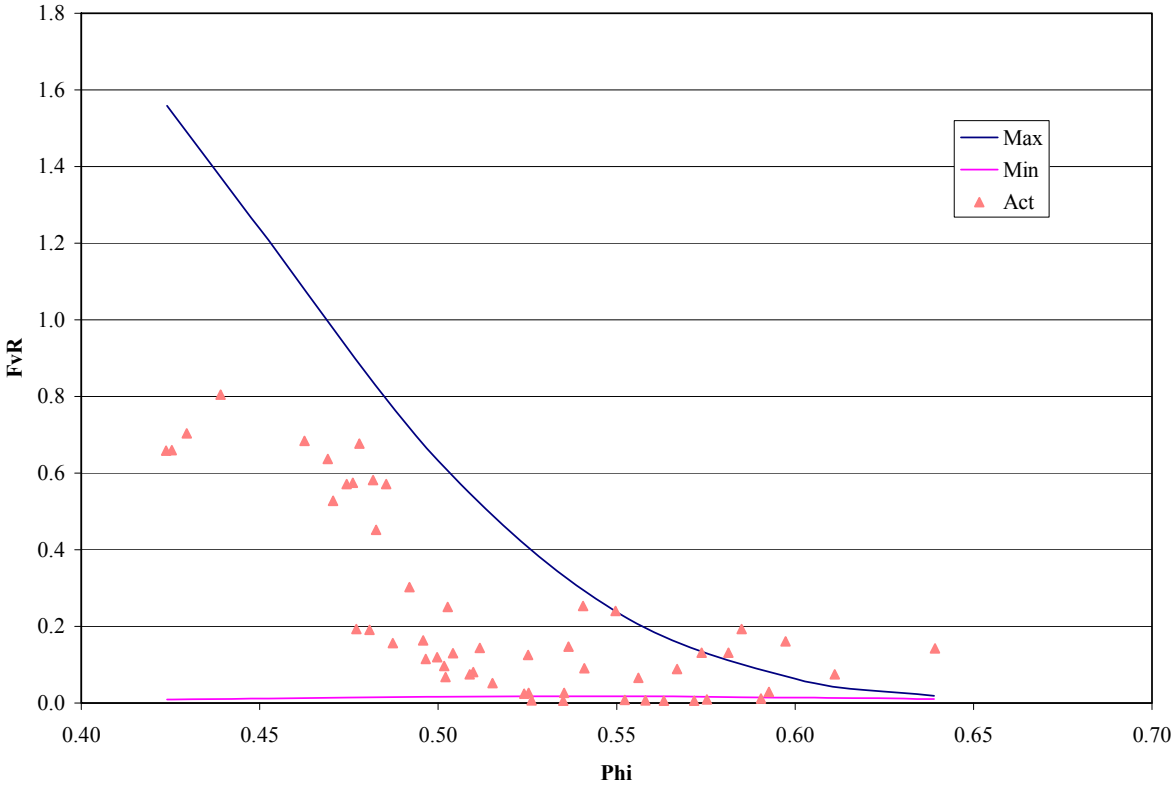

Figure 6-29. Run data and extreme case synthetic F_{vR} vs. combustor inlet equivalence ratio using T_{ad}

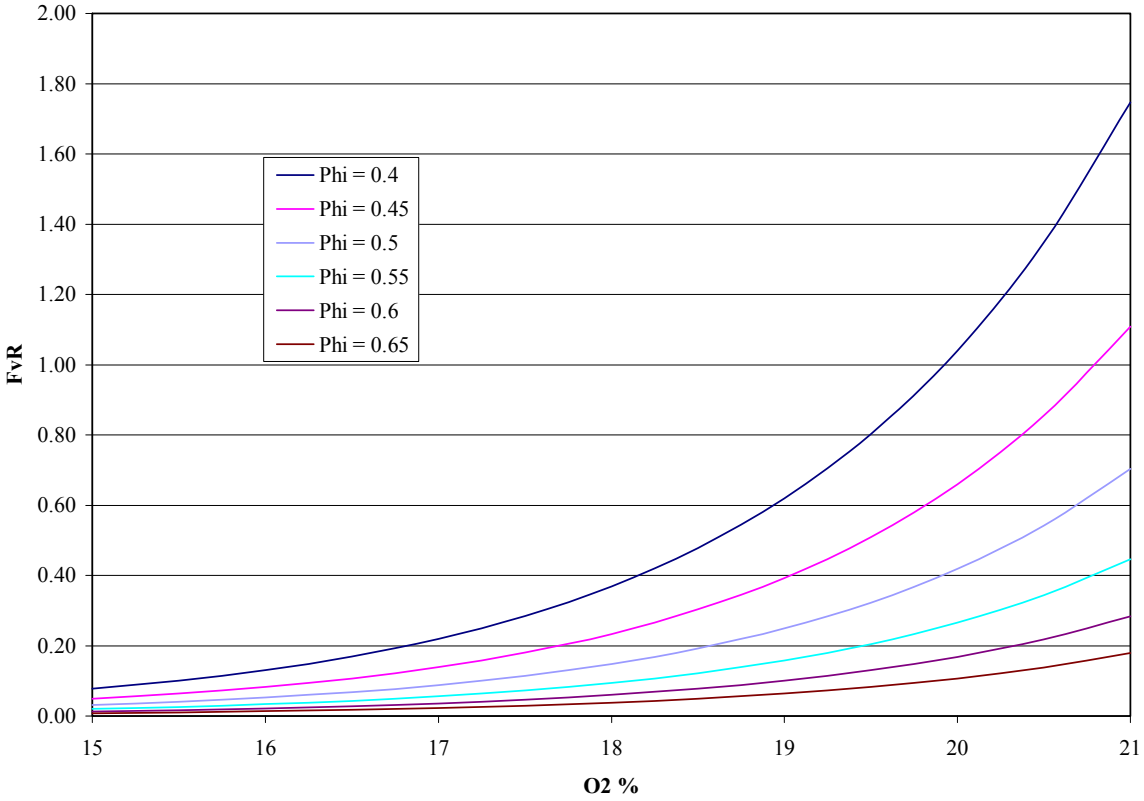

Figure 6-30. Synthetic F_{vR} vs. combustor inlet % O_2 with variable combustor inlet Φ

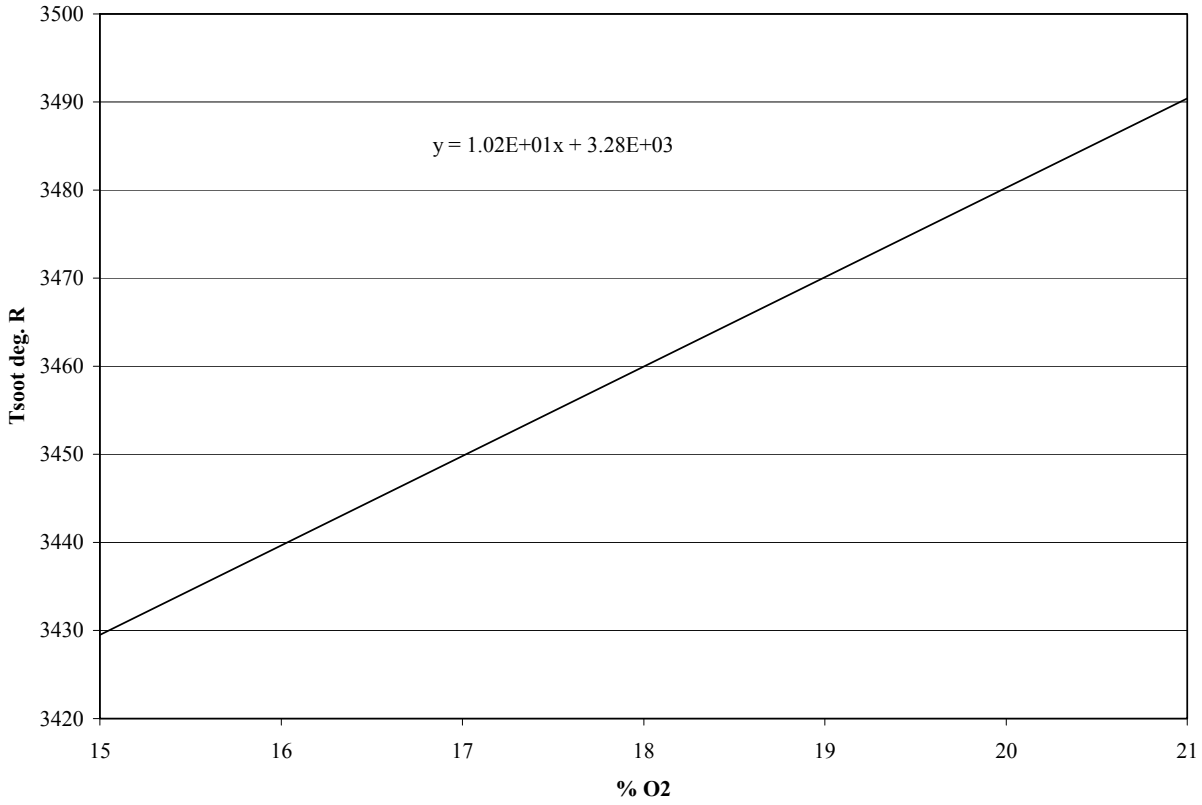

Figure 6-31. Synthetic Tsoot vs. combustor inlet % O_2 with constant P_{comb}

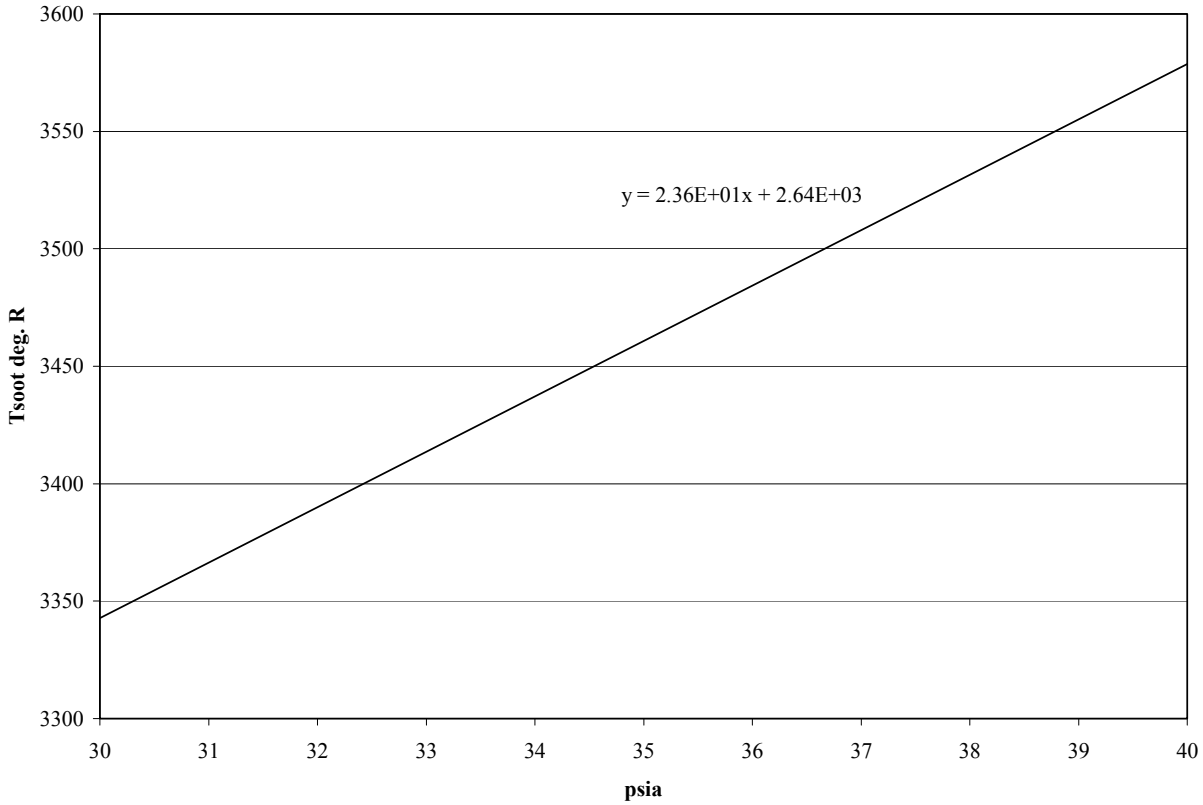

Figure 6-32. Synthetic Tsoot vs. P_{comb} with constant combustor inlet % O_2

CHAPTER 7
CONCLUSIONS

A test program was completed with the High Pressure Recuperated Turbine Engine at the University of Florida Energy & Gasdynamic Systems Laboratory where soot volume fraction was measured in the combustion zone while changing inlet oxygen concentration. A trend of increasing soot formation with increasing oxygen concentration was observed. This trend approximately follows a power relationship. A trend of decreasing soot formation with increasing equivalence ratio was also observed and was approximated by a power relationship.

A regression analysis was performed on soot temperature as a function of percent reactant oxygen and absolute combustion pressure. This relation demonstrated good agreement with test data and predicted a linear dependence on both percent reactant oxygen and absolute combustion pressure.

A regression analysis was performed on soot volume fraction as a function of equivalence ratio, percent reactant oxygen, absolute combustion pressure and soot temperature. Synthetic data generated from the regression reflected trends nearly identical to test data and at extremes of test parameters almost fully bounds the test data. The regression reflected the inverse power relationship between soot volume fraction and absolute combustion pressure at any equivalence ratio or reactant oxygen percent and showed that soot formation diminishes with decreasing reactant oxygen and increasing equivalence ratio. When oxygen concentration was reduced from ambient to 17.5%, soot formation decreased by an order of magnitude.

The test engine operation points ranged between an equivalence ratio of 0.42 and 0.64 and an oxygen concentration between 15.4 and 20.7%. If operating points approached more lean or rich conditions, soot behavior would be expected to deviate from the models.

As an example, if the equivalence ratio approached or exceeded 1.0, clearly the soot and adiabatic flame temperatures would be expected to diminish and soot volume fraction increase. This is not predicted and therefore the models should not be extrapolated to higher equivalence ratios.

For low equivalence ratios, as combustion approaches lean blowout, flame instability would be expected to have an impact and was not studied in this research. Therefore the models should not be extrapolated to lower equivalence ratios.

The limitations to the range of operation and the model are, in part, attributed to the fixed geometry of the combustor liner and performance of engine components. The method of restricting the liner dilution holes to divert flow to the primary zone, did so at the cost of greater pressure drop as well as increased film cooling flow. The effectiveness of the recuperator limited the temperature of the reactants entering the combustion zone. Both of these conditions likely increased the minimum oxygen concentration the engine would tolerate.

This research has demonstrated the significant effect of oxygen concentration on soot formation within a gas turbine. The regression equations developed from this work are useful design tools for circumstances where dilution of combustion air is being considered.

CHAPTER 8
RECOMMENDATIONS

The models developed in this work were useful in predicting behavior of the HPRTE at the University of Florida Energy & Gasdynamic Systems Laboratory. Additional testing with a different semi-closed cycle gas turbine would be warranted in order to investigate the general applicability of the techniques utilized here. Also, while the model coefficients may change with each machine, it may be possible to correlate these with basic design parameters, allowing investigative studies prior to testing.

The data collected in this research did not include operating points approaching or exceeding an equivalence ratio of 1.0. It would be expected to observe increasing soot volume fraction under those conditions and the model does not predict this. Additional testing should be conducted to examine whether a single model is sufficient and if not, whether a boundary exists beyond which a second model can be applied.

The data collected in this research also did not include operating points below ~15% oxygen concentration. It would be expected to observe increasing soot volume fraction under those conditions and the model does not predict this. Additional testing should be conducted to examine whether a single model is sufficient and if not, whether a boundary exists beyond which a second model can be applied.

When the HPRTE was operated at minimum load with no recirculation, an increase in soot volume fraction was observed and attributed to poor atomization. A smaller injector orifice should be evaluated with additional testing to verify whether this is the case.

At the time this investigation was undertaken, two issues were unresolved related to gas analysis. The first concerned the gas analyzer itself. The manufacturer representatives were unsure whether the data collected was on a ‘wet’ or ‘dry’ basis.

Ultimately the answer was neither. Analysis was based on actual concentration at the device without correction for water vapor or condensation. As a result, much more complicated calculations were necessary to determine the composition of the recirculated gases, based on exhaust analysis. Gas analysis data was also taken from a point in the flow path after the mixing of ambient air and recirculation gas, which would have given direct measurement of species concentration at the combustor inlet. The measurement basis was one of the reasons this data could not be exploited.

The second issue was that the seal design used for duct flanges in the recirculation path was inadequate. This allowed introduction of ambient air which could not be accounted for in the measurement of recirculation flow. The significance of the leakage also could not be determined and was the second reason that gas analysis data from the post mixing flow was not utilized. Both of these issues have now been resolved. A limited test program to acquire verification data should be executed in order to evaluate the impact on the model coefficients presented.

Test program requirements included video recordings of the flame to examine changes in observable characteristics. When the optical fiber used to collect spectral data was in position to take data, the view of the camera was obscured. This necessitated a flexible mount so the fiber could be removed and replaced. Further, the fiber was in the vicinity of high temperature components and had to be repositioned to avoid heat damage during transitions between data points. While great care was taken to position the fiber consistently, minor variation was unavoidable. The mounting system for the optical fiber should be redesigned to facilitate precise placement whenever repositioning is needed. The incorporation of a cooling feature or heat shielding would also be advantageous.

Calculation of the soot volume fraction and temperature rely on assumptions relating to the transmission characteristics of the sapphire window and the extinction coefficient of the soot component in the flame. Installation of a second window would allow both of these characteristics to be more directly quantified by taking transmission data using a laser or calibrated light source. If a third widow was feasible, then scattering measurements would also be possible. This would facilitate a more direct measurement of the soot volume fraction as well as future investigations into soot particle characteristics.

Fuel flow is measured volumetrically during operation of the facility. The fuel flow on a mass basis is needed for various analysis calculations. This is accomplished with known fuel density corrected for fuel temperature. The fuel flows through a small diameter line exposed to ambient conditions and for this investigation the fuel temperature was assumed to be equal to the ambient temperature at each data point. Over all testing, the fuel density variation was only ~3% and much less for any single test run. While the potential error is small using this temperature assumption, the fuel temperature should be measured directly upstream of the flow meter to eliminate the need.

APPENDIX A
OPERATING PROCEDURES

The HPRTE Setup Procedure,

Rev. 8/14/07

HPRTE Soot Investigation Test Run #10: Dated 8/1407

_____ OPERATOR'S NAME

Support Systems:

Site Chill Water:

1. ___ Slowly open the source and return overhead isolation valves.

Cooler Chill Water:

1. ___ Connect the process water hoses to the cooler.

2. ___ Supply water to the cooler by opening isolation valves.

3. ___ Verify main cooler flow by listening for flow noise.

4. ___ Record minor leaks for later resolution.

ARU Chill Water:

1. ___ Connect the process water hoses to the ARU.

2. ___ Supply water to the cooler by opening all isolation valves.

3. ___ Verify water flow by checking the ARU flow meter.

4. ___ Record minor leaks for later resolution

Boost Control Valve and Waste Gate Control Air:

1. ___ Set supply air regulator by the South door to 40 psig.

2. ___ Verify the Supply Air Pressure at the control panel is at least 30 psig by adjusting the South door regulator in 1. Above.

3. ___ Close the Fisher boost Control Valve by reducing the controller air pressure to 5 psig. Verify full closing by the valve stem flag.

4. ___ Open the Fisher boost Control Valve by increasing the controller air pressure to 15 psig. Verify full open by the valve stem flag.

12 Volt Battery Check

1. ___ Unplug the battery charger and store the charger.

2. ___ Throw the isolation switch.

3. ___ Verify each start battery has a cold reading of 13.2 volts minimum. This ensures that the batteries are fully charged. Record Voltage:
   N_____VDC, S_____VDC

4. ___ Verify each ignition battery has a cold reading of 12.6 volts minimum. This ensures that the batteries are sufficiently charged. Record Voltage:
   N_____VDC, S_____VDC

Fuel Supply

1. ___ Verify Gravity and speed trim lines to engine skid. Open the ROVER side of the gravity system.

2. ___ Unscrew, remove and replace the fuel Pump accumulator to charge with air.

3. ___ Plug in the fuel transfer pump and verify operation.

4. ___ Check fuel level by sight glass, minimum ¾ full. Fill as necessary.

5. ___ Fill the seven gallon tank under the fuel cabinet, if required.

6. ___ Check the entire fuel cabinet and hoses for leaks.

7. ___ Fill and place on station, auxiliary fuel containers, as required.

8. ___ Dry and position the skid drip pan and the fuel drain drip pan.

Oil Levels

1. ___ Verify Rover engine oil level. Refill with single viscosity 10W oil as necessary up to half way between the high and low markings. Record any amount added.

2. ___ Safety wire the dipstick. Oil added _____

Dynamometer Setup and Oil Cooler Process Water

1. ___ Route system drain lines outside under the main overhead door.

2.___ Adjust Froude Dyno inlet and outlet valve to full open.

3. ___ Fully open the water supply to the Dyno. Purge Dyno.

4. ___ Verify the in-line Rota meter is reading ~ 7 gpm.

5. ___ Verify the water brake is fully unloaded, that is, the geared handle is full to the CCW position.

6. ___ Verify the gear lock remains disengaged.

7. ___ Visually confirm gland leakage.

8. ___ Confirm discharge flow from three drain lines. They are; 1.)The Rover oil cooler, 2.) The dyno, 3.) The dyno drip pan.

Water Recovery

1. ___ Hang the Water Recovery Bucket on the load cell.

2. ___ Route AC extension cord to the drain pumps. Switch on/off to verify rotation

Inlet, Recirculation and Exhaust Start-up Check

1. ___ Check the exhaust system to ensure all penetrations are covered and joints are tight.

2. ___ Verify that the Rover Inlet Isolation Valve is fully open

3. ___ Verify the Rover Recirculation Valve is fully shut.

Engine room Preparation

Room Ventilation:

1. ___ Open the main bay door about five feet (to marked line).

2. ___ Turn on the lab ventilation fan and the compressor room fan.

3. ___ Set up Psychrometer.

Lab Over-watch:

1. ___ Check the lab area for debris that could be ingested into the engine or present a tripping hazard. Remove as necessary.

2. ___ Attach the Safety Chain at the hall outside the Lab.

3. ___ Move fire extinguishers to areas in the lab where they are readily accessible.

ARU Setup

1. ___ Refer to the ARU set up procedure, separate from this document.

Video and Audio Recording

1. ___ Turn on the control room VCR, channel A. Run the cables to the control room to the video monitor.

2. ___ Set up the microphone **(plug in the power supply)** to record the communications loop. Hook this into the VCR sound input and radio receiver.

3. ___ Synchronize VCR time and date with the DAQ.

4. ___ Insert a new VCR tape for the day's activity. Ensure tape is recording on E.P. (extended play).

5. ___ Synchronize Camera time and date with the DAQ.

6. ___ Complete a system check to be sure the monitoring and recording systems are working correctly. This system is used to verify the data set switch points and aids in improving subsequent runs through lessons learned.

7. ___ Check all the communication gear. Change batteries as warranted. All units should be on the same channel and in Push-To-Talk (PTT) mode. All units should be on TX, not INT. Use channel A.

Personnel Safety Equipment and Communications

1. ___ All personnel should wear appropriate clothing for an environment where high temperature piping, heavy equipment and high speed rotating equipment exist. i.e., long sleeve shirt, long pants, closed toe and heel shoes, and no loose fitting items or jewelry.

2. ___ TURN OFF CELL PHONES.

3. ___ All personnel and visitors should have hearing protection, either communication sets or ear muffs.

4. ___ All personnel and visitors should have eye protection.

5. ___ Visitor Policy: all visitors should be checked in, briefed, and supplied with safety equipment before the run set-up begins. Optimally, all visitors should be supplied with Listen-Only communication head gear. No late or unannounced visitors are allowed.

The VARS Operating Procedure

Rev. 8/13/07

This document is for normal start-up and operation, under typical test conditions, of the TRIAD THERMOCHARGER, variously known as the ARU (ammonia refrigeration unit) and the VARS (Vapor absorption refrigeration system). For a more complete understanding of the design, operation and maintenance of this device, refer to the Triad ARU Operation Manual by Energy Concepts Company, LLC, 627 Ridgely Avenue, Annapolis, MD 21401, 410-266-6521, fax 410-266-6539, enerconcep@aol.com, www.energy-concepts.com and

the document ARUvalvebrief.doc by Eric Howell. Conflicts may be noted between the Operation Manual and this document. These are due to operating conditions having changed from the original design constraints.

Set-up for Stand-by

1. Check if the solution receiver is at least half full. If it is lower than 1/2, see "Controlled Start-up" step one.
2. If the solution receiver is empty or very close (level < ~2), notify the Team Leader and review the instructions for transferring fluid from the Rectifier to the Solution Receiver.
3. Connect the Power Cord.
4. Open V2 (TXV isolation valve).
5. Open V14 (pump discharge valve)
6. Open V25 (absorber isolation valve)
7. Set V15 at 3-1/2 turn open (column feed).
8. Set V26 for process chilled water to the condenser at 1.2 to 2 gpm for water temperatures between 44F and 60 F.
9. Set V27 for absorber process chilled water at 1-1/2 turns open.
10. Turn power switch on. Panel lights should go from Red to Yellow. When the Heat Recovery Vapor Generator (HRVG) inlet air becomes hot, the solution pump will start, the solenoid valves will open and the Green light will come on.

Control during Start-up:

1. Observe the Solution Receiver level as the unit comes online. If the fluid level drops below 50%, open V13 1-2 turns until the level begins to rise. As the level approaches 75-80%, begin closing the valve until the solution flow rate is 3.2 gpm again.
2. Expedite the Start-up phase by throttling V13 such that the Ammonia Receiver pressure follows the pump discharge pressure.

Control during Normal Operation:

Note that the two primary "Faults" that will shut down the unit, are when the Solution Receiver Pressure reaches 120 psi or the Ammonia Receiver Pressure reaches 250 psi. Most of your actions will be taken to maintain these at acceptable levels.

TXV:

This is an expansion valve controlling liquid NH3 to the evaporator with two feedback mechanisms: a mercury vapor bulb on the evaporator return line, and a pressure feedback from the same. It is intended to keep the evaporator exit vapor a few degrees superheated, but generally, the evaporator exit temperature (T4) oscillates periodically, until the TXV has fully opened. This valve has an operating range that can be adjusted by removing the stem cap and raising or lifting the stem with a wrench. Consult the valve literature for instructions on this adjustment. Note that the wrong literature was provided by EC for this valve. It's *not* a Danfoss, it is believed to be Sporlan.

V3:

This is the TXV bypass valve, and is invaluable as a manual control for refrigerant flow when the TXV isn't opening sufficiently to carry the evaporator (Cold Gas Cooler, CGC) heat load. It is a needle valve suitable for fine adjustment and establishing a baseline refrigerant flow while the TXV modulates above this level. If the Solution Receiver pressure is exceeding 110psig, it is most sensitive to the TXV/V3 positions. If V3 is open at all, close it in 1 to 2 turn increments, waiting 5 to 10 seconds between adjustments, until the pressure returns to an acceptable value. Note that the CGC exit temperature on the refrigerant side (T4) will be increasing. If unsuccessful, you can still manually adjust the operating range of the TXV and eventually succeed, but again, you're reducing refrigerant flow to the evaporator and increasing the superheat of the refrigerant.

V15:

This is a control valve used to regulate the temperature of the vapor leaving the rectifier (hot side) and proceeding to the condenser (COND). Ideally, this temperature (T1) should be around 110F to 125F for moderate heat loads (<23 TR on the HRVG) and NH3 receiver pressures (200-220). For more extreme heat loads (>25 TR on the HRVG) and high-side pressures (240-250), try to keep this temp around 150F to 160F, for reasonable performance. If it creeps up to 180F, that's probably okay, but there will likely be lots of water carrying over into the NH3 receiver and evaporator, resulting in higher evaporator temperatures (T14). In general, open ¼ to ½ turns as necessary. While opening this valve increases the RECT cold

side flow, it simultaneously takes flow away from the HRVG, increasing T10. Thus, there are two effects competing against one another. However, observation of the solution flow meter (FM on the schematic) has indicated that the first several turns (beyond 3.5 open) opening V15 doesn't detract appreciably from the HRVG flow. Open it slowly. Watch the flow meter. Watch T1 and T10. T10 is best maintained below 270F. It has run as high as 310F, but the system performance was likely degraded. Try to keep it closer to 220F to 230F.

V23:

This control valve bypasses the float valve. It is almost always closed, and should be opened only when the float valve's float chamber is too full (above ¾ full in the sight glass).

V26:

This valve throttles the flow of Process Chilled Water (PCW) to the condenser and is probably the most useful control valve. Decreasing the flow raises the Ammonia (NH_3) Receiver pressure (NH_3 receiver gauge), and increasing the flow lowers the pressure. NH_3 receiver pressure is extremely sensitive to the PCW flow rate and temperature, so use very small turns, and wait for the flow meter to update. If the pressure is approaching the 250 psi limit, and V26 is wide open, and T7 < 85F, then

close V27, ½ turn. Consider also somewhat restricting flow to the warm gas cooler (WGC) if WGC exit temperatures aren't too excessive. If this is successful, you are running close to limits. If not successful, the unit is approaching a 'fault' condition and the HRVG heat load must be reduced. Inform the Team Leader.

V27:

This valve throttles PCW flow to the absorber. Only open this valve, beyond its initial position, during operation if absolutely necessary, as it robs flow from the condenser and the north PCW header (warm gas cooler supply). Things that may necessitate this action:

a) If you see the pump exit temperature (T7) slowly climbing past 90F, open in ¼ turn increments until stable at ~85F. This only happens when the ARU is getting a severe workout or there is a problem or both.

b) If the low-side pressure (solution receiver press. gauge) is climbing past 105 psig, open in half turn increments. Watch the high-side pressure. You're taking flow from the condenser. You'll probably need to simultaneously add flow through V26. Note: Adding to the absorber flow actually has very little effect on the low side pressure; this is a last ditch effort, and then only if you have the flow to spare on the south PCW header.

Planned Shut Down:

A controlled shut down of the THERMOCHARGER is generally uneventful, even if there is an emergency shut down of the turbine. As the heat load decreases and pressures and temperatures drop, the various adjustments can be returned to their Stand-by settings. When the heat load drops sufficiently, the unit will return to Stand-by mode and can then be shut down at the switch panel. **The primary goal is to leave the Solution Receiver 75-80 % full. If it is already at or below this level, do not wait for stand-by mode; turn off the system and close V2, V14 and V25.** If it is above this level, continue to run and allow the pump to bring the level down. **Remember that in stand-by mode, the pump is off, but the level will continue to drop slowly if the valves are still open.**

When shutting down the test facility, unplug the power cord.

Unplanned ('Fault') Shut Down:

This will occur when you are operating at the limits of the system and is generally due to exceeding maximum pressure. The turbine is usually at a high power level and **action must be taken immediately!!** The High Pressure Compressor Inlet Temperature will climb rapidly. Potentially, the rotor may experience a structural failure. Notify everyone repeatedly and with exuberance of this condition until you get confirmation, so an Emergency Turbine Shut down will be initiated. Remember, you are not ending a test, you are saving the facility.

When shutting down the test facility, unplug the power cord.

Transferring Fluid from the Rectifier to the Solution Receiver: Two people required. The primary operator must be wearing a chemical visor. The secondary (spray tank) operator must be wearing full safety glasses. This operation takes about one hour.

To verify the solution is in the Rectifier, check the Rectifier Float Valve sight glass, it should be full. With all valves in shut-down position, proceed as follows;

1. Turn on the exhaust fans.
2. Verify that V 13 and V 14 are closed.
3. Bring both water sprayers to the vicinity.
4. Check that both water sprayers are ¾ full of water, then pressurize. (Note there is a pressure bleed on the tank.)

When making or breaking any connection, irrigate with a continuous spray of water. All valves tend to leak and all hoses are probably charged with ammonia.

5. Connect a hose from V 20 at the Rectifier to V 7 at the solution Receiver.
6. Connect the ammonia tank (upright) to V 21 on the SHX (recuperative heat exchanger).
7. Open the tank valve to pressurize the line.
8. Crack open the hose fitting connection to V 21, allowing air to purge from the line, then re-seal.
9. Open V 7 then V 20 to allow the fluid to transfer.
10. Open V 21 to pressurize the circuit with ammonia vapor.
11. Continue fluid transfer until the solution receiver is ~ ¾ full. On the sight glass this would be a reading of ~ 7. The transfer causes oscillation in the sight glass reading. As the level approaches 7, stop transfer occasionally to be sure what the level actually is.
12. Before disconnecting the ammonia tank hose from V 21, de-pressurize the hose by opening the pressure relief ball valve at the tank end. Ammonia will bleed out of the line into a water bucket through the relief line. Do not allow water to draw back into the line as pressure drops.

Lab Data Acquisition System Procedure

Rev. 8/5/07

HPRTE Soot Investigation Test Run #10: Dated 8/10/07

OPERATOR'S NAME_____ Date _____

System Set-up: Record Barometric pressure _____ in Hg
This information can be obtained from http://www.phys.ufl.edu/weather/ .

1. ___ Switch on the National Instruments unit at least one hour before the run.
2. ___ Turn on the monitor and computer.
3. ___ Turn on the Fluke VOM for fuel flow rate readout.
4. ___ Turn on the Pressure Transducer regulated power supply.
5. ___ Switch on the thermal couple readouts (control panel below the selectors).
6. ___ Switch on the surge protected power strip behind the control panel.
7. ___ The computer password is, lear2005
8. ___ On the desktop, open the "Rover data acquisition" folder.
9. ___ Double click the latest program version, currently Rover5enomod4.vi; this will open the LabView data panel.
10. ___ Click the "Continuous Run" button and wait for the "Not Recording" light to begin blinking.
11. ___ Verify that all thermocouples are reading properly by both the analog and digital data acquisition systems. Confirm agreement with the instrumentation map. This should be completed a day in advance of the run.
12. ___ Verify that all pressure taps are reading properly by both the analog and digital data acquisition systems. Confirm agreement with the instrumentation map. This should be completed a day in advance of the run.
13. ___ Verify the analog pressure, temperature, and manometer reading legends are clearly displayed on the panel near the instruments.
14. ___ Observe the readouts for a sufficient period of time to deduce an average, then enter the offsets for the following:
    a) On the "Rover Vitals" tab;
        1) ___ HP Comp exit Press.
        2) ___ Prvci, (recirc. venturi inlet pressure)
        3) ___ HP Comp inlet Press.
        4) ___ Seal Tip Pressure
    b) ___ On the "LP Spool" tab, Comp. exit Pressure

15. ___ On the "Rover Vitals" tab, press the 'Write Data' toggle, on command of the test manager, during the start-up sequence.

16. ___ At the end of the run, stop data recording by pressing the 'Write Data' toggle again. The readouts are still active and can be monitored during cool-down.

Data Post Processing:

1. The data is recorded in C:\Rover\day,date,year.xls, e.g. Thursday, March 02, 2006.xls. It is in two columns. The first is the index, the second is the data value. Each scan of the DAQ is recorded sequentially, so the information must be put into a spreadsheet as follows.
2. Open Matlab and run MatLab program Edecimate('filename'), the filename being today's run file. It is easiest to copy the filename as text and paste it between the apostrophes to insure correctness.
3. Press 'Enter' and wait for the post-processed data file to be written. Its location is C:\Old_Rover_Data\filename.
4. The Excel data template is now required and the easiest way to get one is to open a previous run.
5. Save the previous run in a folder created for the current test program.
6. On the "All Data" worksheet, delete the <u>data only</u> in the first 64 (currently) columns. This is the data template.
7. Open the new data in the C:\Old_Rover_Data\filename location.
8. Copy the data, paste it in the data field of the template and save the file.
9. Change the source data of the plots to include data from start-up to shut-down of the current run.
10. Examine the plots for stray data points caused by signal noise. Find these data points in the data columns and replace them with an average of the five previous or subsequent data points.
11. The lead-in cells on the'PresDat' worksheet, still contain the range from the old run data you have deleted to get the template. Change this by going to the 'AllData' worksheet and finding the cell containing the ET recorded at Engine Start Solenoid Engaged. Now go to the 'PresDat' worksheet and copy the row number of the cell. Copy the row number of this cell address (e.g. 144 for cell A144) into each of the "lead-in" cells, such that they are the second input into each of the AVERAGE functions. For example, if the correct

ET at Engine Start Solenoid Engaged is in cell A144 of the 'AllData' worksheet, then AVERAGE(TU3,TU190) would become AVERAGE(TU3,TU144). The lead in data is now averaged over the proper time period for the new run. This time range may also be deduced by examining the plots and choosing, as your ET, the time just before temperature excursions indicate engine start.

12. The LabView and operating system combination has a "Bug" that causes jumps in the ET clock. When this occurs a blank region is observed in the plots where data seems to stop then begin again many seconds later. This may occur more than once during a run. Handle each occurrence in sequence. Repair the problem as in the following example.

    (1) Determine the amount of time "lost", e.g. ET = 3997, 3999, 4001, 4003, 4005, 4055, 4057, 4059 . . . about 50 seconds

    (2) Determine the average delta-t preceding the time loss, in the above, it's two seconds

    (3) Subtract the delta-t from the time lost, in this example, 48 seconds

    (4) Create a new column at the end of the spreadsheet, beginning with the first row following the time loss. That is, the same row as ET = 4055 in the above example. This column will replace the corrupted ET column, by subtracting 48 seconds from every ET, e.g. 4055-48, 4057-48, 4059-48 . . . etc to the end of the data.

    (5) Select the partial column with the new ET's, from where you started it, e.g. 4055-48 and cut it (ctrl + x).

    (6) Select the cell where the time loss begins, the cell with the 4055 in the above example, and right click.

    (7) Select the "Paste Special" option; a dialog box will appear.

    (8) Select the "Values" radio button, and press "Okay".

    (9) Check out the plots to ensure success.

    (10) Repeat this process for any additional time gaps farther into the run.

13. Post processing is now complete. Copy the post-processed spreadsheet to the flash drive provided.

Spectrometer Operating Procedure

Rev., 7/22/07

HPRTE Soot Investigation Test Run #10: Dated 8/10/07

_____ OPERATOR'S NAME

This document defines the operating procedure for the Ocean Optics spectrometer system available from Dr. David W. Hahn at the Laser Lab in the MAE A lower level. It consists of a laptop computer, mouse, 500-770nm S2000 spectrometer, SAD 500 signal conditioner, fiber optic cable, a magnetic base with holder and shield, signal cable, laptop power supply and spectrometer power supply. Note that the spectrometer is a precision instrument; take care not to damage it or the optical fiber cable. Use large radius loops when handling the cable, sharp bends will break it.

Set-up:

1. Connect the laptop mouse and power supply and turn on the computer.
2. At the prompt, press ctrl-alt-del and enter the password "lab".
3. Synchronize the date and time with the control room DAQ computer.
4. Verify the spectrometer is the correct 500-770 nm range.
5. Connect the signal cable between the laptop and the SAD500.
6. Connect the spectrometer power supply.
7. Create a folder on the Desktop named 'Run # mm/dd/yy'.
8. On the Desktop, double click the OOIBase32 Icon.
9. Set Integration time to 100ms.
10. Set Average to 20.
11. Set Boxcar to 0.
12. The X axis scale should read 500 to 760, if it does not;
    a) Open the "Spectrometer" menu.
    b) Open "Spectrometer Configuration"
    c) Go to C:\program files\ocean optics\OOIBase32
    d) Double click 500-770.spec
    e) At the prompt click yes for default configuration
13. Mount the magnetic base/fiber holder/inner light shield assembly approximately at the location marked on the Rover inlet duct. Be sure the 'V' of the mag base is fully seated

on the duct. The holder shield must be centered and co-axial in the viewport light shield. There should be 5/8" axial clearance between the cable holder and the viewport light shield. These should also be parallel.

14. Remove the blue fiber cable protector and connect the cable to the S2000 spectrometer. The cable nut must be fully engaged, finger tight is sufficient.

Data Acquisition:

1. Grasp the other end of the fiber optic cable, with the protector still in place, fully shrouded, in the palm of your hand.
2. Take a data point and save in the run folder with the filename 'Dark Signal'.
3. Remove the black cable protector and install the cable into the magnetic base holder, finger tight.
4. Take a data point and save in the run folder with the filename 'Stray Light'.
5. **When taking test data points during the run, the goal is to use <u>maximum signal integration time for each data point</u>, without saturating the Spectrometer CCD. The table shows acceptable combinations.**

Integration Time and Signal Averaging Table							
Integration Time	13	15	20	30	40	50	100
Averaging	150	130	100	70	50	40	20

6. Saturation is indicated by a horizontal line on the screen where there should be a continuous smooth curve. If the curve peak is off the screen, use Spectrum Auto scale to view the entire curve.
7. If saturation is not occurring, increase the Integration time until it does, then choose the next lower Integration Time and Averaging from the table before taking the data.
8. Save all additional data points, taken when called for by the team leader, in the run folder, use filenames 'DP1' 'DP2' etc.
9. At the end of the run, close the program.
10. Remove the mouse from the USB port and install the flash drive provided.
11. Copy the run data folder and paste it to the flash drive.
12. Shut down the system, disconnect the hardware, and return it to the storage location.

The COSA 1600 IR Gas Analyzer Operating Procedure

Rev., 5/9/07

1. Remove the analyzer from their storage case and re-locate to the control room counter top. Disconnect the sampling wand from the rubber sample tube, if attached.
2. Remove the battery from the analyzer carry case and connect it to the charger.
3. Install the charged battery into the analyzer carry case and connect it to the analyzer.
4. The screen will prompt with start-up and calibration date information. Press 'Enter' at each prompt until the "Warming up" sequence begins. Warm up will take ~ 4 minutes and the suction pump will start.
5. When warm up completes, and the screen will prompt "Set to zero please wait". Zeroing takes about 1 minute.
6. When zeroing completes, the screen will change to the menu.
7. Select 'Settings' and 'Clock'.
8. Synchronize the Analyzer clock to the Lab DAQ computer.
9. Connect the sampling hose to the sample diverter valve port.
10. Press 'Enter' to begin sampling for measurement. The memory location number will be in the upper right corner of the screen.
11. **Allow the analyzer to stabilize for one and one half minute (90 sec.).**
12. To record gas composition data, press 'Enter'.
13. The unit will immediately begin sampling for the next measurement.
14. At the end of the run, press 'Off' to put the unit in Standby mode.

Notes:

1. The condensate trap must always be vertical, drain and dry after each run.
2. **Always put the unit in standby mode before the battery is disconnected, otherwise the data will be lost.**
3. It should be assumed that fully charged batteries go dead within 3 days of non-use. The battery for each run must be on charge overnight before the run.
4. The unit must re-zero from time to time during the run, usually when you are trying to record a measurement. The screen notifies you and instructs you to disconnect, wait for

zero and reconnect the sample hose. Do not disconnect the hose, simply remove the lower cap of the condensate trap.

5. If the screen returns to the mode menu, the data point was recorded. Press 'Enter to begin sampling. If the screen returns to data readout, the data point was not recorded (check the memory location on the screen). In this case wait for stable readings (1min.) and record.

Stored data retrieval

1. The unit must warm up and zero before retrieval can begin.
2. At the opening menu, move the curser to "Stored Data" with the up/down arrow buttons.
3. Press Enter.
4. With the left/right arrow buttons select the data point 1-50.
5. Starting at data point 1, press the up or down arrow and the stored data for that point will be displayed.
6. Subsequent data points are selected with the left/right arrow buttons.
7. Transcribe all data to the Gas Analysis Run Data Sheet file.
8. To return to the main menu, press Enter.
9. To clear memory, select "Stored Data" then press the "print" button. The options are return, print actual, send data and "Del all Data"
10. Scroll to "Del all Data" and press the Enter button. The screen will return to the "Place 1" memory location. **Note that once deleted, the memory is not recoverable. Double check that you have accurately transcribed the data before executing steps 9. and 10.**
11. Press Enter to begin taking Measurements again.
12. Press the Off button to end the session, confirm at the "yes" prompt by pressing the Enter button to put the unit in standby mode.
13. To completely shut down the unit, disconnect the battery.
14. Distribute the Gas Analysis Run Data Sheet file as instructed.

Digital Camera Set-up Procedure

Rev. 7/22/07

Setting up for a test run:

1. Set up the tri-pod with the legs fully extended and locked. If applicable, lock the tri-pod central support.
2. Attach the tri-pod adaptor to the camera and mount the camera to the tri-pod.
3. Connect the power supply adapter to the camera. Note that the cord is at the top when installed.
4. Connect the power supply adapter cord to the power supply.
5. Connect the AC power cord to the power supply.
6. Plug the AC power cord into a receptacle.
7. Open the AV jack cover at the right rear of the camera.
8. Plug the AV jack into the AV receptacle (top one, yellow).
9. Connect the yellow and white AV, RCA jacks into the overhead AV cables.
10. Turn on the camera. The switch is at the top, rear of the camera.
11. Open the camera view screen.
12. Synchronize your timepiece to the Control room DAQ system. If you don't have a timepiece and/or don't know how to synchronize it, find someone who has these assets and ask them to finish setting up while you go do something else.
13. Press the menu button at the back of the camera.
14. Using the central grey button on the mode dial, Select "Basic"
15. Using the central grey button on the mode dial, Select "Clock set"
16. Using the central grey button on the mode dial, Select "Yes"
17. Press the central grey button on the mode dial, to bring up the time and date display.
18. Set the time and date using your synchronized timepiece.
19. Press the menu button to exit.
20. Aim the camera at the rig and adjust the zoom for maximum picture with both the fuel pressure gage and the combustion chamber viewport visible.
21. To record on the internal tape, press the silver "record" button at the back of the camera.

Note: It is not necessary to record internally to record on the control room VHS deck.

To rewind the internal tape:

1. Turn the mode dial to the green arrow with the green border.
2. Select rewind (left) with the central grey button on the mode dial.

APPENDIX B
DATA SHEETS

Test Matrix

Bill Ellis, Rev. 5/30/07

RCV	Dynamometer Net Load (lbf)				
ΔP	**9**	**15**	**25**	**35**	**45**
0	*Run 1, DP1*	*Run 1, DP2*	*Run 1, DP3*	*Run 1, DP4*	*Run 6, DP13*
.5		*Run 6, DP1,12*		*Run 1, DP5*	*Run 6, DP11*
1.0		*Run 6, DP2*		*Run 1, DP6*	*Run 6, DP10*
1.5		*Run 6, DP3*		*Run 1, DP7*	*Run 6, DP4*
2.0		*Run 5, DP12*		*Run 1, DP8*	*Run 6, DP5*
2.5		*Run 5, DP11*		*Run 1, DP9*	*Run 6, DP6*
3.0		*Run 2, DP1*		*Run 1, DP10*	*Run 6, DP7*
3.5		*Run 2, DP2*	*Run 3, DP1*	*Run 1, DP11*	*Run 6, DP8*
4.0		*Run 2, DP3*	*Run 4, DP1*	*Run 1, DP12*	*Run 6, DP9*
4.5		*Run 2, DP4*	*Run 4, DP2*	*Run 1, DP13*	*Run 7, DP1*
5.0		*Run 2, DP5*	*Run 4, DP3*	*Run 5, DP10*	*Run 7, DP2*
6.0		*Run 2, DP6*	*Run 4, DP4*	*Run 5, DP9*	*Run 7, DP3*
7.0		*Run 2, DP7*	*Run 5, DP1*	*Run 5, DP8*	*Run 7, DP4*

HPRTE Soot Investigation Test Run #7: Dated 8/10/07

Rev. 8/2/07

_____ OPERATOR'S NAME

Note: The AC vent blows on the table in front of the ARU/VARS unit. Locate the Psychrometer where it is not affected by AC airflow.

Calculate RH % before handing in the data sheet please !!!

Engine room Watch Data Sheet										
Data Point	WET Bulb (F)	DRY Bulb (F)	RH (%)	NH_3 Rec Press. (PSIG)	Sol. Pump Press. (PSIG)	Sol. Rcvr Press. (PSIG)	Sol. Flow Rate (GPM)	Cond Flow Rate (GPM)	NH_3 Level (inch)	Sol. Level (inch)
1										
2										
3										
4										
5										
6										
7										
8										
9										

HPRTE Soot Investigation Test Run #7: Dated 8/10/07

Rev. 8/2/07

_____ OPERATOR'S NAME

Switch Position A: High Compressor Exit

Switch Position B: High Turbine Exit

Gas Analysis								
Data Pt	Sw. Pos.	Mem Loc.	time	Ch4 %	CO %	CO2 %	NO ppm	O2 %
1	A	1						
	B	2						
2	A	3						
	B	4						
3	A	5						
	B	6						
4	A	7						
	B	8						
5	A	9						
	B	10						
6	A	11						
	B	12						
7	A	13						
	B	14						
8	A	15						
	B	16						
9	A	17						
	B	18						
10	A	19						

HPRTE Soot Investigation Test Run #7: Dated 8/10/07

Please take care that all entries are legible and fill in the page #'s
Rev. 8/5/07

_____ OPERATOR'S NAME

ENGINE START: _____ AM/PM

ENGINE STOP: _____ AM/PM

Operator's Panel Data Sheet							
		Data Point					
Instrument		1	2	3	4	5	6
STRAIN	DYNO LOAD (LBf)						
FUEL	FUEL LEVEL						
GAGE	FUEL PRESSURE (PSIG)						
ENG. OIL P	PRESSURE (PSIG)						
ENG. OIL T	TEMPERATURE(^{0}C)						
DYNO PRESSURE	DYNO INLET PRESSUE (PSIG)						
DYNO FLOW	TOTAL DYNO INLET FLOW (GPM)						
MAI	VALVE POSITION						
RECIRC	VALVE POSITION						
ROTAMETER	FUEL FLOW (g/s)						
RPM	ENGINE SPEED						
J11	HPCI (^{0}F)						
K5 (1150 max)	HPTX (^{0}F)						

HPRTE Soot Investigation Test Run #7: Dated 8/10/07

Please take care that all entries are legible and fill in the page #'s
Rev. 8/2/07

_____ OPERATOR'S NAME

Pressure Data Sheet							
		Data Point					
Instrument		1	2	3	4	5	6
M0	BRNR DP (S.G. 1.75)						
M4	RECRC DP (S.G. .827)						
M9	MAI (S.G. 1.91)						
M12	EVAP (S.G. 1.00)						
G5	HPCX (PSIG)						
G7	Seal P (PSIG)						
G8	HPRI (PSIG)						
G2-2	BRNR IN (PSIG)						
G1-1	HPTI (PSIG)						
G2-1	HPCI (in Hg Vac.)						

HPRTE Soot Investigation Test Run #7: Dated 8/10/07

Please take care that all entries are legible
Rev. 4/29/07

_____ OPERATOR'S NAME

Temperature Data Sheet							
		Data Point					
Instrument		1	2	3	4	5	6
T1	ARU-T14						
T2	NCWS						
T4	SCWS						
T11	ARU-T9						
T12	ARU-T10						
T16	ARU-T4						
J2	HPCX						
J5	WGCE						
J11	HPCI (W)						
J12	HPCI (E)						
K2	HPTX (t,e)						
K3	HPTI						
K4	HPTX (b,e)						
K5	HPTX (t,w)						
K12	HPTX (b,w)						
Ambient	Thermometer						

HPRTE Soot Investigation Test Run #10: Dated 8/10/07

Please take care that all entries are legible and fill in the page #'s
Rev. 5/30/07

_____ OPERATOR'S NAME

Record the beginning and ending time for each data point.

Timekeeper Data Sheet		
Computer Clock Time (h/m)	Computer ET (h/m/s)	Brief Description of occurrence
		Engine Start Solenoid Engaged
		Engine Ignition, Solenoid fuel valve on

Test Plan Shakedown Run
HPRTE Soot Investigation Dated 03/22/07
Bill Ellis, Rev. 3/16/07

The Soot Investigation shakedown run will be the first time the HPRTE has been in operation for several months. Some personnel who will assist in the run have no previous experience with HPRTE operation. This document defines the goals for this run.

There are two primary goals:

The first is to provide an opportunity for everyone on the team to observe the test rig in operation, become familiar with procedures, our methods of data acquisition, gain confidence with the controls and acquire an understanding of rig response to control changes.

Considering the time elapsed since the last run, even the experienced operators will benefit from the initial run in this regard.

The desired result is an increased proficiency of the team that will enhance our ability to complete future data runs in a timely and economical manner.

The second primary goal is more closely related to data acquisition. The operating limits we will approach are not yet clearly defined for the proposed conditions. It will be necessary to establish these.
Specifically; (see Soot Investigation Test Plan)

1. The minimum dynamometer load for data points 1-11.
2. The dynamometer load possible at maximum turbine inlet temperature for data points 56-66.
3. The maximum recirculation venturi Dp possible before restricting the boost control valve.
4. The maximum optical radiation intensity the spectrometer is expected to encounter is at data point 66. The spectrometer integration time may need to be reduced to avoid CCD saturation.
5. Flame transition can be expected at high recirculation ratios. We'll find it at some point and avoid it in subsequent runs.

The data will be taken in three runs after the shakedown. Knowledge gained on control positions will allow the rig to be brought up from start to the next test point more quickly.

To accomplish these goals four data points will be attempted on the shakedown run. These are 1, 66, 56 and 11, in that order. Since these are at the extremes of the matrix, encountering one of the above limitations is likely. This will begin to define the performance characteristics of the current configuration combustion liner.

APPENDIX C
RELEVANT DATA

Table C-1. Processed data

Data Point	F_{vR}	Φ	R_m	T_{soot} Deg. R	T_{ad} Deg. R	% O_2	P_{comb} psia
1	1.000	0.427	0.000	3559	2864	20.71	36.17
2	0.904	0.417	0.000	3590	2841	20.72	36.08
3	0.805	0.439	0.000	3587	2923	20.73	36.10
4	0.684	0.463	0.000	3582	3012	20.58	35.96
5	0.677	0.478	0.132	3511	2977	19.64	35.94
6	0.637	0.469	0.201	3514	2904	19.21	35.66
7	0.574	0.476	0.244	3468	2906	19.01	35.74
8	0.571	0.474	0.279	3491	2893	18.82	35.83
9	0.581	0.482	0.320	3489	2901	18.64	35.87
10	0.571	0.485	0.361	3462	2893	18.43	35.99
11	0.452	0.483	0.394	3491	2864	18.21	35.88
12	0.156	0.487	0.432	3472	2871	18.15	35.94
13	0.115	0.497	0.471	3472	2881	17.90	35.81
14	0.302	0.492	0.428	3309	2893	18.24	35.41
15	0.304	0.514	0.464	3317	2966	18.36	35.31
16	0.253	0.541	0.497	3309	3050	18.39	35.11
17	0.241	0.550	0.542	3306	3058	18.18	34.91
18	0.147	0.537	0.605	3307	2976	17.78	34.77
19	0.131	0.574	0.685	3303	3067	17.67	34.58
20	0.131	0.581	0.777	3297	3058	17.36	34.30
21	0.160	0.597	0.853	3294	3011	16.34	34.13
22	0.193	0.585	0.897	3261	2960	16.16	33.85
23	0.143	0.639	1.038	3228	3060	15.74	33.45
24	0.687	0.500	0.415	3323	2920	18.17	34.04
25	0.526	0.477	0.487	3356	2789	17.79	35.15
26	0.193	0.477	0.508	3400	2776	17.62	35.11
27	0.191	0.481	0.548	3408	2788	17.64	34.80
28	0.163	0.496	0.614	3381	2794	17.15	34.53
29	0.125	0.525	0.717	3387	2851	16.81	34.18
30	0.091	0.541	0.814	3393	2860	16.36	33.71
31	0.088	0.567	0.885	3373	2907	16.05	33.10
32	0.120	0.500	0.680	3383	2794	17.01	34.80
33	0.081	0.510	0.753	3389	2795	16.71	34.70
34	0.024	0.524	0.840	3473	2814	16.45	34.50
35	0.027	0.535	0.898	3434	2820	16.14	34.30
36	0.028	0.593	0.922	3411	2952	15.69	34.20
37	0.009	0.575	0.860	3554	2944	16.07	34.50
38	0.008	0.552	0.777	3569	2925	16.56	34.60
39	0.006	0.535	0.694	3648	2939	17.22	34.80

Table C-1. Continued.

Data Point	F_{vR}	Φ	R_m	T_{soot} Deg. R	T_{ad} Deg. R	% O_2	P_{comb} psia
40	0.027	0.525	0.624	3477	2923	17.38	35.00
41	0.066	0.556	0.538	3396	3074	18.04	35.20
42	0.607	0.523	0.319	3453	3067	19.04	35.20
43	0.547	0.500	0.291	3404	3009	19.15	35.10
44	0.186	0.423	0.127	3623	2797	19.57	35.12
45	0.704	0.430	0.191	3469	2787	19.12	34.76
46	0.659	0.424	0.271	3454	2737	18.78	34.89
47	0.144	0.512	0.241	3470	3035	18.70	34.93
48	0.129	0.504	0.284	3421	2979	18.42	35.07
49	0.068	0.502	0.346	3434	2937	18.07	35.11
50	0.074	0.509	0.372	3426	2950	18.00	34.74
51	0.052	0.515	0.421	3462	2948	17.80	34.88
52	0.007	0.526	0.470	3692	2961	17.54	34.72
53	0.097	0.502	0.203	3475	3026	18.90	34.46
54	0.251	0.503	0.152	3490	3063	19.21	34.29
55	0.660	0.425	0.146	3463	2797	19.37	34.03
56	0.528	0.471	0.000	3548	3052	20.34	33.77
57	0.007	0.553	0.517	3721	3030	17.48	34.86
58	0.007	0.558	0.552	3682	3019	17.19	34.76
59	0.006	0.563	0.630	3693	2999	16.87	34.36
60	0.006	0.572	0.707	3685	2978	16.47	34.26
61	0.011	0.590	0.866	3562	2959	15.74	33.82
62	0.074	0.611	0.906	3426	2955	15.39	34.48

Table C-2. Sample Labview Output

0	0
1	79.40388
2	1649.221
3	77.6002
4	78.30279
5	62.4443
6	61.94059
7	75.00613
8	77.82876
9	76.79381
10	76.94235
11	80.43185
12	78.13914
13	81.17278
14	79.61881
15	81.75643
16	-0.42701
17	-0.11914
18	0.043567
19	2.665943
20	0.150181
21	4.906085
22	1.580672
23	-0.41621
24	0.036023
25	-0.78179
26	-0.22353
27	3.19627
28	-3.59566
29	0.136194
30	2.724582
31	2600.127
32	19.58565
33	12.17088
34	-0.51699
35	78.25413
36	78.96556
37	78.76843
38	76.83228
39	0.041883
40	46.49488
41	19.03054
42	61.63222

Table C-2. Continued.

43	61.6227
44	0.025831
45	77.00661
46	74.11941
47	75.82267
48	70.80216
49	70.24372
50	68.22599
51	67.36043
52	77.67521
53	75.27425
54	78.36711
55	77.45163
56	77.55927
57	77.75253
58	75.5365
59	73.61412
60	74.46709
61	62.07341
62	63.19882
63	80.846

Measurement Error Analysis

Values for T_{soot} and F_{vR} are directly related to the emission intensity, measured with the spectrometer, after correcting for distance and set-up assumptions. The values of interest are the physical location of the optical fiber in its holder, the assumed radius of the flame and signal attenuation by the sapphire window. The average for these values was used to obtain the results presented in this work. The location of the optical fiber was known within +/- 0.12" of its mean, the radius of the flame was known within +/- 0.5" and the window transmissibility was known within +/- 0.08. A minimum and maximum corrected signal intensity was calculated using extreme values for these variables along with the corresponding values for T_{soot} and F_{vR}. These were compared to the results of this research. One half of the range was considered to be the measurement uncertainty.

Combustion pressure, P_{comb}, was measured using a bourdon tube mechanical gage with a 100 psi range and a 60 inch u-tube manometer. The accuracy of the gage was quoted to be +/- 0.75 % of full scale or 0.75 psi. The accuracy of the manometer was quoted to be +/- 0.04 psi. The contribution to uncertainty by the manometer was much less than the gage. Therefore the overall uncertainty was determined by rounding off the gage specification and presented as +/- 0.8 psi.

Values for O_2 % and Φ were dependent on the accuracy of fuel, humidity and exhaust gas measurements. The instrumentation for fuel and humidity measurements had a quoted accuracy of 1 %. For the exhaust gas analyzer, measurement accuracy for CO and CO_2 was +/- 5 % and for oxygen it was +/- 0.2 %. Uncertainty was calculated as follows.

$$7.2\% = \left[(1\%)^2 + (1\%)^2 + (5\%)^2 + (5\%)^2 + (0.2\%)^2\right]^{1/2}$$

LIST OF REFERENCES

1. IPCC, 1995. Climate Change 1995. *Intergovernmental Panel on Climate Change.* Cambridge Univ. Press, London (1995).

2. Haywood, J.M., and Shine, K.P., *Quart. J. R. Meteorol. Soc.*123:1907–1930 (1997).

3. Seinfeld, J. H., *Nature,* 391:837 (1998).

4. Shine, K. P., and M. de F. Forster, Piers, *Global and Planetary Change* 20:205–225, (1999).

5. Kirkeva, A., Iversen,T., and Arne, D., *Atmospheric Environment* 33:2621-2635 (1999).

6. American Lung Association, *Selected Key Studies on Particulate Matter and Health: 1997 – 2001,* New York (2001).

7. Gupta, A.K., *Energy Convers. Mgmt.* 38:10-13:1311-1318, (1997).

8. Lefebvre, H., *Int. J. Heat Mass Transfer.* 27:9:1493-1510, (1984).

9. Moss, J.B., and Stewart,C..D., *Experimental Thermal and Fluid Science* 28:575-583, (2004)

10. Frenklach, M., *Phys. Chem. Chem. Phys.*, 4:2028–2037, (2002).

11. Glassman, I., *Combustion, 3d ed.*, Academic Press, New York, 1996

12. Thomson, K. A., Gülder, Ö. L., Weckman, E. J., Fraser, R. A., Smallwood, G. J., and Snelling, D. R., *Combustion and Flame* 140:222–232 (2005).

13. Roditcheva, V. X., and Bai, S., *Chemosphere* 42:811-821, (2001).

14. McCrain, L. L., and Roberts, W. L., *Combustion and Flame* 140:60-69, (2005).

15. Brooks, S. J., and Moss, J. B., *Combustion and Flame* 116:49-61, (1999).

16. Gollahalli, S.R., and Puri, R., *Energy Convers. Mgmt*. 38:10-13:1073-1081, (1997)

17. Konishi, N., Kitagawa, K., Arai, N., and Gupta, A. K., *Journal of Propulsion and Power*, 18:1, (2002)

18. Shimo, N., and Fujisou, A., *Second International Symposium on High Temperature Air Combustion and Gasification,* Kaohsuing, Taiwan, 1999, pp B6

19. Weber, R., Verlaan, A. L., Orsino, S., and Lallemant, N., *Second International Symposium on High Temperature Air Combustion and Gasification,* Kaohsuing, Taiwan, 1999, pp C2

20. Gupta, A. K., and Hasegawa, T., *Second International Symposium on High Temperature Air Combustion and Gasification,* Kaohsuing, Taiwan, 1999, pp A4

21. Caveliere, M. de Joannon, and Ragucci, R., *Second International Symposium on High Temperature Air Combustion and Gasification,* Kaohsuing, Taiwan, 1999, pp B4

22. Hottel, H. C. and Broughton, F. P., *Industrial and Engineering Chemistry, Analytical Edition*, Vol. 4, No. 2, (1932)

23. Zhao H., and Ladommatos, N., *Prog. Energy Combust. Sci.* 24:221-255, (1998).

24. Chang, H., and Charalampopoulos, T. T., *Proc. R. Soc. Lond. A*, 430:577-591 (1990).

25. Choi, M. Y., Hammins, A., Mulholland, G. W., and Kashiwagi, T., *Combustion and Flame*, 99:174-186 (1994).

26. Jenkins, T. P., and Hanson, R. K., *Combustion and Flame*, 126:1669-1679 (2001).

27. Howell, E. B., Masters Thesis, University of Florida Gainesville, Department of Mechanical Engineering, 2007.

28. Sonntag, R. E., and Van Wylen, G. J., Introduction to Thermodynamics: Classical and Statistical, John Wiley & Sons, Inc., New York, 1971.

29. di Stasio, S. and Massoli, P., *Meas. Sci. Technol.,* 5:1453-1465, (1994).

BIOGRAPHICAL SKETCH

William J. Ellis, Jr. was born in West Palm Beach Florida. His primary education was completed in Fort Lauderdale Florida. He graduated in the top 10% of his class in 1970. Early undergraduate work was undertaken at Broward Junior College (Davie, Florida) and the University of South Florida (Tampa) where he received an Associate of Arts degree. After transferring to the University of South Carolina at Clemson in 1977, he graduated with a Bachelor of Science in mechanical engineering in 1979 with honors. After a career spanning 27 years, he enrolled for graduate studies at the University of Florida in Gainesville Florida and received a Master of Science in mechanical engineering in 2008.